PETROGRAPHY

OF THE CARDIUM SANDSTONES IN THE

RICINUS, CAROLINE, AND GARRINGTON FIELDS

ALBERTA

PETROGRAPHY OF THE CARDIUM SANDSTONE IN THE RICINUS, CAROLINE, AND GARRINGTON FIELDS, ALBERTA

BY

DOUGLAS ELLIOTT SWEENEY

A THESIS SUBMITTED TO THE
DEPARTMENT OF GEOLOGY
IN PARTIAL FULFILLMENT OF REQUIREMENT
DEGREE OF BACHELOR OF SCIENCE

McMASTER UNIVERSITY
APRIL 18, 1983

THESIS: BACHELOR OF SCIENCE

TITLE: PETROGRAPHY OF THE CARDIUM SANDSTONES RICINUS, CAROLINE AND GARRINGTON FIELDS, ALBERTA

AUTHOR: DOUGLAS ELLIOTT SWEENEY

SUPERVISOR: DR. R. G. WALKER

NUMBER OF PAGES: 197

ACKNOWLEDGEMENTS

The author wishes to extend his sincere appreciation to Dr. R. G. Walker for suggesting the topic of this thesis and for his remarkable patience.

Thanks go to a friend and a colleague, Chris Kasserra for humoring me in my weaker moments.

Most of all I wish to thank my wife and son, who tolerated a husband and a father who was little more than a voice on the telephone for the duration of this research.

ABSTRACT

Seventy-nine thin sections were prepared from cores of the Upper Cretaceous Cardium sandstone, obtained from wells in the Ricinus, Caroline and Garrington fields in Alberta. Petrography of each thin section was studied to determine if any comparisons could be made between sands of differing fields, or between the Upper (A) and Lower (B) sands of the same field.

Two sandstone types have been determined based upon modal percentages of three major mineral constituents. A chert rich sublitharenite generally contains 60% chert, 30% quartz, and 10% unstable rock fragments. A chert poor sublitharenite contains 70% quartz, 15% chert and 15% unstable rock fragments. The chert sublitharenite were coarse grained to conglomerate, poorly sorted, with subround to rounded grains. The chert poor sublitharenite were fined grained, well sorted, and contained subangular to angular grains.

Within the Caroline and Garrington fields, the Upper and Lower sands can be distinguished on the basis that the former is of the fine grained, chert poor sublitharenite type, and the latter is of the conglomeratic, chert rich sublitharenite type of sandstone. The Lower Garrington sand can be distinguished from the Lower Caroline sand, because the Lower Garrington sand tends to be more chert rich. Similarly, the Upper Garrington sand

and the Upper Caroline sand can be distinguished on the basis that the Upper Garrington sand contains a greater abundance of unstable rock fragments. The Upper sands of the Caroline and Garrington fields can not be distinguished from the Ricinus sand, whereas the Lower sands can, as they tend to be richer in chert, and are coarse grained to conglomeratic in grain size.

The cementing sequence of; siderite, calcite and silica (in chronological order) was observed in all of the sands. Variations in cement abundances were a function of both depth and grain size. The deeper sands such as in the Ricinus field were predominantly silica cemented. The shallower sands tended to be siderite cemented, as did all those coarse grained to conglomeratic sands.

TABLE OF CONTENTS

TABLES OF FIGURES

FIGURE NO. - PAGE

TABLE OF PLATES

CHAPTER 1

PURPOSE OF STUDY

The focus of this paper is to compare and contrast three existing hydrocarbon bearing fields with respect to their petrography. Specifically, the fields from west to east are Ricinus, Caroline, and Garrington. Previous work is somewhat limited, as only hydrocarbon production has been used for a data base to establish the field boundaries. Nevertheless, a base has been established from which petrographic data can be compared. Well logs indicate that the Caroline and Garrington fields contain an upper (A) sand and lower (B) sand. The Ricinus field is composed of only one sand unit (Walker, 1983) which cuts into the A sand as a 5 Km wide scour with depths varying from 20 to 40 meters (Fig. 1). The purpose of this paper is to study the mineralogic or textural differences between these sand bodies. In particular, the following questions will be addressed:

1. Are there any significant petrographic differences between the Ricinus and Caroline fields, or between Ricinus and Garrington fields?
2. Are there any significant petrographic differences within either the Caroline or the Garrington fields? That is, can the A and B sands be distinguished on a petrographic basis?

FIGURE 1 : Stratigraphic cross section of the Ricinus, Caroline, and Garrington fields (Walker, 1983).

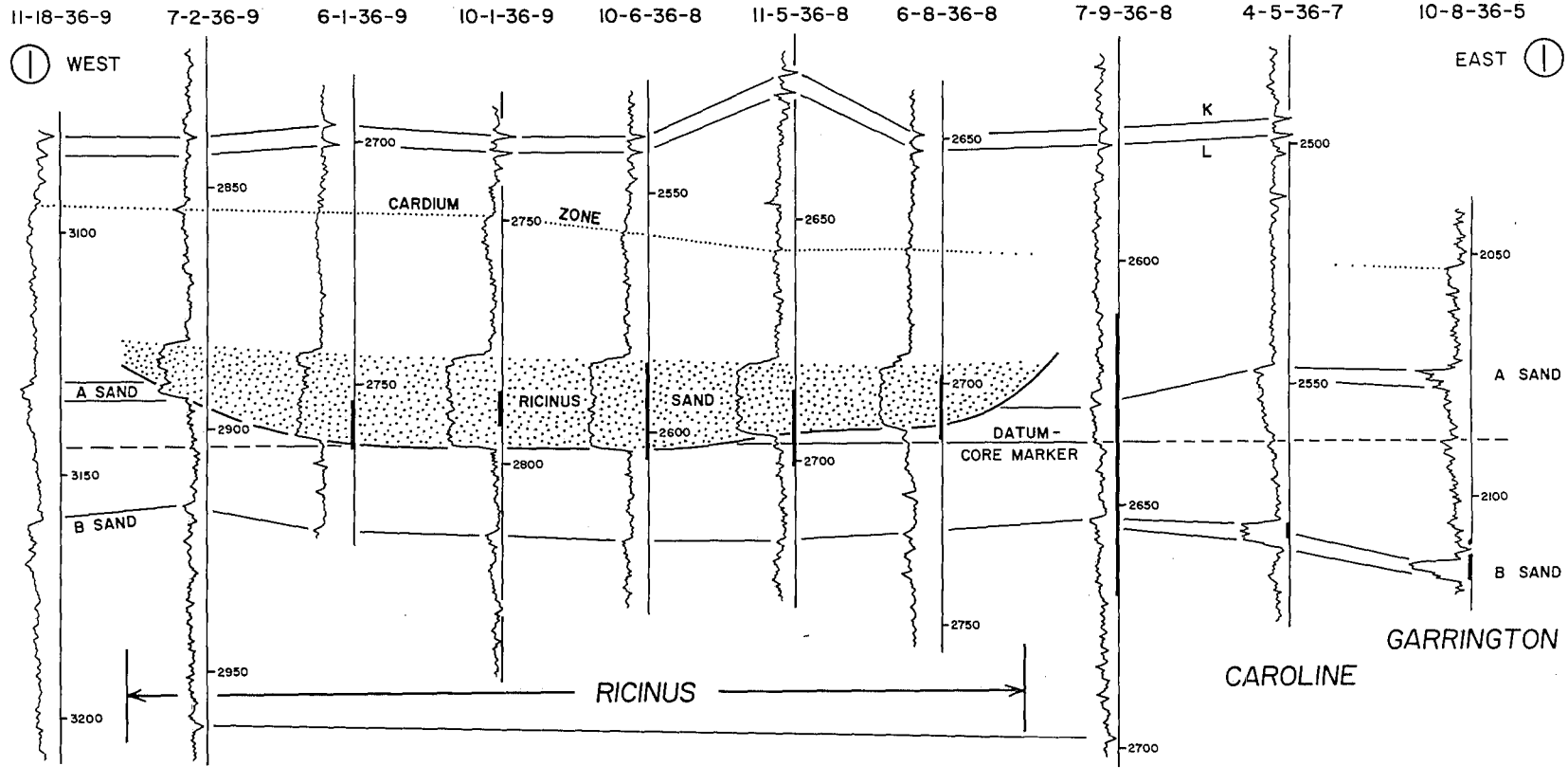
11-18-36-9
7-2-36-9
6-1-36-9
10-1-36-9
10-6-36-8
11-5-36-8
6-8-36-8
7-9-36-8
4-5-36-7
10-8-36-5
WEST
EAST
CARDIUM
ZONE
A SAND
B SAND
RICINUS
SAND
DATUM-
CORE MARKER
K
L
A SAND
B SAND
RICINUS
GARRINGTON
CAROLINE
2700
2850
3100
2750
2900
3150
2800
2550
2600
2650
2700
2750
2950
3200
2650
2500
2600
2550
2050
2100
2650
2700

AREA OF STUDY

The Ricinus, Caroline and Garrington fields are located approximately 85 Km northwest of Calgary, Alberta (Fig. 2). The wells penetrating the sand bodies are located within ranges 7 to 9, townships 31 to 37, west of the fifth meridian (Fig. 3). The three fields are defined by three lenticular "pod", like sandstone bodies which lie at a depth of approximately 2700 meters. The sandstone bodies occur en echelon, striking approximately northwest to southeast, with varying sand thicknesses in between. The sand bodies increase in length towards the east from approximately 30 Km in the Ricinus to 60 Km in the Garrington field, and vary in thickness from 2 to 7 meters in any given sand body. They are generally sharp based but have convex upper surfaces. Laterally, the sand bodies range from fairly straight sided in Garrington, to more sinuous in Caroline, to very irregular sided in Ricinus, due to the effects of faulting in the latter field. The Caroline body appears to thin southeasterly, whereas no such relationship is apparent for the Ricinus and Garrington sand bodies (Walker, 1983).

FIGURE 2 : Map of Alberta indicating location of the study area.

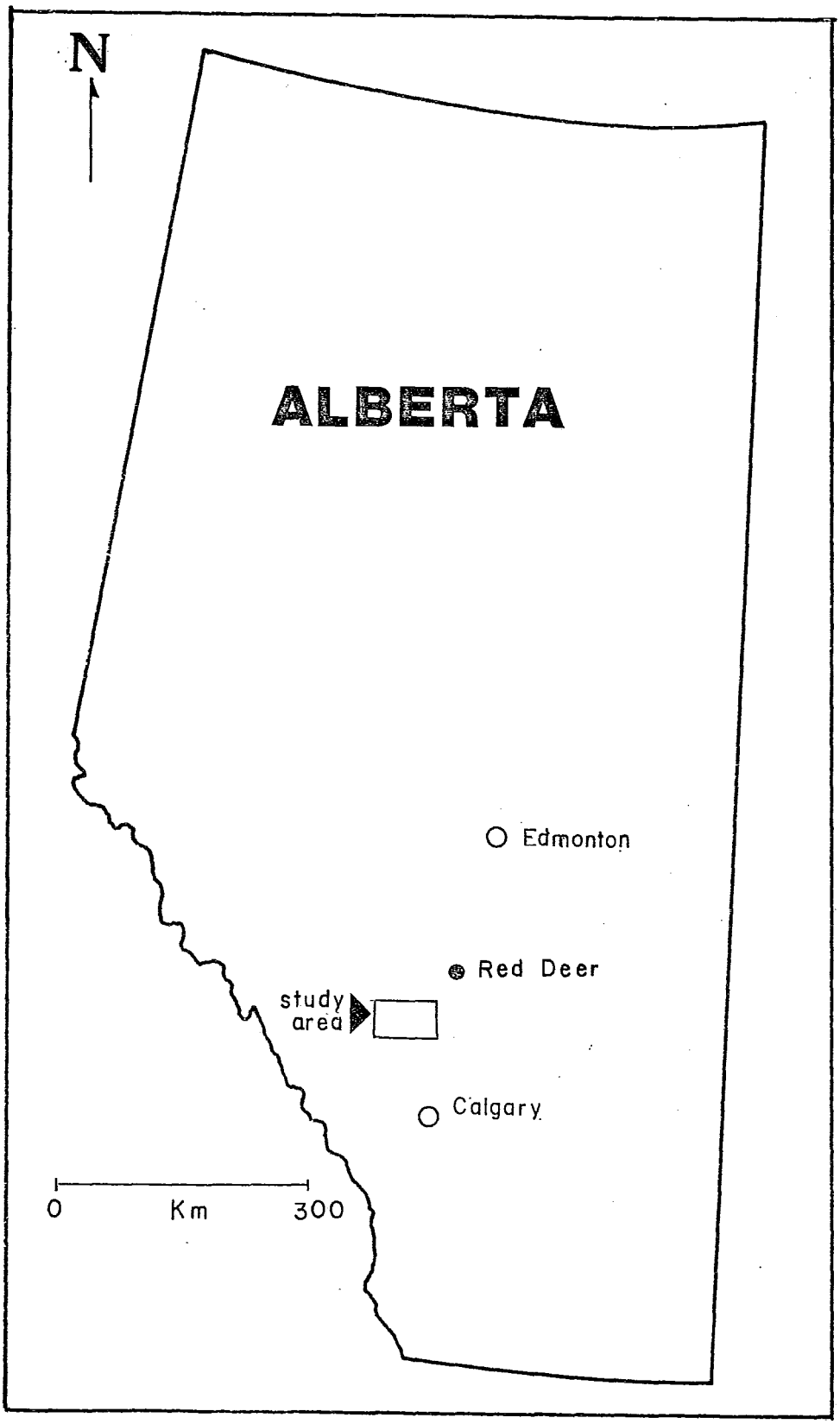
N
ALBERTA
Edmonton
Red Deer
study area
Calgary
0
Km
300

FIGURE 3 : Schematic diagram of study area illustrating field size and shape (Walker, 1983).

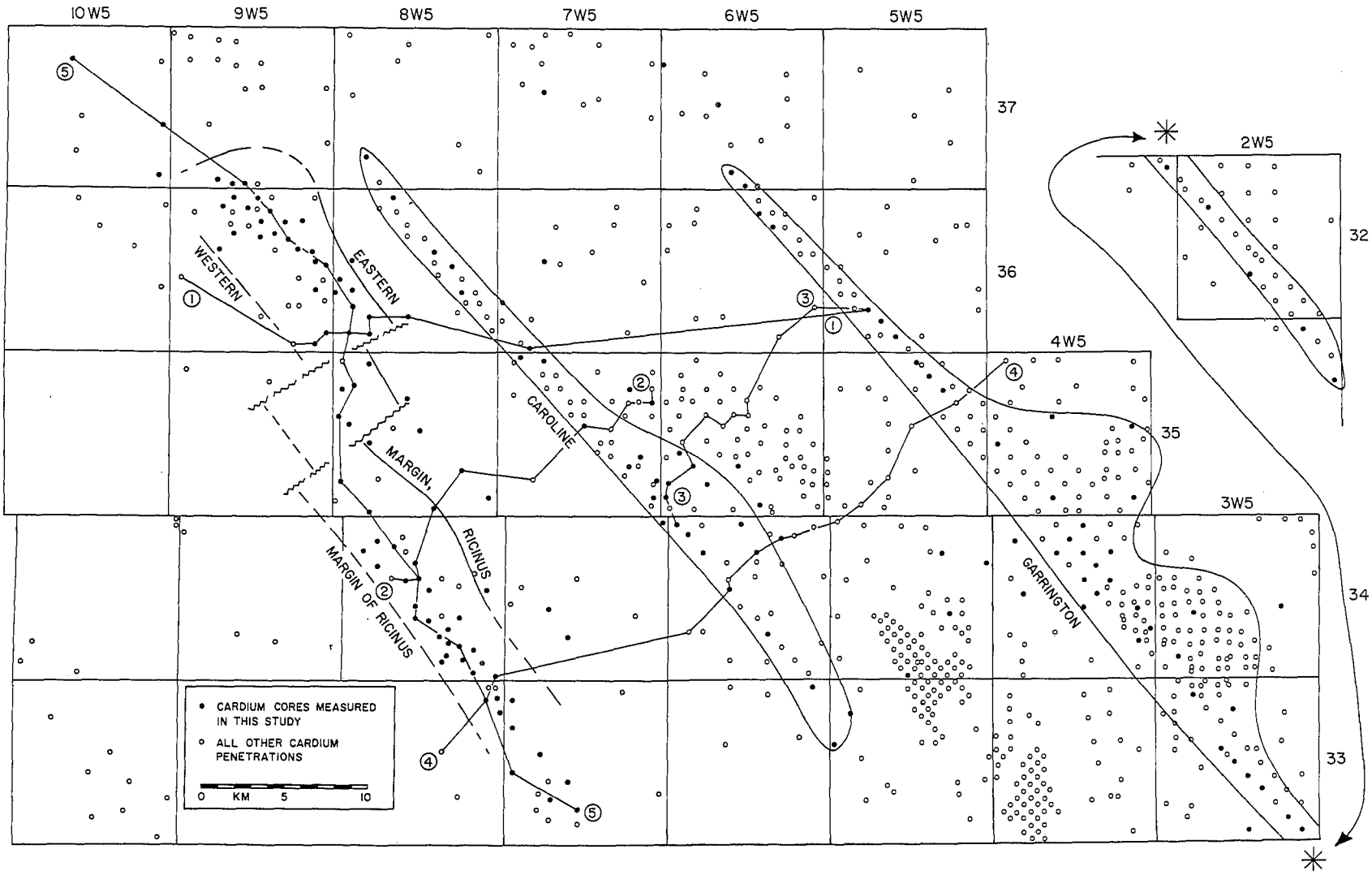
10W5
9W5
8W5
7W5
6W5
5W5
4W5
3W5
2W5
37
36
35
34
33
32
WESTERN
EASTERN
CAROLINE
MARGIN,
RICINIUS
MARGIN OF RICINIUS
GARRINGTON
CARDIUM CORES MEASURED IN THIS STUDY
ALL OTHER CARDIUM PENETRATIONS
0 KM 5 10

GENERAL STRATIGRAPHY

The Ricinus, Caroline, and Garrington fields contain the Cardium sandstone as the hydrocarbon-bearing sand body, and hence an important unit of study. The Blackstone, Cardium and Wapiabi formations collectively comprise the Alberta Group (Upper Cretaceous). The Cardium Formation (Turonian) was named by Rutherford in 1927 after Hector introduced the Cardium Shale in 1895, based upon the discovery of the fossilized bivalve Cardium within the sediments. The Cardium Formation contains six members, and, in ascending order, they are the Ram, Mossehounds, Kiska, Cardinal, Leyland and Sturrock (Fig. 4). In addition to this, a series of coarsening upwards cycles has been observed, ranging from clays up through sandstone (Stott, 1963). Unfortunately, the physical boundaries of the cycles cross the member boundaries, hence a re-assessment of the stratigraphy is necessary. The Cardium is exposed in outcrop in a north to south running belt, referred to as the Central Foothills Belt (Currie, 1974). Drill holes intersect the Cardium in the subsurface along the eastern margin of the foothills and eastward towards the plains. Outcrops of the Cardium can be found within the foothills, between Grande Prairie and the international border.

The interpreted depositional environment is that of a shallow marine environment dominated by storm activity

(Wright and Walker, 1983). The Cardium is characterized by coarsening upwards sequences of shale to sandstone containing ubiquitous hummocky cross stratification. Anomalous conglomeratic horizons are also associated with the Cardium sandstones, capping many of the coarsening upwards sequences. The sharp based coarsening upwards sequences reflect a more proximal source area, whereas the fine grained shale intervals between cycles reflect a more distal source. In this sense, the coarsening upwards sequences suggest transgressive and regressive controls on the deposition of the Cardium sediments.

FIGURE 4 : Diagram indicating the Cardium stratigraphy.

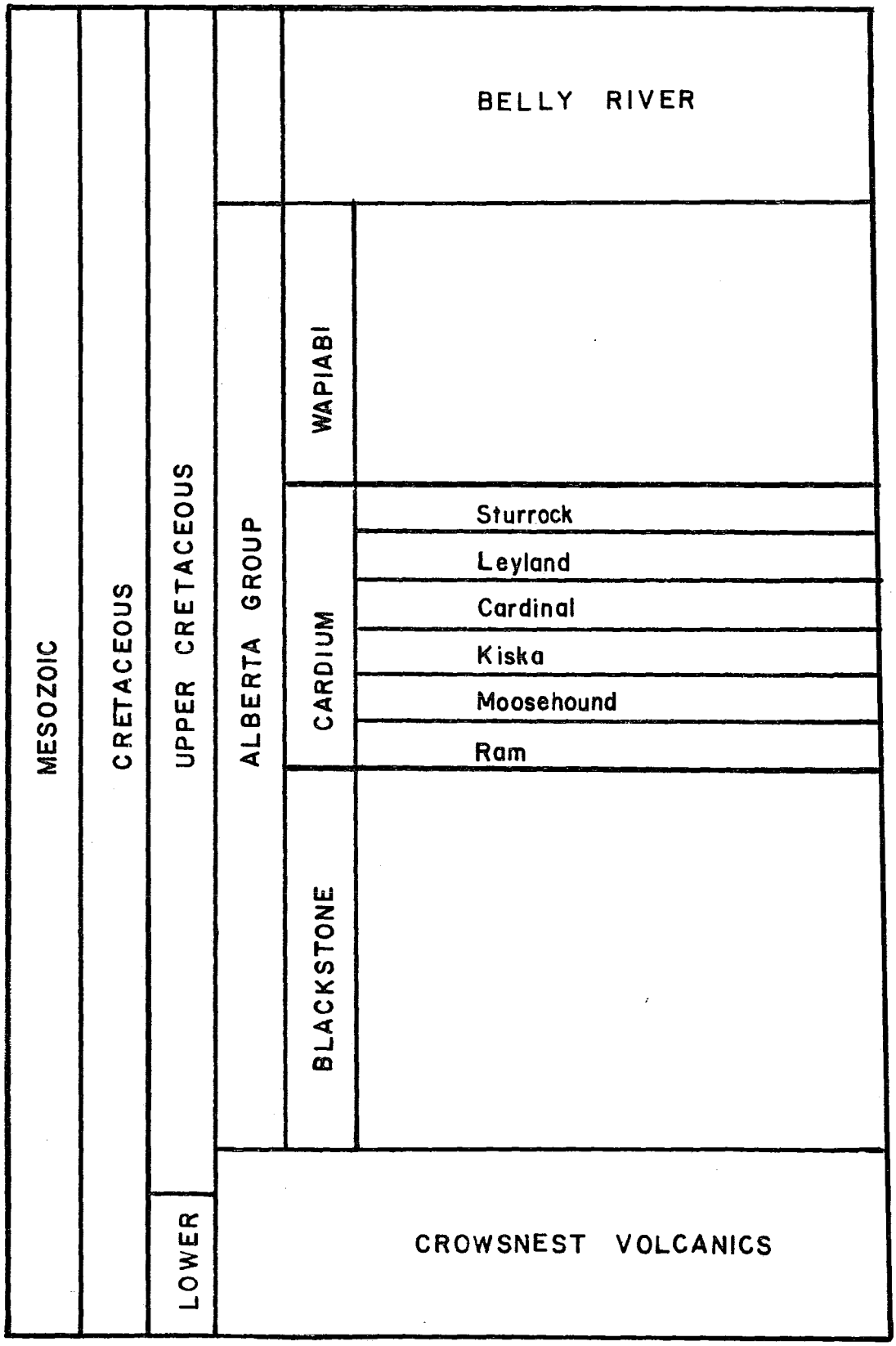
MESOZOIC
CRETACEOUS
UPPER CRETACEOUS
LOWER
BELLY RIVER
ALBERTA GROUP
WAPIABI
CARDIUM
Sturrock
Leyland
Cardinal
Kiska
Moosehound
Ram
BLACKSTONE
CROWSNEST VOLCANICS

STRUCTURAL HISTORY

With the exception of the Ricinus field, there is very little structural deformation of the Cardium Sandstone, within the local study area. The Caroline and Garrington fields are located far enough east of the Foothills Deformed Belt as not to have been affected. In Ricinus, the Cardium sand is observed to repeat itself up to five times, as a result of extensive thrust faulting. Faults dip mostly westward, but some dip eastward because the Ricinus sand body is located on the "triangle zone" in the Foothills Deformed Belt (Fig. 5). Nevertheless, all of the fields in question are in a region that, because of tectonic uplift, accompanied by erosional unloading, are going to experience some form of microscopic deformation. This may be manifested in thin sections by the occurence of fractures, styloliths and compaction.

FIGURE 5: Map of the local area, indicating the extent of structural control in the Ricinus, Caroline, and Garrington fields (Walker, personal communication).

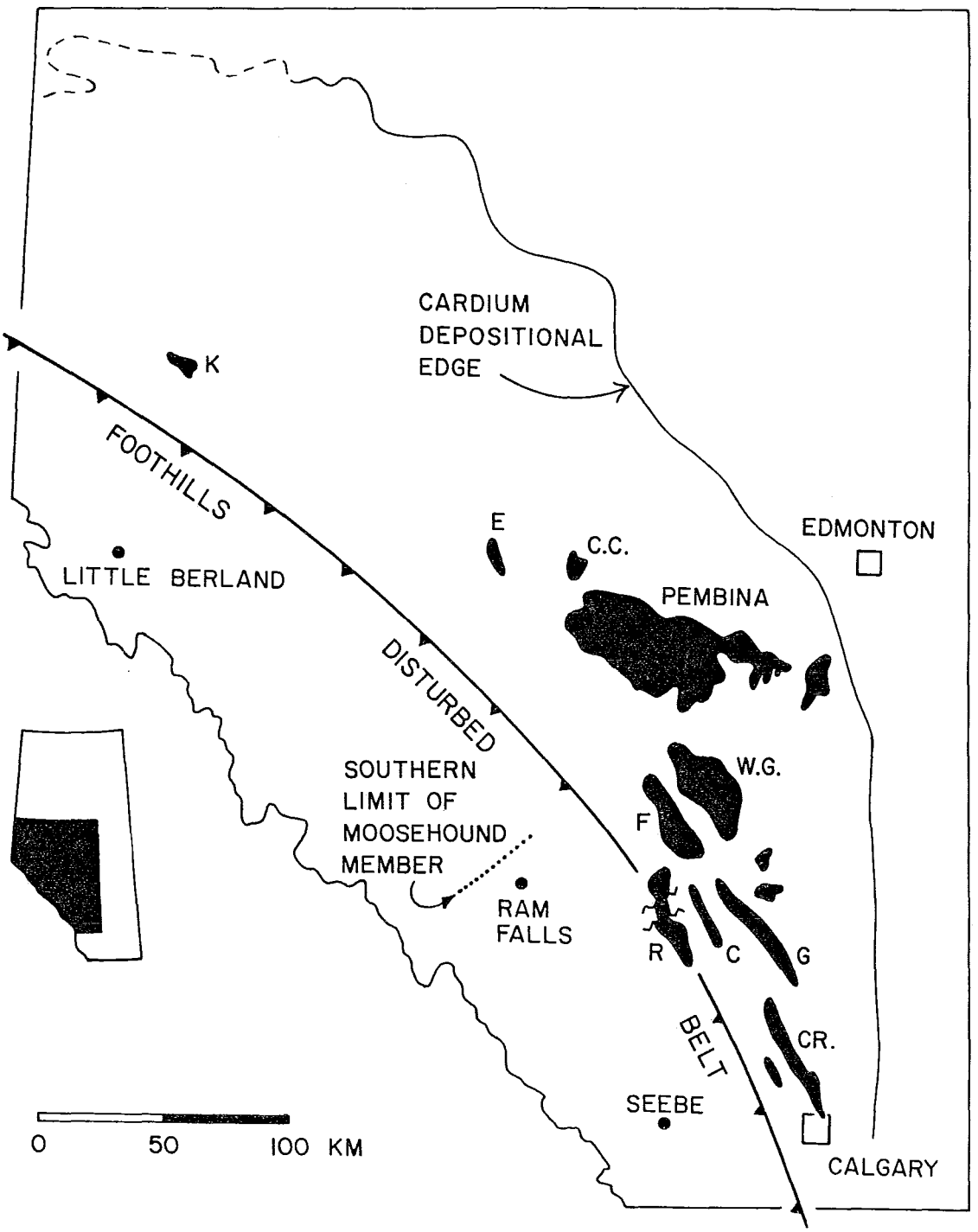
CARDIUM
DEPOSITIONAL
EDGE
K
FOOTHILLS
LITTLE BERLAND
E
C.C.
EDMONTON
PEMBINA
DISTURBED
SOUTHERN
LIMIT OF
MOOSEHOUND
MEMBER
W.G.
F
RAM
FALLS
R
C
G
BELT
CR.
SEEBE
CALGARY
0
50
100 KM

LOCAL GEOLOGIC HISTORY

Within the local area of study, the Crowsnest Volcanics lie underneath the Alberta Group. The Alberta Group was deposited in a broad depositional trough, the source being the rising Rocky Mountains to the west. By the Late Cretaceous, the region bounded by the Rocky Mountains to the west, and the Canadian Shield to the east, was inundated by an epeiric Sea. The Blackstone shales were first deposited in a marine environment with an orogenic source area becoming increasingly less stable with time. The deposition of the Cardium was characterized by recurrent uplifts of the borderland, followed by periods of erosion giving rise to an oscillating source area. Hence the geologic record shows the Cardium sediments as intercolated silts and shales with coarse clastic wedges of sandstone. These cycles are thought to represent relatively rapid marine transgressive and regressive episodes within the depositional basin (Berven, 1966). Subsidence of the basin re-established the marine enviornment manifested by the Wapiabi shales, until the emergence of the nonmarine Belly River sandstones. This period of emergence was interrupted by a brief marine transgression, represented in the geologic record as the Bearpaw shales. Subsequent sedimentation resulted in as much as 3700 meters of overburden accumulating on top of the Cardium Formation (Currie, 1974). By the late Tertiary, the foothills and plains had

experienced uplift and the associated tilting of strata.

PREVIOUS WORK

The initial motivation for research in the Cardium was in 1953 when oil was discovered within the sandstones at Pembina. Initially, the research was centered around the controversy of the turbidite mechanism as means to deposit the coarse clastic sediments so far out from the hypothetical source area. Papers by Beach in 1955, and DeWeil in 1956, were representative of this debate. Numerous other depositional models were submitted at the Cardium symposium held by the A.S.P.G. in Calgary in 1957. One opinion was a barrier beach environment (Michaelis, 1957). The next topic of research was extensive stratigraphic compilation of most of the Cardium outcrops in Alberta, as well as those containing the Wapaibi and Blackstone Formations (Stott, 1963). It was not until 1963, however, that the first comparative subsurface study was published on the Cardium (Burk, 1963). The Cardium formation as well as three other marker horizons, have been correlated using spontaneous - potential logs in 1966, containing detailed petrography of some of the Cardium cores (Berven, 1966). In this research, correlation was made with respect to the Crossfield and Garrington fields, but unfortunately the number of cores studied was not sufficient to nail down any concrete relationships. In 1969, more subsurface studies were completed, but this time emphasis was placed on the identification of sedimentary structures

in cores. In subsequent years, more intensified studies were made on individual fields with regard to sedimentary structures, paleoflow determination, petrography and environmental interpretations. Fields examined in detail were; Edson Field (Sinha, 1970), Carrot Greek Field (Swagor et al, 1976), Ferrier Field (Griffith, 1982), and Pembina Field (Krause, 1982).

Once again, the question of environment of deposition of the Cardium sandstones was emphasized, using sedimentary structures, primary stratification, and trace fossils. A tidally-influenced shoal complex was suggested (Michaelis and Dixon, 1969), as well as a storm dominated depositional shelf enviornment at Seebe, Alberta (Wright and Walker, 1980).

From the history of previous research, it is apparent that, inasmuch as the Cardium sandstones have been studied extensively within individual fields, relatively little research has been applied with respect to comparisons between two or more fields on a petrographic basis.

CHAPTER 2

METHODS OF STUDY

The data for this study are based upon cores taken from 35 wells within the study area. Seventy-nine thin sections were prepared from core samples that had been injected with a blue epoxy to highlight porosity. Each thin section was examined with a petrographic microscope, as well as a cathode luminescence microscope. Under the petrographic microscope, each thin section was point counted, with four traverses of one hundred counts each. Details such as grain size, sphericity, contacts, porosity and modal mineral composition were recorded. The mineral categories recorded were quartz, chert, rock fragments, feldspar, porosity, cement, matrix and other.

Rock Fragments included shale clasts, siltstone grains, volcanic debris, and polymineralic grains. Feldspars were generally of the plagioclase variety, by virtue of their polysynthetic twinning, although alkali feldspars were occasionally observed. Porosity was noted whenever the blue stain was encountered. Cement refers to the silica variety only. Clays, calcite and siderite comprise the matrix whether they occur as cements or otherwise. The "other" category usually included such accessory minerals as pyrite, muscovite, tourmaline or hydrocarbons.

In the case of those thin sections out from a conglomeratic sandstone, a second mineralogic evaluation was required with respect to the composite clasts. The clasts were generally composed of chert, with lesser proportions of quartz, siderite, shale, and porosity. The method utilized in these instances was similar to that used by Terry and Chilingar, 1955 (Appendix VI).

Since in any given conglomeratic thin section, the extent and type of impurities within the chert were consistent, the resulting composition of the composite clasts could be added to the original modal composition, as determined by the point count procedure. In this regard, conglomeratic and polymineralic clasts could be normalized with respect to their mineralogy and compared with the monomineralic grains.

Error Analysis

Inasmuch as the observations and conclusions presented in the body of this paper must ultimately reflect the data generated by the operator, an assessment as to the source and extent of error would be appropriate. This was attempted by recounting a randomly selected thin section, with respect to its modal composition. A recount was made by the same operator to establish the degree of reproducibility by the same operator. An additional recount was performed by a second operator to establish the

degree of reproducibility between operators. The results were recorded and tabulated (Appendix V).

The reproducibility of data generated by the same operator is good, as most of the modal compositions were within 5% agreement between the two counts. The exceptions were chert and rock fragments. A lesser amount of chert was observed in the first count and recorded as rock fragment. As a much greater amount of petrographic experience had been obtained by the time of the second count was made, the operator was more easily able to discern siderite invaded chert as chert. In this sense it is to be expected that some of the earlier thin sections might have a very minor error associated with the rock fragments.

The reproducibility of the data generated by different operators is also very good. In all cases the mineral modal percent estimates were within 5% error, so that little error can be attributed to operator bias.

CATHODE LUMINESCENCE

The major power of this technique was the ability to distinguish various types of authigenic cements. Quartz overgrowths as silica cement are rendered transparent under cathode luminescence, while the carbonate cements luminesced a vivid orange-red (Plate 5B). Volcanic rock fragments and feldspars were also enhanced under cathode luminescence, but to a less obvious degree. In the instance of silica cements, a visual approximation was made as to the percentage of quartz grains in the thin section which were cemented, and the percentage of the grains that were composed of quartz overgrowths. In this regard, a quantitative approximation of the amount of silica cement was achieved. This was necessary as, under the petrographic microscope, the quartz overgrowths were in optical continuity with the quartz grains, and could not be distinguished, except in the rare instances where dust rims were present (Plate 1B).

Carbonate cements could be point counted, using the petrographic microscope, upon their identification by means of the cathode luminoscope. Other features that were evident under the cathode luminoscope were fractures, sutures, and embayments of grains (Plate 3B). A second observation was made as to those grain shapes previously obscured by quartz overgrowths. Based upon observations such as these, the diagenetic history of the Cardium sandstones was revealed.

GRAIN SIZE ANAYLSIS

Grain size determinations were made with a petrographic microscope equipped with a micrometer. The micrometer was able to measure grains with an accuracy of .03 mm. Initially, each thin section was traversed at random, measuring the long axes of 100 grains. The largest and smallest grains were recorded as the range, and an average grain size calculated. It soon became apparent, however, that one hundred grain counts were redundant, depending upon the degree of sorting of the sandstone. This sorting varied from extremely well to moderately well, to poor, for the fine grained, coarse grained, and conglomeratic sandstones, respectively (Plate 40A-C).

The nature of the conglomeratic sandstone was such that the number of grain counts was limited by the number of clasts. In some cases, as few as a dozen clasts comprised nearly all the thin section.

It was determined that 25 grain and 50 grain counts would be sufficient for the coarse grained and fine grained sandstone, respectively, by the following approach: A series of histograms were constructed for 25, 50 and 100 grain counts on representative thin sections, for each of the coarse and fine grained sandstones (Figs. 6, 7). The grain size was plotted in millimeters on the abscissa axis, while the percentage of the thin section represented by each grain size interval is plotted on the ordinate. The

number of grains corresponding to each grain size is printed within each of the histogram rectangles.

In the case of the coarse grained, moderately-sorted sandstone, the 25 grain count histogram appears sufficiently dissimilar to the 50 grain count histogram to be invalid in representing grain size. The 100 grain count histogram is sufficiently similar to the 50 grain count histogram to indicate that 50 grain counts are valid in establishing an average grain size. Similarly, in the case of the fine grained sandstone, the 50 grain count histogram is close enough in similarity to the 25 grain count histogram to reveal that 25 grain counts are sufficient.

Grain shapes were assessed with the aid of a diagram (Powers, 1953), illustrating standard grain sphericities (Appendix VII).

FIGURE 6 : Grain size histograms used to establish the required number of grain counts to statistically represent the coarse grained sandstones.

COARSE GRAINED

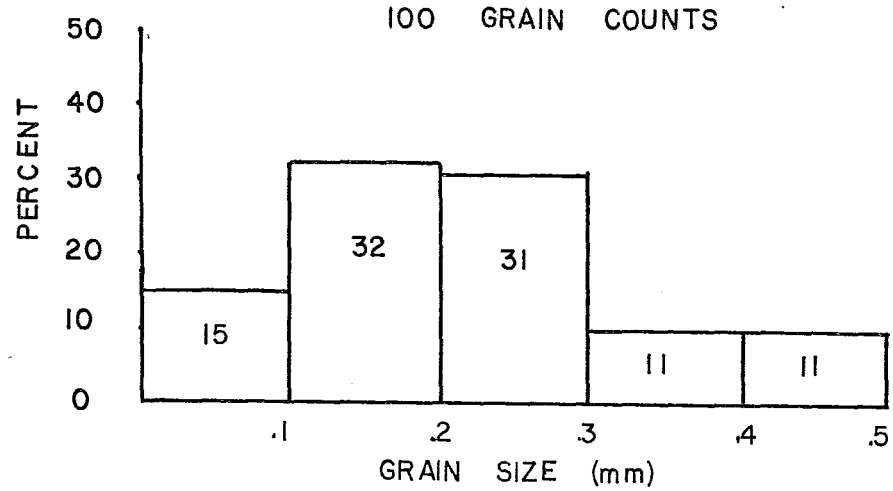

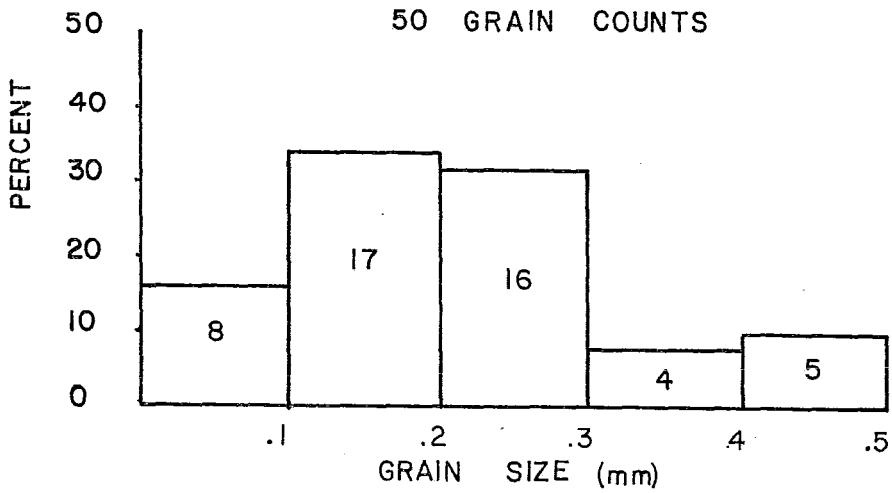

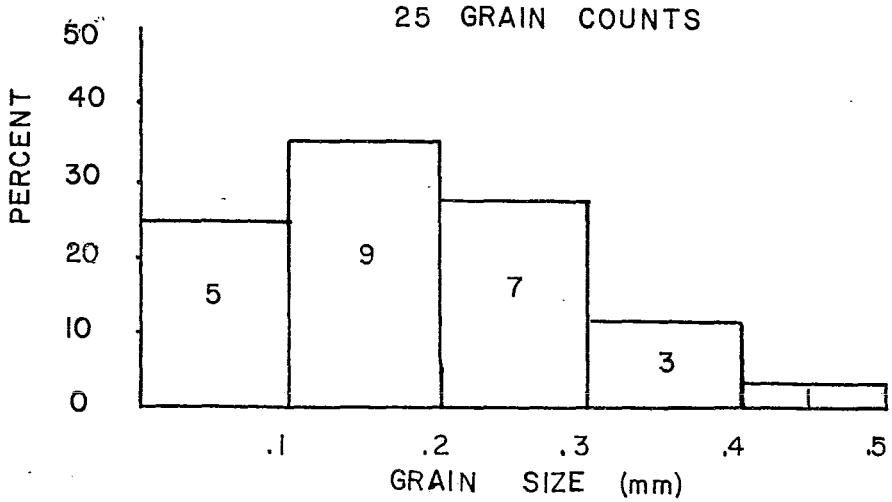

FIGURE 7 : Grain size histograms used to establish the required number of grain counts to statistically represent the finer-grained sandstones.

FINE GRAINED

50 GRAIN COUNTS

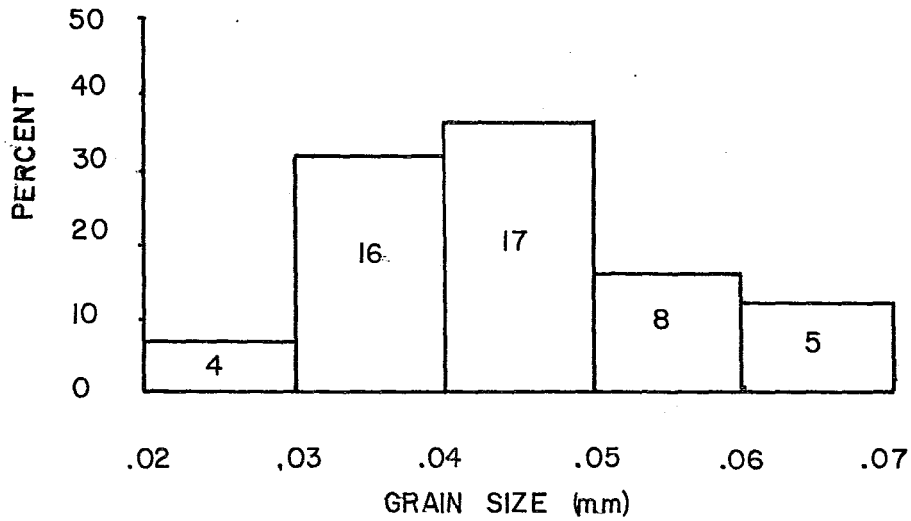

25 GRAIN COUNTS

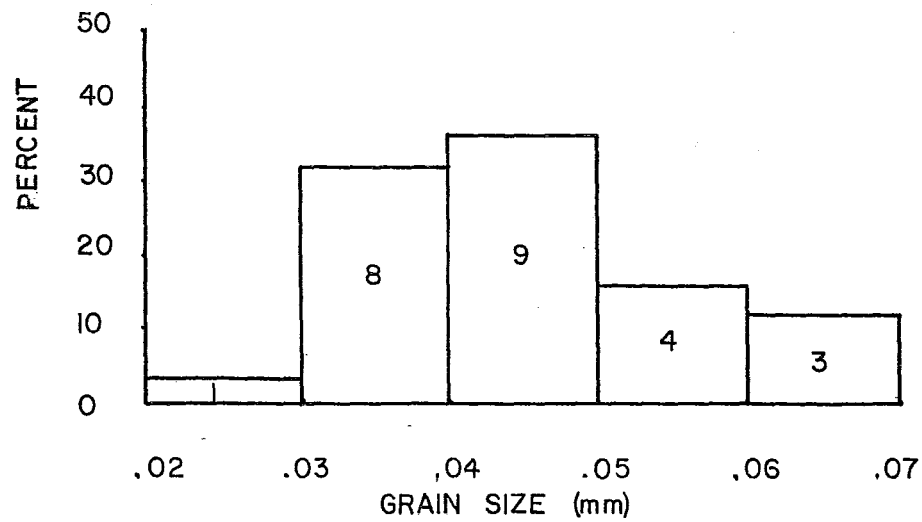

QUARTZ ANALYSIS

For each thin section containing quartz grains greater than .05 mm in size, an estimation was made as to the proportion of undulose to nonundulose quartz. The relative proportions of polycrystaline quartz containing greater than three grains, and those containing fewer than three grains, was also recorded. Those grains that exhibited strained extinction under crossed nicols, upon five degrees or less rotation of the microscope stage, were said to be undulose, and vice versa (Basu, 1974). Polycrystaline quartz were those grains of chert that showed sub-grains of quartz upon rotation of the stage. That is, the sub-grains were not in optical continuity with one another. Furthermore, those microcrystaline varieties of quartz that are more properly referred to as chert are discounted from the analysis. The point count technique was again utilized to quantify the varieties of quartz, but because of the subjective nature of the criterion for undulosity, repetition of any undulosity counts could only be made with an accuracy of 20 percent. Hence, in the table presenting the data, values in multiples of 20 represent the degree of error which may have been introduced into the analysis due to operator error, or the limitations inherent in not utilizing a universal stage (Appendix III).

PETROGRAPHY OF THE RICINUS SAND

Quartz (56%) and chert (19%) comprise most of the Ricinus thin sections. Porosity (9.5%) and rock fragments (9.5%) make up most of the remaining modal composition, with matrix (5%), feldspar (.5%) and muscovite (.5%) as minor constituents. Comparisons between different wells within the Ricinus field indicate that quartz and chert show greatest variation in modal abundances (Fig. 8). This is indicated by very irregular "sawtooth" profiles. In addition to this, it is evident that quartz abundances increase or decrease at the expense of chert and vice-versa. In contrast, the matrix and rock fragments show more regular profiles containing comparably straight segments.

The ternary diagram indicates that most of the Ricinus sandstone plot in the quartz-rich region of the diagram containing greater than 50% quartz (Fig. 9). Those points outside this region contain greater amounts of chert and are the contribution made by the conglomeratic fraction of the thin sections. In this sense, the mineralogic distribution of the Ricinus sand appears to be bimodal.

The grain size within the Ricinus sand has a bimodal distribution. Excluding the conglomerates, the Ricinus sand is very fine grained, with an average grain size of .2 mm and a standard deviation of .1. They are angular and extremely well sorted, as evident by their standard deviation (Plate 40C). The conglomeratic clasts

are generally between .5 and 8 mm in size, very poorly sorted and are round in shape (Plate 40A). They are supported by a population of smaller sized grains, mostly composed of quartz which are sub-rounded and moderately sorted. The grain size histogram illustrated the bimodal distribution best, with two populations - one concentrated below the .2 mm range of the diagram and the other at the coarse end of the diagram, greater than 1.0 mm (Fig. 10).

In all the fine grained sandstones, grain on grain contacts were evident, whereas in the conglomerates the grains were matrix supported by siderite (Plate 25A). Accessory minerals such as muscovite, tourmaline, pyrite, and garnets were infrequent. Feldspar was only identified when polysynthetic twinning was observed, and therefore of the plagioclase variety (Plate 15A). Staining for feldspar, as attempted by colleagues, was deemed to be unreliable and not effective in sandstones with low amounts of feldspar, at the time of this study.

The chert in the fine grained sandstones showed the characteristic pinhead extinction, under crossed nicols (Plate 19A). Only in this basis could it be distinguished from quartz, as it displayed the same size and shape, with very little alteration evident under ordinary light. The clays have a patchy distribution and are usually associated with porosity, as indicated by the blue stain (Plate 9B).

Clays are observable only as masses of fine grained sucrosic material containing anhedral "blebs" of black organic material. X-Ray diffraction was not done to indentify the clay minerals, but kaolinite and illite were identifiable by their textures.

By far, the major cement is silica, comprising approximately 10% of the modal composition of the fine grained sandstone, as discerned by cathode luminescence (Plate 4B). The cement varied in colour from black to chocolate brown and infilled all the fractured grains. In some cases, both colours of cement were present, indicating more than one generation of silica cement (Plate 2). The grains were observed to have mainly sutured contacts with the rare embayment of quartz grains (Plate 3B). Under ordinary light the cement "blanketed" the grains to give the thin section a "mosaic" texture. Calcite cement, however minor in abundance, was present in all the fine grained thin sections. It was found to be patchily distributed by its orange-red fluorescence, under cathode luminescence (Plate 4B). Calcite was observed to exploit fractures within chert grains (Plate 6).

In the case of the conglomeratic sandstone, siderite cement is dominant, with very minor amounts of silica cement. As much as 20% of the thin section was composed of the reddish brown cement, having a radially

fibrous habit, and exhibiting the characteristics iron cross extinction (Plate 13). In addition to this, siderite was observed as euhedral rhombs, both within the chert grains and the matrix (Plate 12). Although the siderite was observed to embay and alter all other minerals, chert was especially susceptible to invasion. To crystallographic nature of the chert was preserved in most cases, as evident by the pinhead extinction, but the colour and transluscency of the mineral was greatly changed, depending upon the degree of invasion. In this regard, a complete spectrum of chert composition was produced (Plates 35-39). Also, within the chert clasts of the conglomerates, were numerous varieties of inclusions, ranging from silicified, biogenic remains to quartz crystals and rock fragments. The biogenic material appeared to be crinoid stems, sponge spicules and bryozoans (Plates 28-34). Numerous fractures criss-cross the chert clasts, or run parallel as "railway tracks". In both cases, the fractures are infilled with quartz, some of which display a prismatic combstooth texture (Plate 25, 26).

Slight compaction was evident by the presence of curved muscovite (Plate 1), embayed quartz grains, micro styloliths (Plate 24B) and deformed shale clasts between grains. Straight muscovite was also observed (Plate 15B).

FIGURE 8: Mineral modal percent graphs for the Ricinus sand.

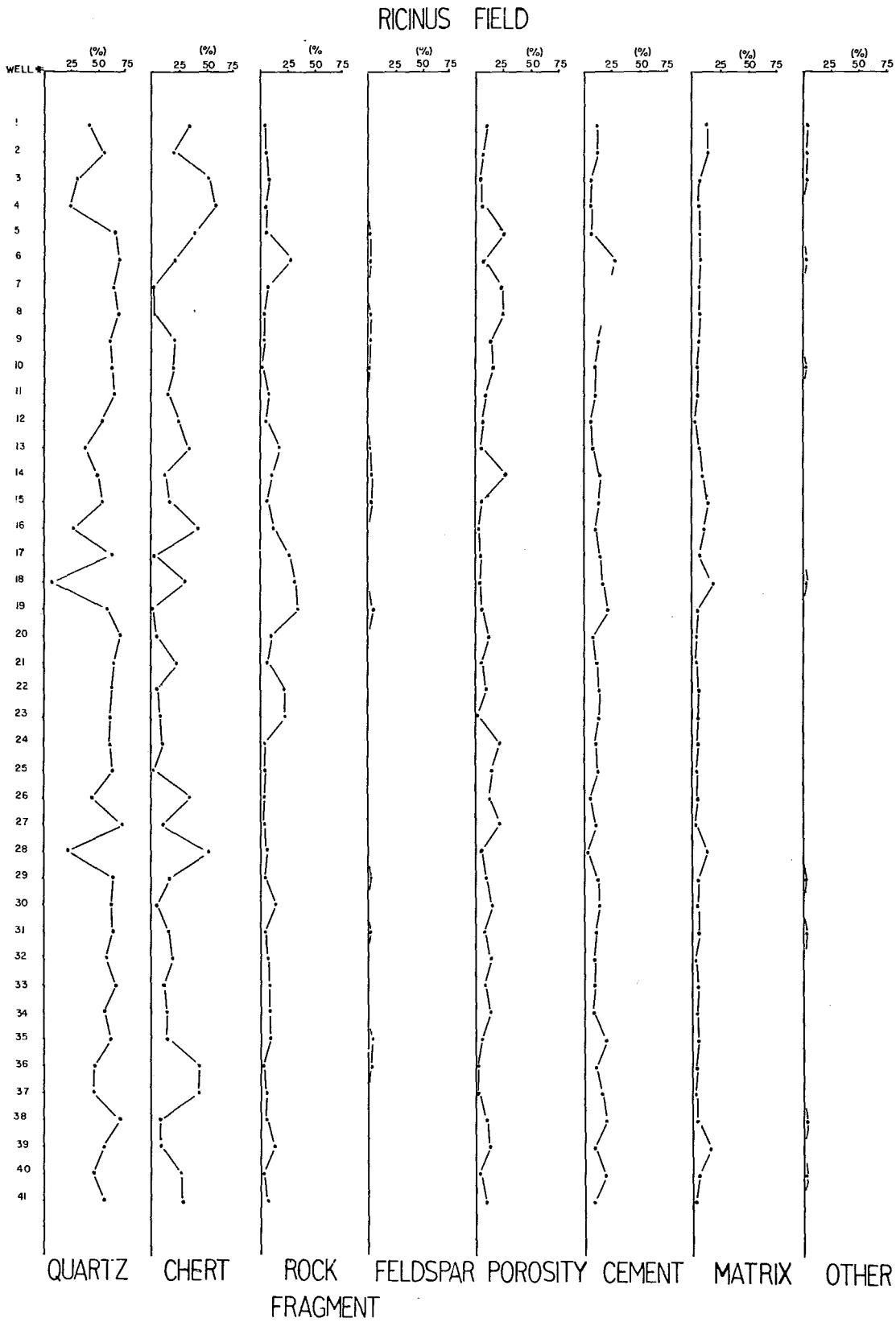
RICINUS FIELD
WELL #
(%)
25 50 75
1
2
3
4
5
6
7
8
9
10
11
12
13
14
15
16
17
18
19
20
21
22
23
24
25
26
27
28
29
30
31
32
33
34
35
36
37
38
39
40
41
QUARTZ
CHERT
ROCK FRAGMENT
FELDSPAR
POROSITY
CEMENT
MATRIX
OTHER

FIGURE 9 : Ternary diagram for the Ricinus sand.

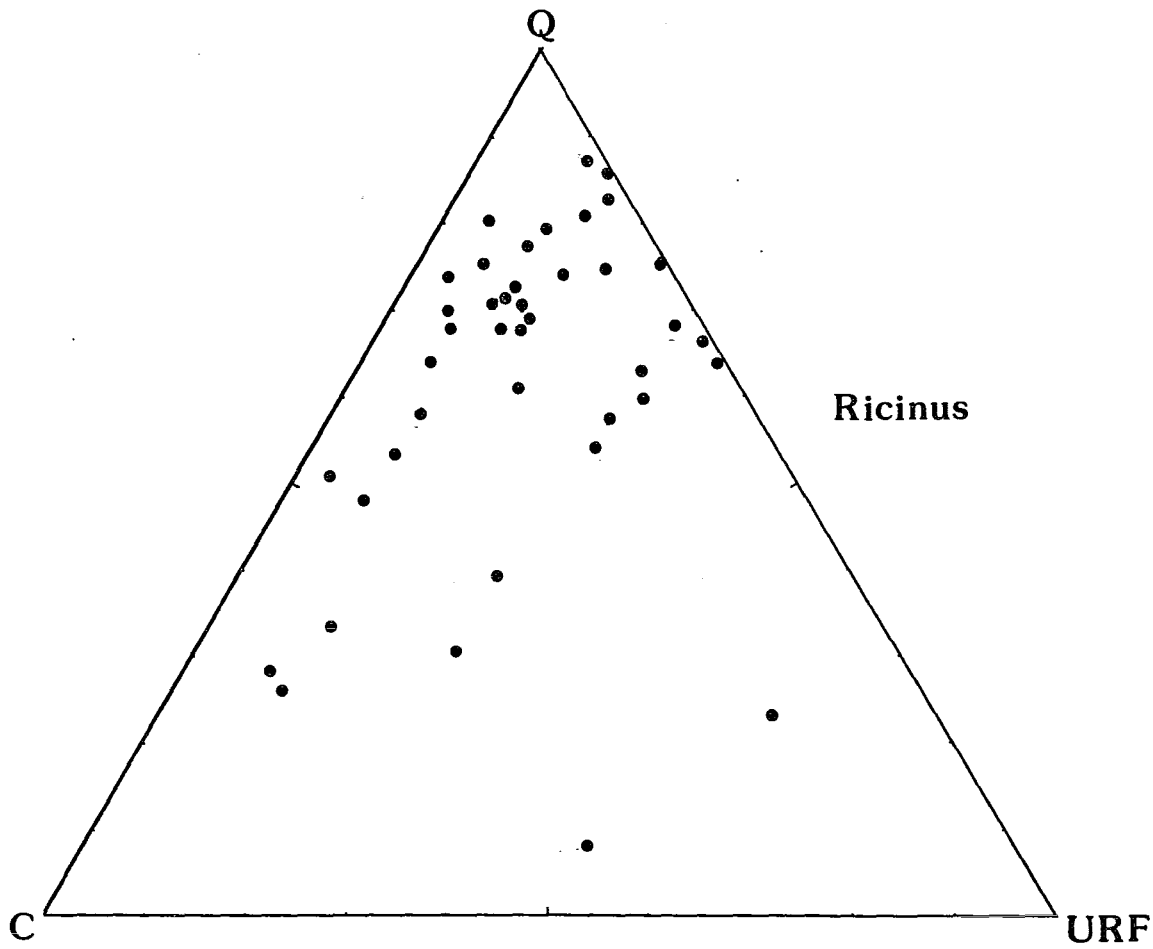
Q
Ricinus
C
URF

FIGURE 10 : Grain size histogram for the Ricinus sand.

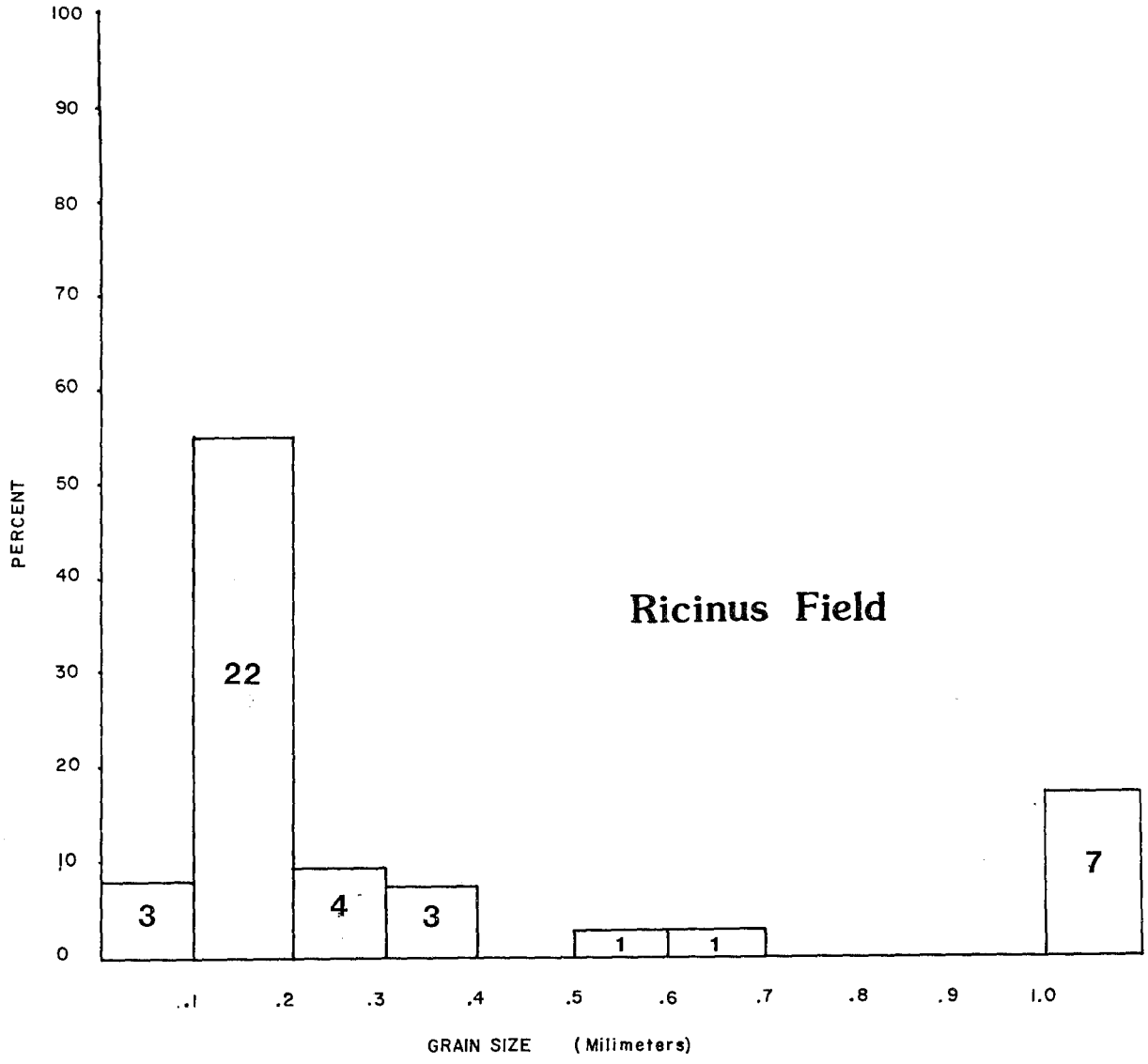
Ricinus Field
PERCENT
100
90
80
70
60
50
40
30
20
10
0
3
22
4
3
1
1
7
.1
.2
.3
.4
.5
.6
.7
.8
.9
1.0
GRAIN SIZE (Milimeters)

PETROGRAPHY OF THE LOWER CAROLINE SAND

The modal percent of quartz (31%) is significantly less relative to the Ricinus sand. The abundance of chert (35%), however, has nearly doubled, with an additional increase observed in matrix (15.25%). Rock fragments (7.5%) and porosity (6%), comprise the remainder of the modal composition, with only trace amounts of feldspar (.25%). Comparison of different wells within the Lower Caroline sand indicates that quartz and matrix show the greatest variation in modal abundances, as shown by their irregular profiles (Fig. 11). In contrast with the Ricinus sand, a mirror image relationship exists between the quartz and matrix profiles, instead of the quartz and chert. The chert, rock fragments and porosity reflect consistent modal abundances between the wells, as evident by their more linear profiles.

Feldspar abundances were consistent when present, but accessory minerals, such as muscovite and pyrite were absent.

The ternary diagram illustrates a bimodal distribution of sandstone mineralogy (Fig. 12). The largest population is located within the chert rich region, and the second population within chert poor, rock fragment poor region of the triangle. With the exception of two anomalous thin sections, the two population

show relatively little scatter.

The grains within the Lower Caroline sandstone have a bimodal distribution. The finer grained population dominates the sandstone and is moderately well sorted, with an average grain size of approximately .4mm and a standard deviation of .15. The grains vary from sub-nagular to sub-round in shape and have grain on grain contacts. The conglomeratic sandstone tend to be matrix supported with clasts ranging from .5 mm to 10 mm in size, are poorly sorted, and very rounded (Plate 40A). The clasts are primarily composed of chert, with minor amounts of siderite, quartz and rock fragments. The matrix is composed of siderite and small grains of quartz. The grain size histogram illustrates a very distinct bimodal distribution, with the larger population between .2 mm and .5 mm (Fig. 13). The conglomeratic fraction of the thin section is represented at the coarse end of the diagram as greater than 1 mm in size.

Accessory minerals were absent, as was feldspar in the majority of the thin sections. The chert in both the fine grained and the coarse grained sandstone showed a diversity in textures, as controlled by siderite invasion (Plate 38). In the finer grained sandstone, the chert appears larger and rounder than the neighbouring grains of quartz and rock fragments. The chert, in many

instances, is altering to chalcedony (Plate 12A), and appears to embay quartz grains. Both quartz and chert grains are embayed by siderites (Plate 13B). The quartz grains tend to be subangular in shape, as a result of silica cement which fills in between chert grains. Fluid, as well as rutile inclusions, are frequent (Plate 23B). Dust rings, indicative of the original grain boundaries, predominate within the Lower Caroline sand (Plate 22). The quartz grains often display pastel yellow and pinkish brown tints, diagnostic of impurities within the crystal. Grains of metamorphic quartz are also abundant (Plate 20A).

Clay minerals were virtually absent within the Lower Caroline sand, except as trace amounts lining pore space. Siderite cement (16.25%) was the major cementing agent, with minor amounts of calcite (1%), and silica cement (4%). The silica cement was only observed within the finer grained sandstones as quartz overgrowths. The calcite cement was observed only in a few of the finer grained thin sections as a very pristine poikiolitic cement, with a high birefringence (Plate 7). It appeared to have gradational contacts with the siderite cement and was relatively unreactive with all minerals except siderite and feldspar. Calcite was replacing siderite, as evident by the prismatic linings of siderite between calcite and chert clasts (Plate 5A). Siderite appeared

to manifest itself by its radially fibrous habit (Plate 13), as well as rhombohedrons (Plate 11). In some cases, the siderite rhombs were dissolved by pore fluids, leaving fluid filled euhedral inclusions within the chert (Plate 13A).

In the case of the conglomeratic thin sections, silica cement was all but absent, and the calcite cement was observed to be actively altering the siderite cement. This is evident, as calcite is observed to completely surround and embay the siderite cement (Plate 5). The dominance of these carbonate cements in coarse grained to conglomeratic sandstones, would suggest that a greater effective permiability is condusive to carbonate cements. Siderite also appears to be pseudomorphed by the calcite cement, especially at grain boundaries (Plate 8B).

In one thin section, wilkeite, a rare calcium silico-phosphate was observed to fill pore spaces between large chert clasts and quartz grains. Wilkeite displays a high birefringence under crossed nicols, but otherwise, appears not unlike quartz.

The chert clasts again exhibit a great diversity of texture because of siderite invasion and mineral inclusions. The biogenic material tends to be particularly prolific in the Lower Caroline sands, with moderate preservation of the fossil assemblages (Plates 28 to 34).

In addition to the crinoids, bryozoans and sponge spicules observed in the Ricinus conglomerate, foraminifera and brachiopod shell fragments can be observed in the Lower Caroline Sand. Secondary porosity is observed as dissolved siderite crystals (Plate 31A), and as enlarged fractures (Plate 27).

FIGURE 11 : Mineral modal percent graphs for the Caroline sands.

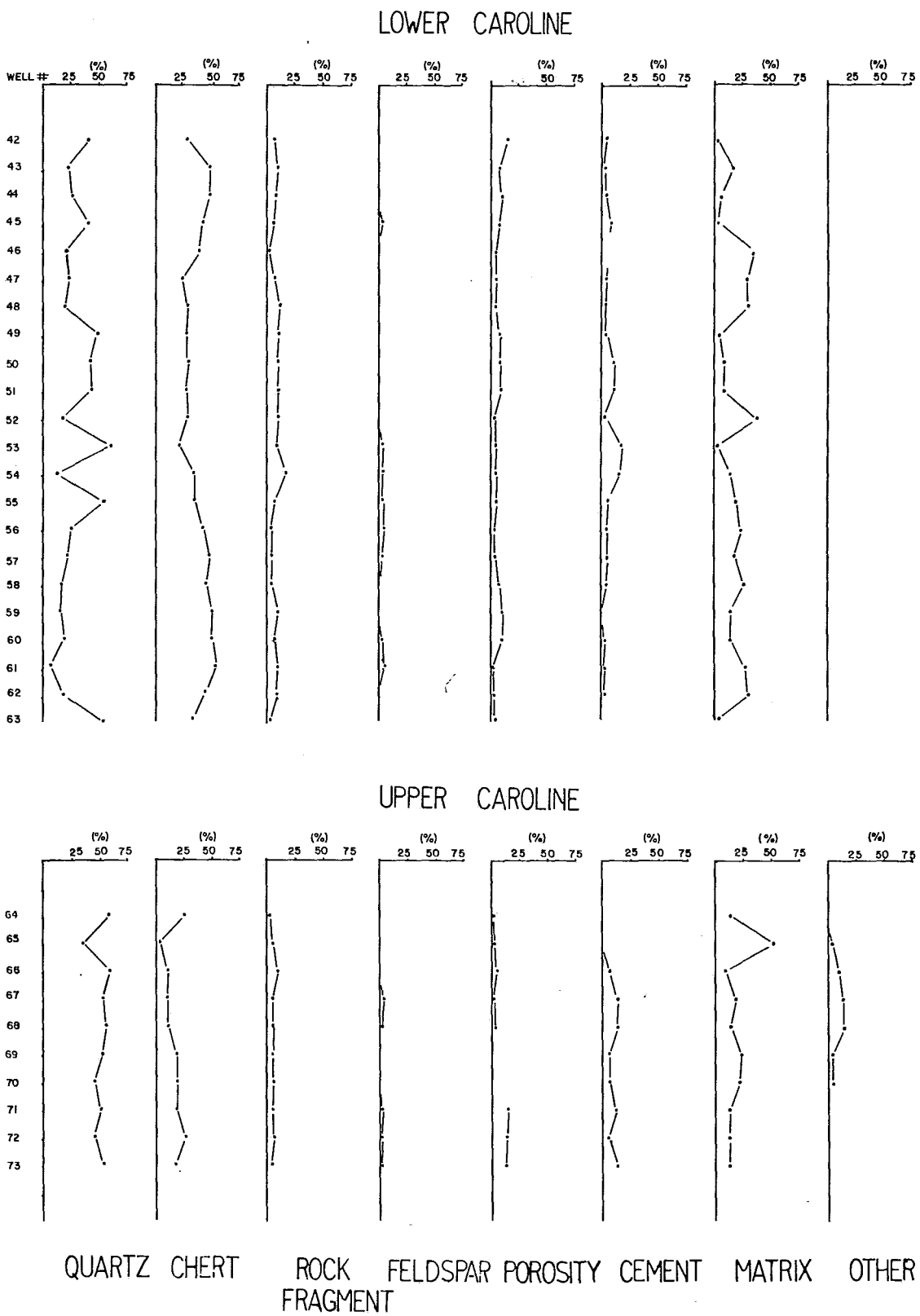
LOWER CAROLINE
WELL #
(%)
25 50 75
42
43
44
45
46
47
48
49
50
51
52
53
54
55
56
57
58
59
60
61
62
63
UPPER CAROLINE
64
65
66
67
68
69
70
71
72
73
QUARTZ
CHERT
ROCK FRAGMENT
FELDSPAR
POROSITY
CEMENT
MATRIX
OTHER

FIGURE 12 : Ternary diagram for the Lower Caroline sand.

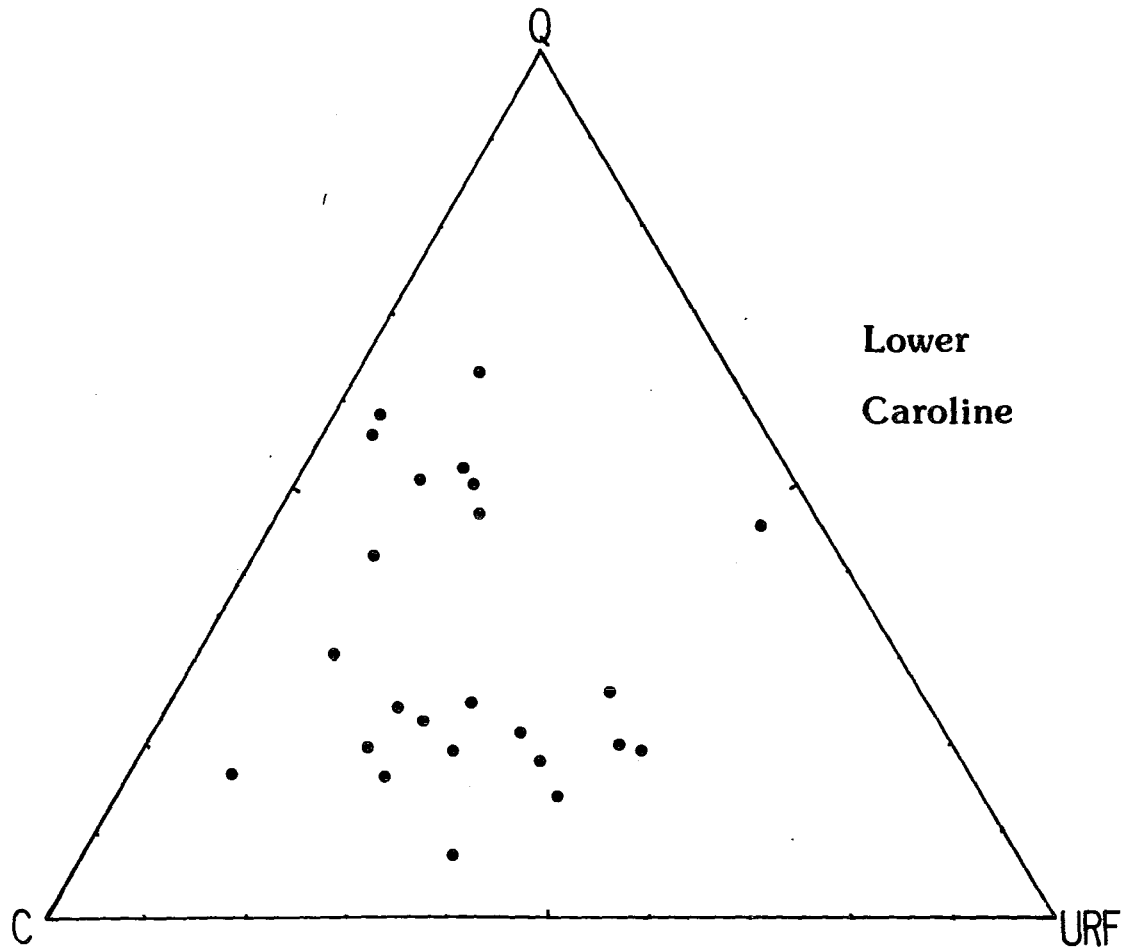
Q
C
URF
Lower
Caroline

FIGURE 13 : Grain size histogram for the Lower Garrington sand.

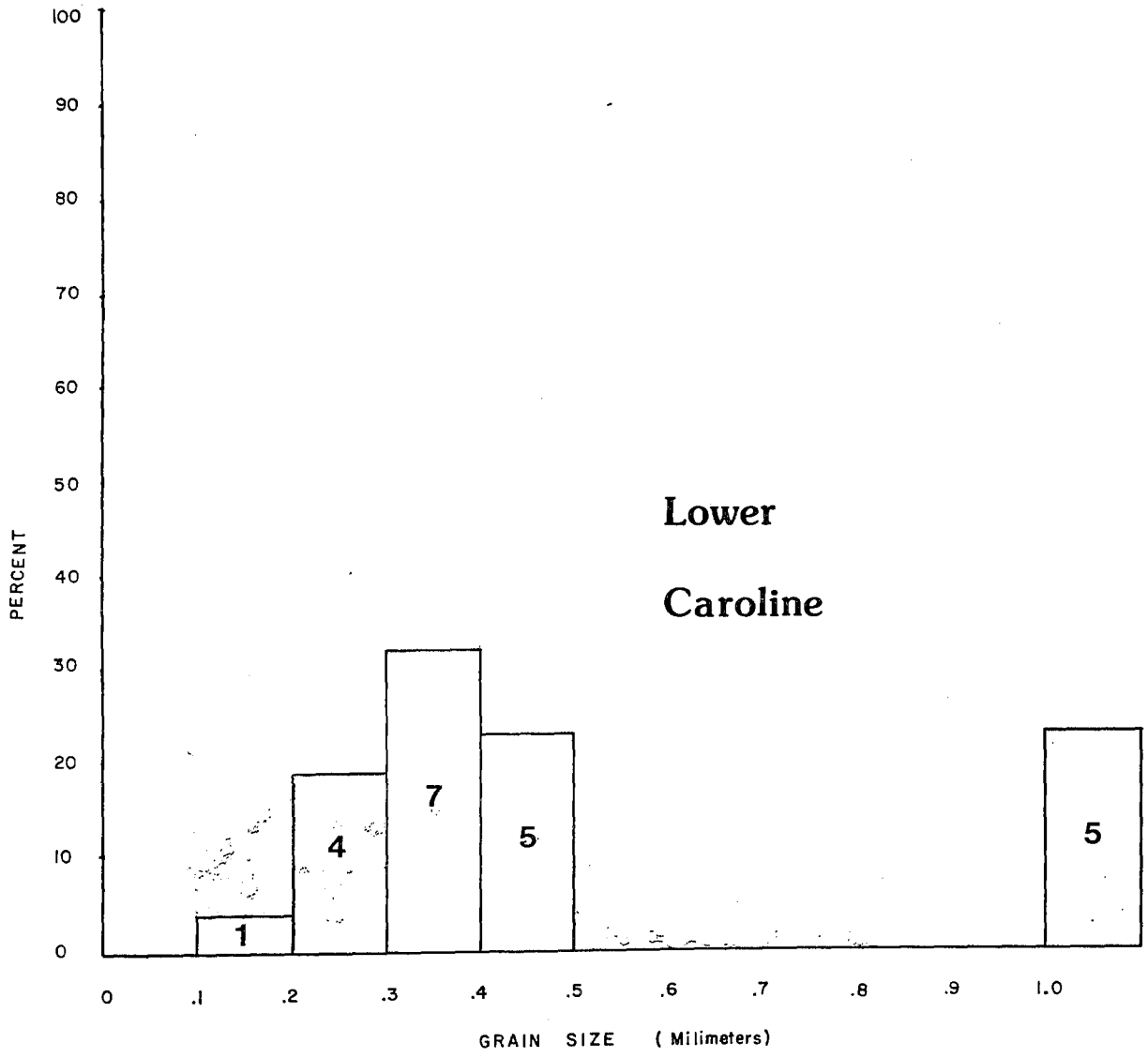
100
90
80
70
60
50
40
30
20
10
0
PERCENT
Lower
Caroline
1
4
7
5
5
0
.1
.2
.3
.4
.5
.6
.7
.8
.9
1.0
GRAIN SIZE (Milimeters)

PETROGRAPHY OF THE UPPER CAROLINE SAND

Quartz (52%), chert (15.5%) and matrix (18.5%) comprise the greatest proportion of the Upper Caroline thin sections. Rock fragments (4%), accessory minerals (4%), and porosity (5.5%), make up the remaining modal composition. Comparisons between the wells within the sandstone reveal again that quartz and matrix show the greatest variance in abundance, and that, in fact, the profiles are mirror images of each other (Fig. 11). Rock fragments, chert and accessory minerals show more regular profiles.

The ternary diagram illustrates a single population (disregarding one point), with little scatter at the chert poor - quartz rich region of the triangle (Fig. 14). This sandstone appears to be enriched with respect to unstable rock fragments, relative to previous sands.

Discounting one coarse grained, thin section, the Upper Caroline sand has a unimodal grain size distribution. The average grain size is .15 mm and the grains tend to be extremely well sorted. The grain size histogram depicts a very well sorted sand body, with the majority of sand grains located at the fine end of the diagram, less than .2 mm (Fig. 15). The grains are angular to subangular in shape and show grain on grain contacts. Within the thin sections fine laminations are evident with the naked eye.

The accessory minerals are pyrite and organic rich shale fragments (Plate 13). The shale fragments appear to be associated with well established sub-parallel fracture systems, and hence the fine, laminated appearance of the thin section. The pyrite was detected by reflecting microscope, and shows a well defined euhedral crystal habit (Plate 23). The crystals appear to coalesce into masses which tend to line pore spaces (Plate 23A) and grain boundaries (Plate 23B). In this sense, they may be considered a cementing agent. The chert is identical to quartz in all respects, except under crossed nicols, where it exhibits the characteristic pinhead extinction. Siderite invasion of chert is not well established in these sandstones. Fine grained tan and grey coloured clays are evident, especially near the altering rock fragments, and probably comprise a significant but undetermined amount of the matrix. The clays have a patchy distribution and are undistinguishable from the anhedral organic "blebs" that exhibit isotropic properties (Plate 13B).

Siderite (17%) comprises the majority of the matrix and equals silica (9.5%) in its capacity as a cementing agent. Calcite appears only as trace amounts, with the exception of two thin sections where it excludes all other cements. In these thin sections the grains are supported by the calcite cement and are not in contact

with each other. The calcite exhibits a regular pristine texture, with distinct growth lamallae (Plate 8A). Under luminescence, it is observed to surround grains of chert and quartz devoid of silica overgrowths, suggesting it formed prior to silica cementation. This is in keeping with the fact that in most thin sections, calcite is observed as altered patches surrounded by silica cements (Plate 4).

By virtue of the fine grained nature of the thin sections, pressure solution effects were difficult to observe, but extremely deformed muscovite and extensive fracture systems would suggest evidence of compaction.

FIGURE 14 : Ternary diagram for the Upper Caroline sand.

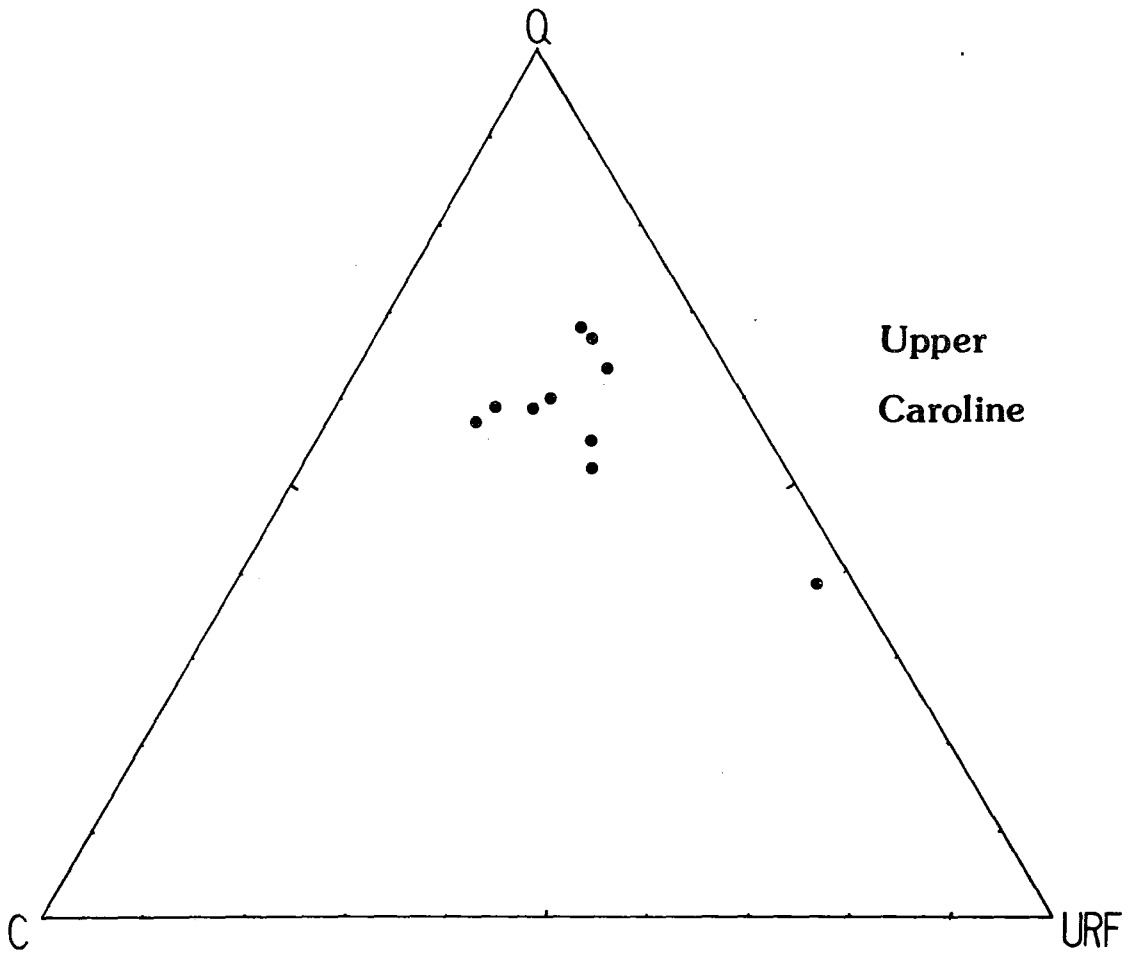
Q
C
URF
Upper
Caroline

FIGURE 15 : Grain size histogram for the Upper Caroline sand.

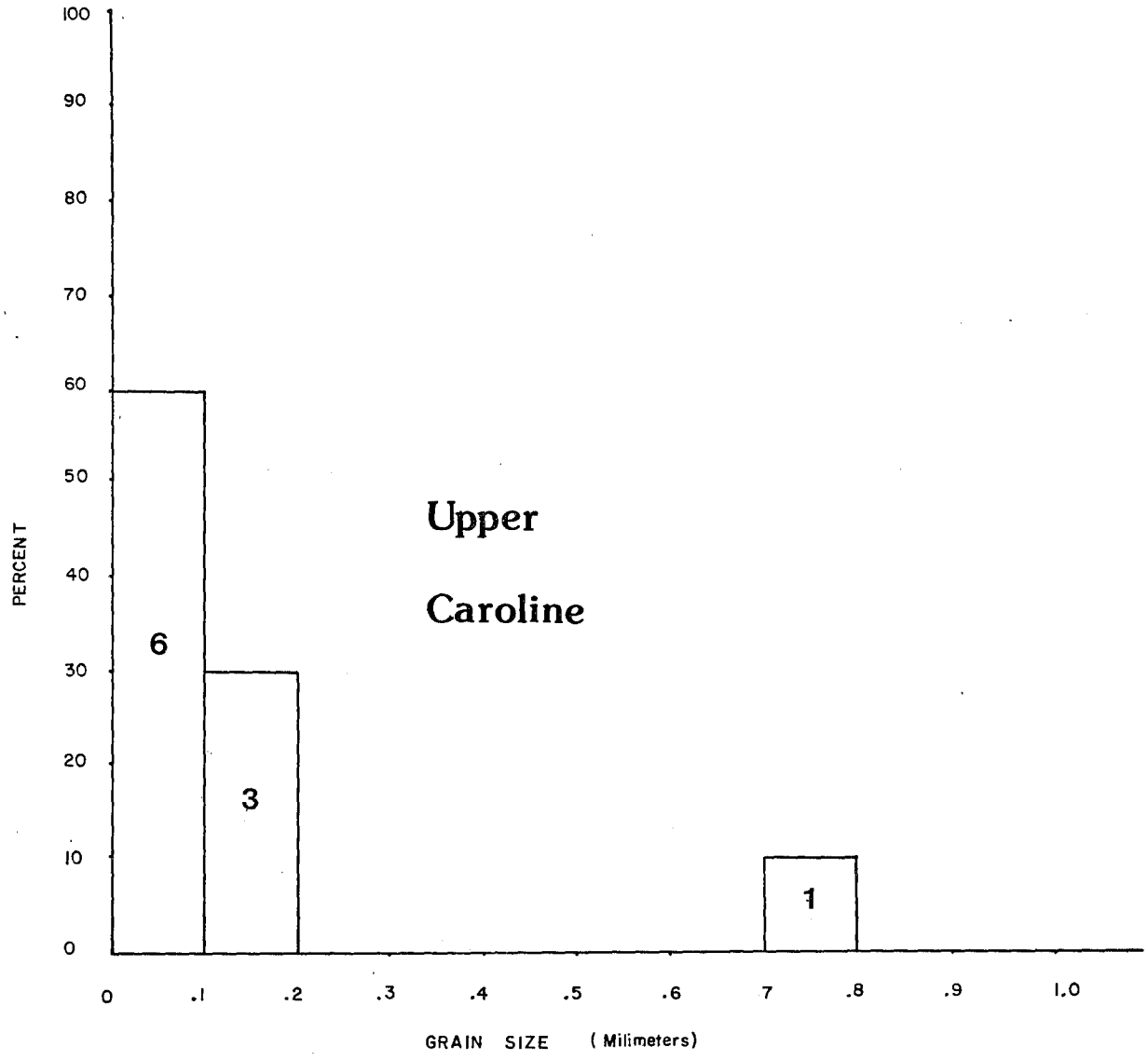
100
90
80
70
60
50
40
30
20
10
0
PERCENT
Upper
Caroline
6
3
1
0
.1
.2
.3
.4
.5
.6
7
.8
.9
1.0
GRAIN SIZE (Milimeters)

PETROGRAPHY OF THE GARRINGTON SANDS

There is an unfortunate lack of data for both the Upper and the Lower Garrington sands. For this reason it is difficult to draw any conclusions, generalizations, or graphically represent the data with any statistical validity. Nevertheless, there are distinct differences between the two sands in the Garrington field, which make themselves apparent.

The Lower Garrington Sand

The Lower Garrington sand is predominantly composed of chert (59.5%), quartz (13%), and matrix (12%). Rock fragments (3.5%) and feldspar (.25%) comprise only a minor amount, whereas porosity (11%) contributes the remaining modal percent. Analysis between the three wells in this sand reveal only that accessory minerals are absent (Fig. 16).

The ternary diagram indicates that the Lower Garrington sand is poor in unstable rock fragments, but abundant in chert (Fig. 17). The grain size histogram reflects the fact that all the thin sections in the Lower Garrington sand are conglomeratic (Fig. 18). The clasts range from .5 mm to 12 mm and are very round in shape, with poor sorting. Generally, the grains are matrix supported, with grain on grain contacts occurring only near portions of the thin sections having abundant porosity.

Siderite comprises the matrix, having a variety of textures. Siderite spherules are the most striking of these textures found next to grain boundaries, and within pore spaces (Plate 9). Siderite also occurs as fibrous aggregates,rhombohedral grains (Plate 12), and as prismatic crystals growing normal to grain boundaries. The latter texture is in some cases being pseudomorphed by calcite (Plate 8B). An extremely small amount of silica cement (1%) was observed in one section.

Clays are absent, as are accessary minerals. Chert clasts show numerous quartz filled fractures, some exhibiting combstooth texture (Plates 25, 26). Grains of metamorphic quartz are also abundant (Plate 20A). Biogenic material, quartz and rock fragments also occur in the chert as inclusions, but, to a lesser degree, relative to the conglomerates of the Ricinus and Garrington fields. Invasion by siderite is also less evident in this sand. Post depositional compaction is evident by the mutual embayment of chert and quartz grains.

FIGURE 16 : Mineral modal percent graphs for the Garrington sands.

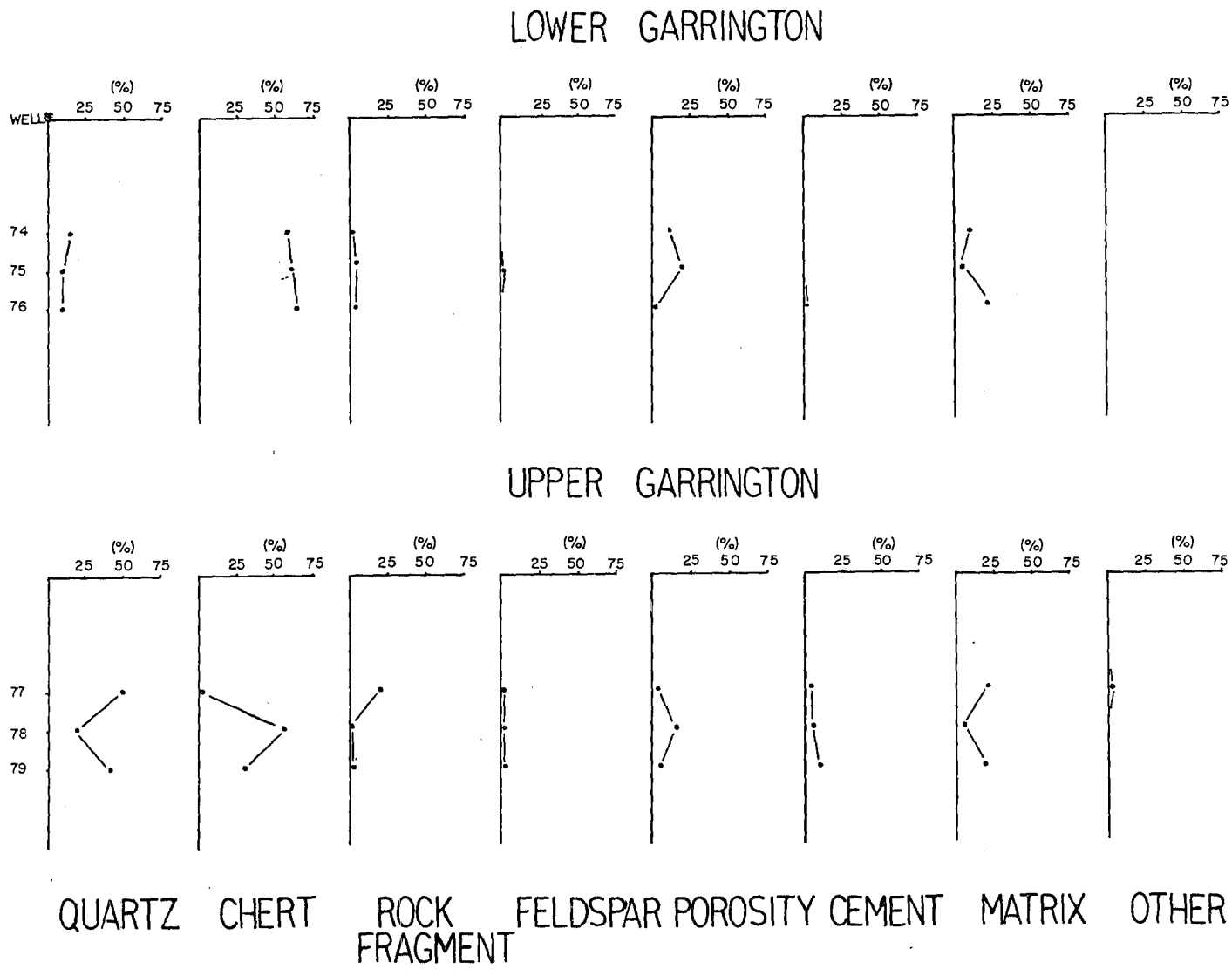
LOWER GARRINGTON
(%)
25 50 75
WELL#
74
75
76
UPPER GARRINGTON
77
78
79
QUARTZ
CHERT
ROCK FRAGMENT
FELDSPAR
POROSITY
CEMENT
MATRIX
OTHER

FIGURE 17 : Ternary diagram for the Garrington sands.

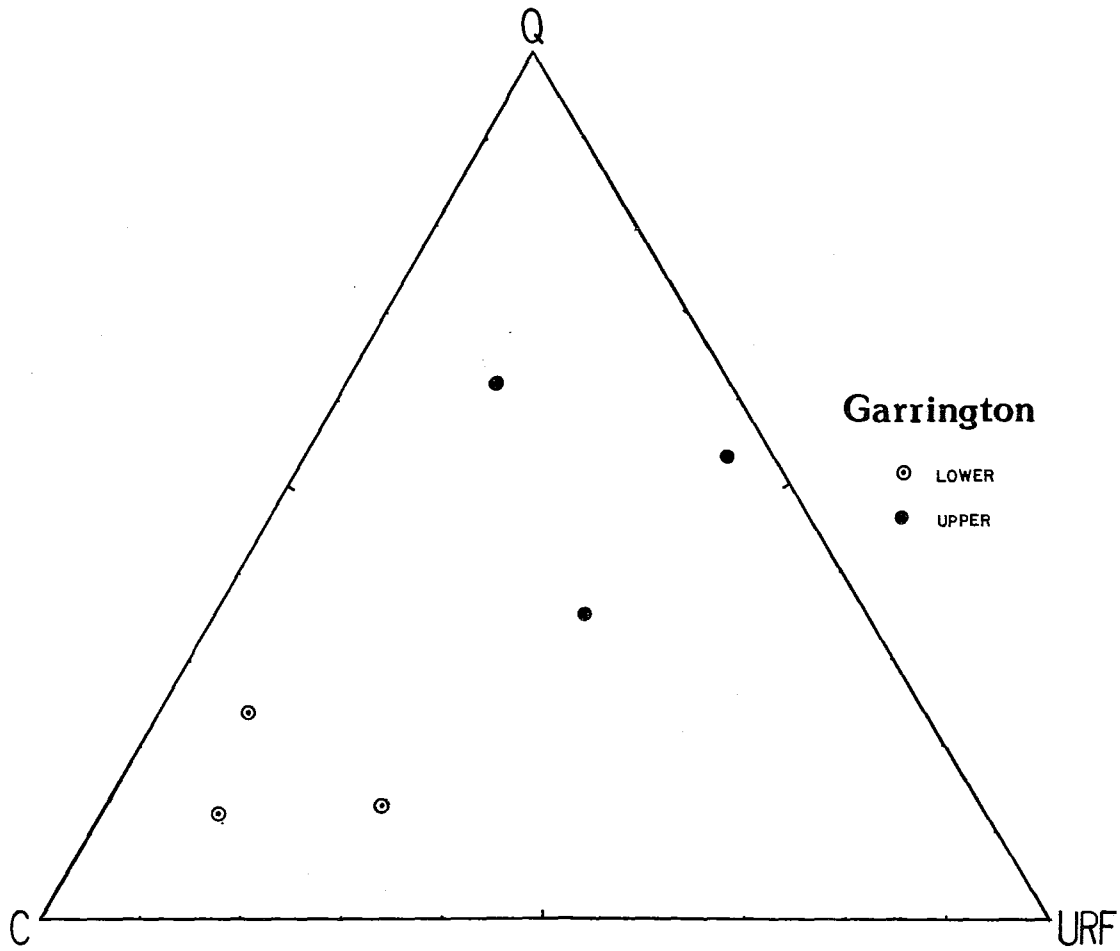
Q
C
URF
Garrington
LOWER
UPPER

FIGURE 18 : Grain size histogram for the Garrington sands.

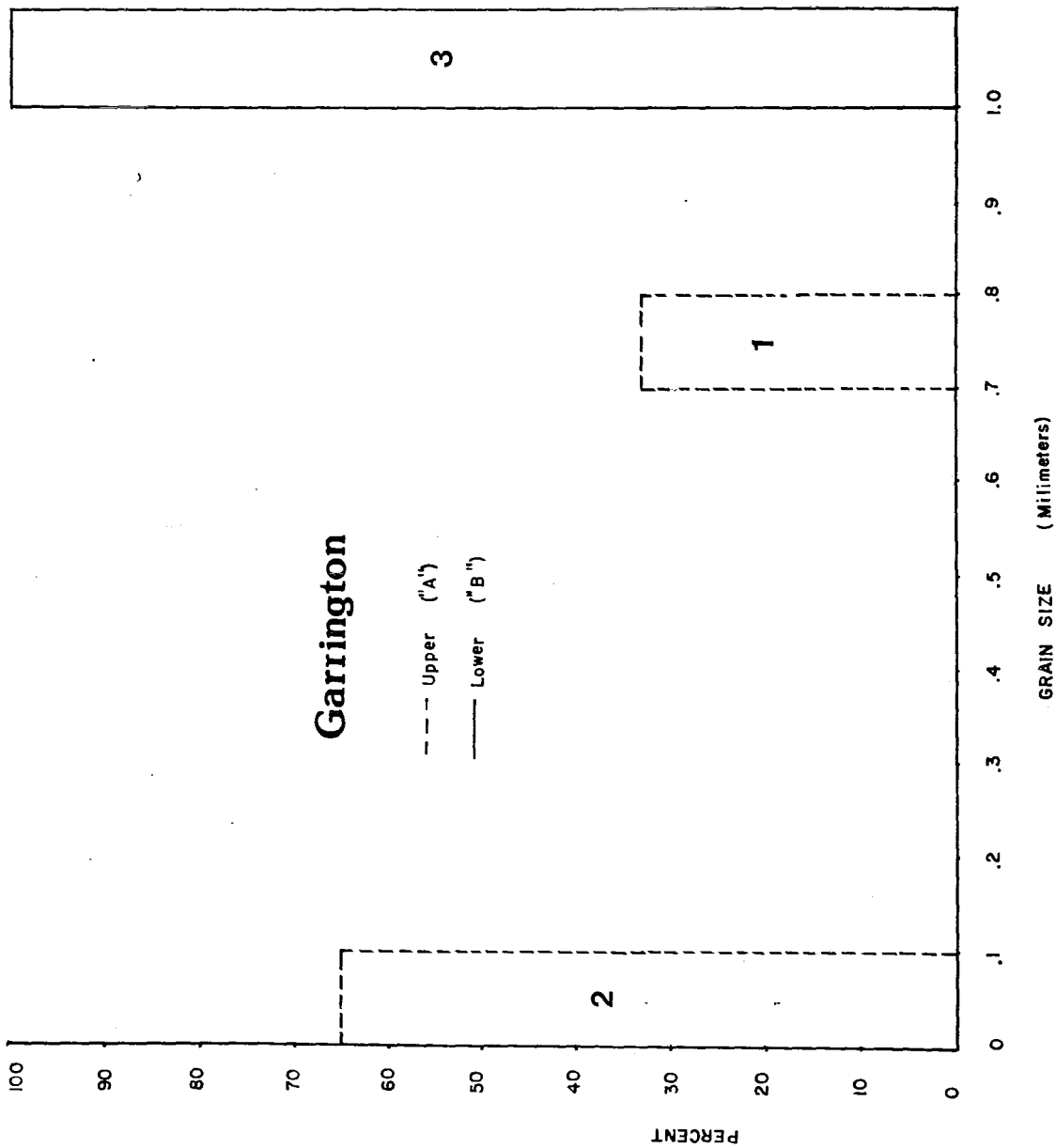
Garrington
Upper ("A")
Lower ("B")
1
2
3
PERCENT
100
90
80
70
60
50
40
30
20
10
0
0
.1
.2
.3
.4
.5
.6
.7
.8
.9
1.0
GRAIN SIZE (Milimeters)

Upper Garrington Sand

The Upper Garrington sand is mainly composed of quartz (38%), chert (31%) and matrix (15%). Porosity (7.75%) and rock fragments (7.25%) comprise the remaining modal precent, with minor feldspar (.5%) and accessory minerals (.5%). A comparison between the three wells in this sand indicates a mirror image relationship between the chert and quartz profiles, as well as a consistent feldspar abundance (Fig. 16).

The ternary diagram illustrates a sandstone poor in chert but richer in quartz, with a slightly larger scatter in the Lower Garrington sand (Fig. 17).

The grain size histogram shows two populations, one very fine grained and the other coarse grained (Fig. 18). Taking into consideration the lack of the data base, it would be expedient to consider this a bimodal distribution, therefore the coarser population will be considered anomalous. The average grain size of the finer population is about .05 mm, with a subangular shape and extremely good sorting. The grain contacts appear to be dominantly of the grain on grain type, with the matrix having a patchy distribution.

The extremely fine grained nature of the Upper Garrington sands permits description of only the largest grains and structures. For this reason, no positive state-

ment can be made as to the presence of absence of clays and accessary minerals. Organic rich shale fragments were evident by virtue of their isotropic nature. Cathode luminescence revealed that silica cement (6.5%), as well as siderite cement (15%), are the principle cementing agents. The cherts appeared to be significantly altered by siderite, but were otherwise indistinguishable from quartz under ordinary light. Compaction and pressure solution effects could not be observed because of the fine grained nature of the sandstone.

CAROLINE AND GARRINGTON FIELDS

From the ternary diagram (Fig. 19), and grain size histogram (Fig. 20), constructed for the Caroline and Garrington sandstones collectively, it is apparent that a bimodal relationship exists in both illustrations. Two populations of grain size, one fine grained and the other coarse grained, are evident in the grain size histogram. Similarly, two populations exist, with respect to mineralogy in the ternary diagram, one being chert rich and the other chert poor. In fact, the two diagrams are related in that the coarser grained sandstones plot within the chert rich population of the ternary diagram, and the fine grained sandstones correspond to the chert poor population. Furthermore, the two populations correspond to the Lower and Upper sands respectively of the Caroline and Garrington fields.

FIGURE 19 : Ternary diagram for the combined Caroline and Garrington sands.

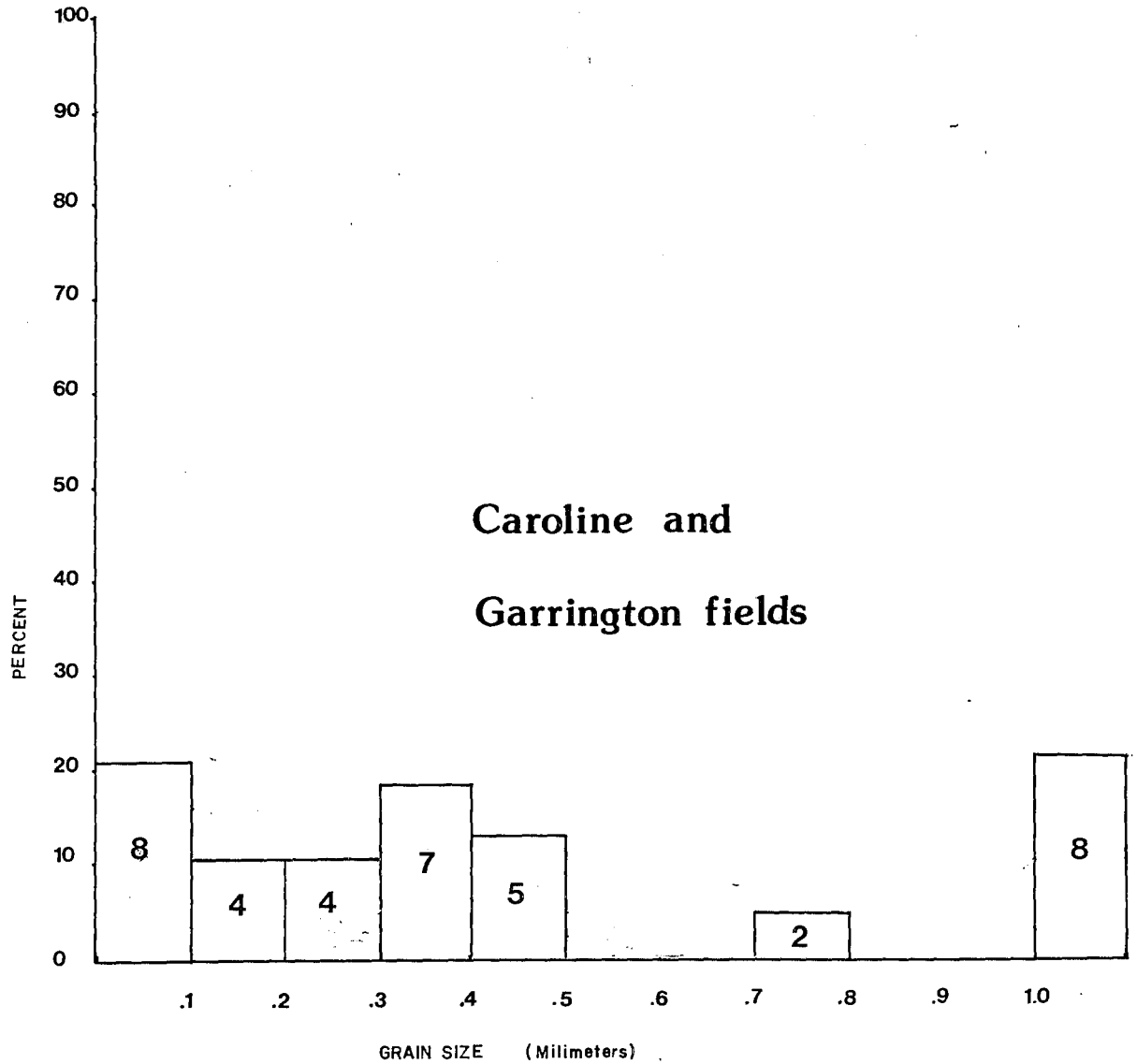
Caroline and
Garrington fields
PERCENT
100
90
80
70
60
50
40
30
20
10
0
8
4
4
7
5
2
8
.1
.2
.3
.4
.5
.6
.7
.8
.9
1.0
GRAIN SIZE (Milimeters)

FIGURE 20 : Grain size histogram for the combined Caroline and Garrington sands.

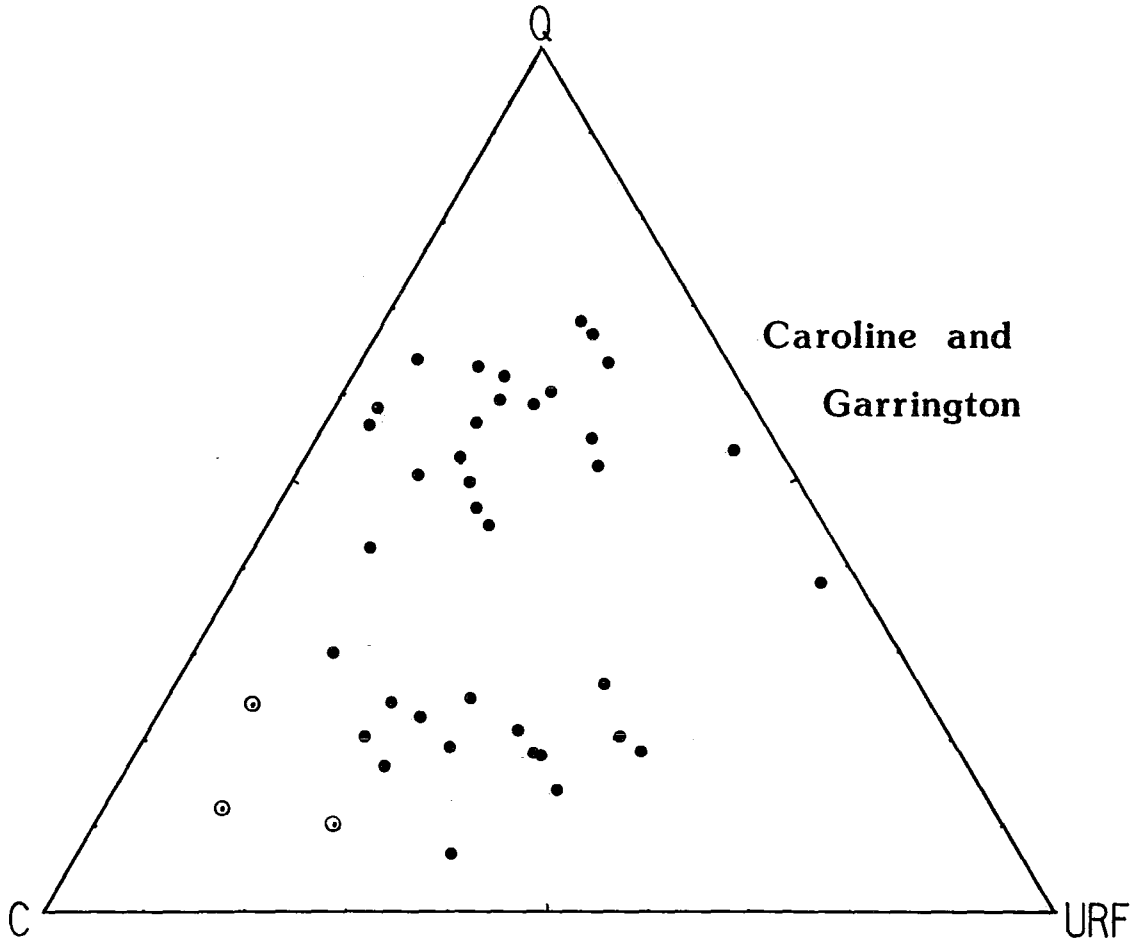
Q
Caroline and
Garrington
C
URF

QUARTZ ANALYSIS

A comparison in quartz grains has been made between the Ricinus field and the combined Caroline-Garrington fields. This was necessary as there is not sufficient data to represent the Garrington field with any statistical validity.

The data is presented on a diamond-shaped graph which has been constructed to aid in provenance determination (Basu, 1974). On the horizontal axis, the percent of non-undulose, versus undulose, quartz grains is determined (Fig. 21). Then all the remaining quartz grains having a polycrystaline nature are represented on one of the other axes, depending upon whether 75% of the polycrystaline grains are the "less than" or "greater than" three grain type. In this sense, these two categories are mutually exclusive.

The Ricinus sandstone contains quartz grains which are approximately 8% polycrystaline. Of the 92% monocrystaline quartz grains, approximately 83% are of the undulose variety. The combined Caroline and Garrington sandstones, on the other hand, show that 18% of the quartz grains are polycrystaline, and that only 61% of the monocrystaline quartz grains are of the undulose variety.

The further towards the upper left hand region of the diagram a sandstone is plotted, the higher degree

of metamorphism the grains are thought to have experienced (Blatt et al, 1980). In this respect, the Caroline and Garrington sandstones have been significantly more metamorphosed than the Ricinus sandstone in this analysis.

In addition to this, one can achieve a more general provenance determination, in terms of the tectonic regime of a sandstone. The illustration designed for this purpose is in the form of a ternary diagram, with Quartz-Chert, Feldspar, and unstable rock fragments as the end members (Dickinson, 1978). In this illustration, all of the Ricinus, Caroline and Garrington sands plot within the Recycled Orogen Provenance region of the diagram (Fig. 22). This is by virtue of the fact that they contain very little feldspar, but abundant quartz and chert components.

FIGURE 21 : Diagram determining the differences in metamorphic provenance for the Ricinus sand, and the combined Caroline-Garrington sands (Basu, 1974).

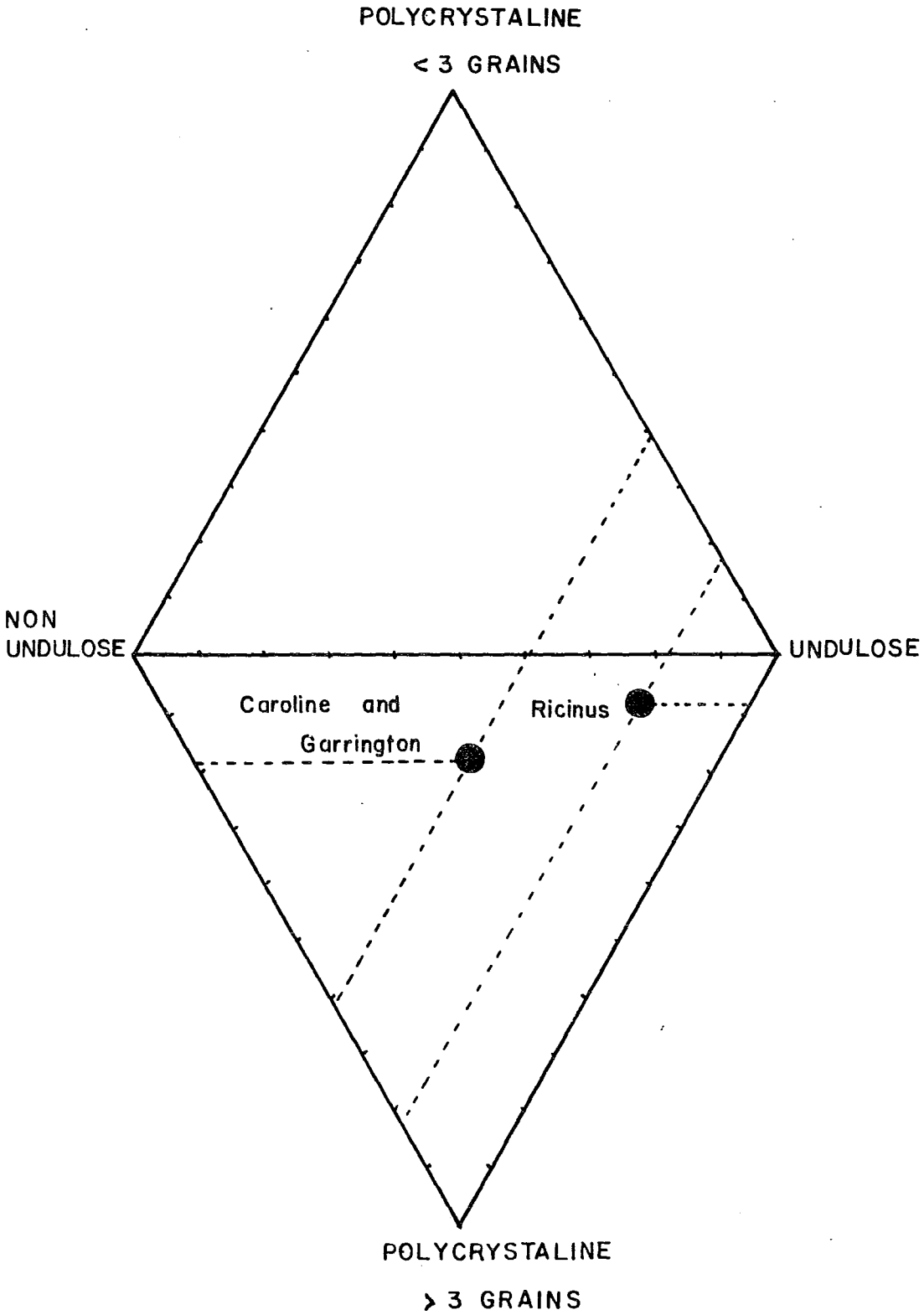
POLYCRYSTALINE
< 3 GRAINS
NON
UNDULOSE
UNDULOSE
Caroline and
Garrington
Ricinus
POLYCRYSTALINE
> 3 GRAINS

FIGURE 22 : Ternary diagram determining the tectonic provenance of the Ricinus, Caroline and Garrington sandstones (Dickinson, 1978).

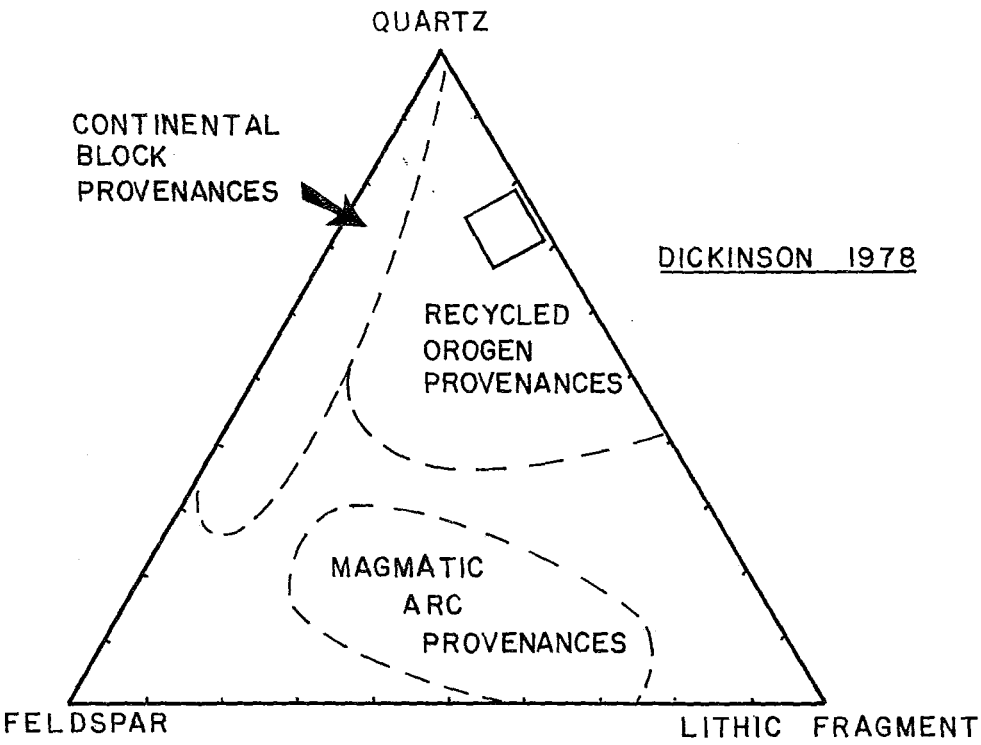
QUARTZ
CONTINENTAL
BLOCK
PROVENANCES
DICKINSON 1978
RECYCLED
OROGEN
PROVENANCES
MAGMATIC
ARC
PROVENANCES
FELDSPAR
LITHIC FRAGMENT

DEPTH VERSUS POROSITY ANALYSIS

It has been shown by recent researchers that the amount of porosity in any given sand body is a function of the diagenetic characteristics and the depositional history (Thomas and Oliver, 1979). One can assume that the depositional history of the Ricinus, Caroline and Garrington fields is for all intents and purposes similar, and therefore need not be considered further. We therefore can infer that any differences between the fields in question with respect to depth-porosity relationships is a result of varying diagenetic histories.

In the depth versus porosity graphs, the ordinate represents the depth of burial of the sand from which the thin sections were cut, and the abscissa represents the amount of porosity observed, by the presence of blue stain. In all three fields, there is evidence that a good relationship does not exist between depth and porosity, linear or otherwise (Fig. 23, 24). In fact, the plotted points are quite random with a large scatter.

This is the keeping with a study done on the comparison of depth-porosity relationships between the Viking and the Cardium Formations in Alberta (Oliver, 1979). It was discovered that the Viking showed a decrease in porosity with increase in depth, as a result of increased compaction and pressure solution. The Cardium revealed no such relationship, and it was argued that this was a result

of the inhibitive nature of hydrocarbons, with respect to the diagenetic processes which plug the pore spaces by clays and cements at depth.

FIGURE 23 : Depth versus porosity graph for the Ricinus sand.

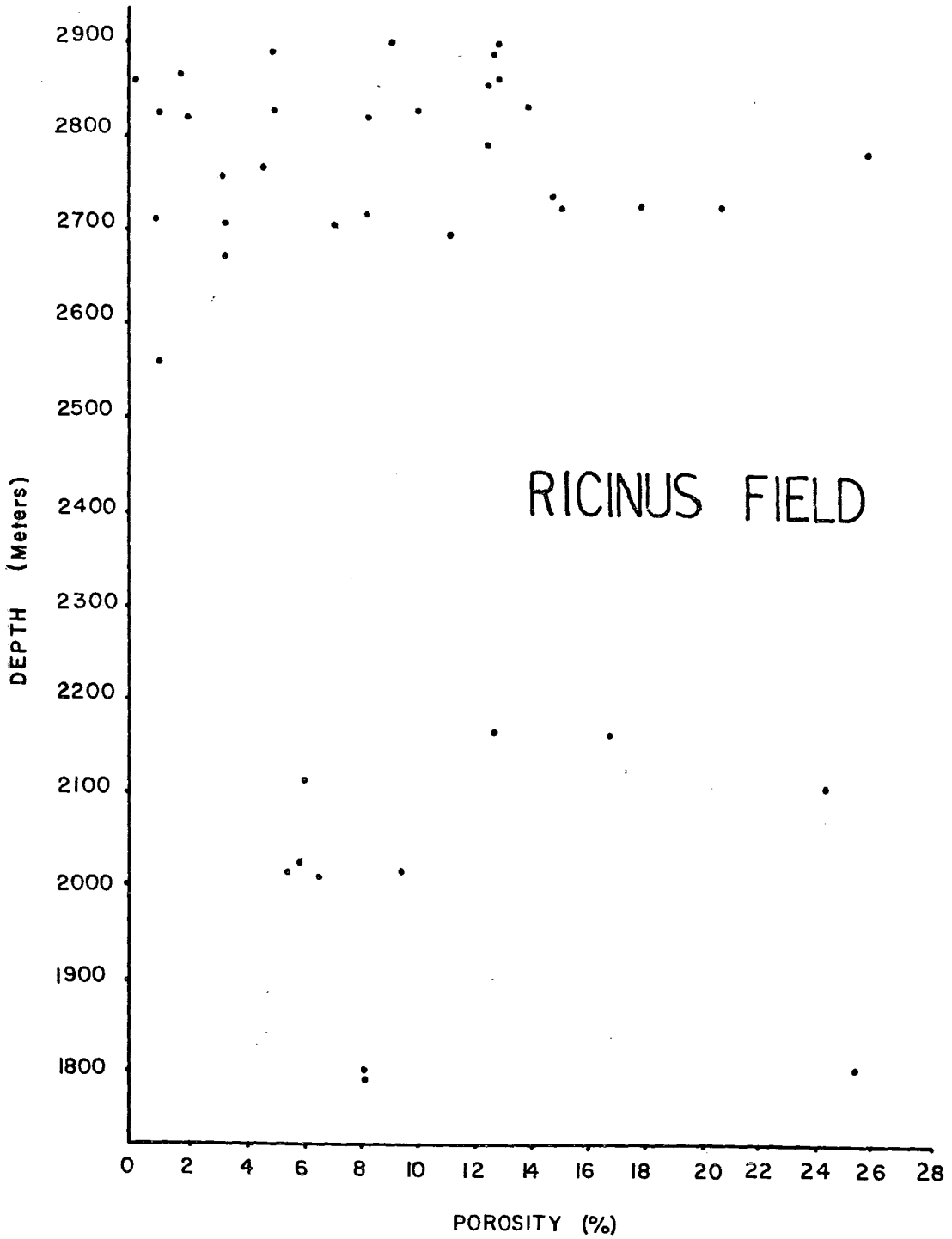
RICINUS FIELD
DEPTH (Meters)
2900
2800
2700
2600
2500
2400
2300
2200
2100
2000
1900
1800
0
2
4
6
8
10
12
14
16
18
20
22
24
26
28
POROSITY (%)

FIGURE 24: Depth versus porosity graph for the Caroline and Garrington sands.

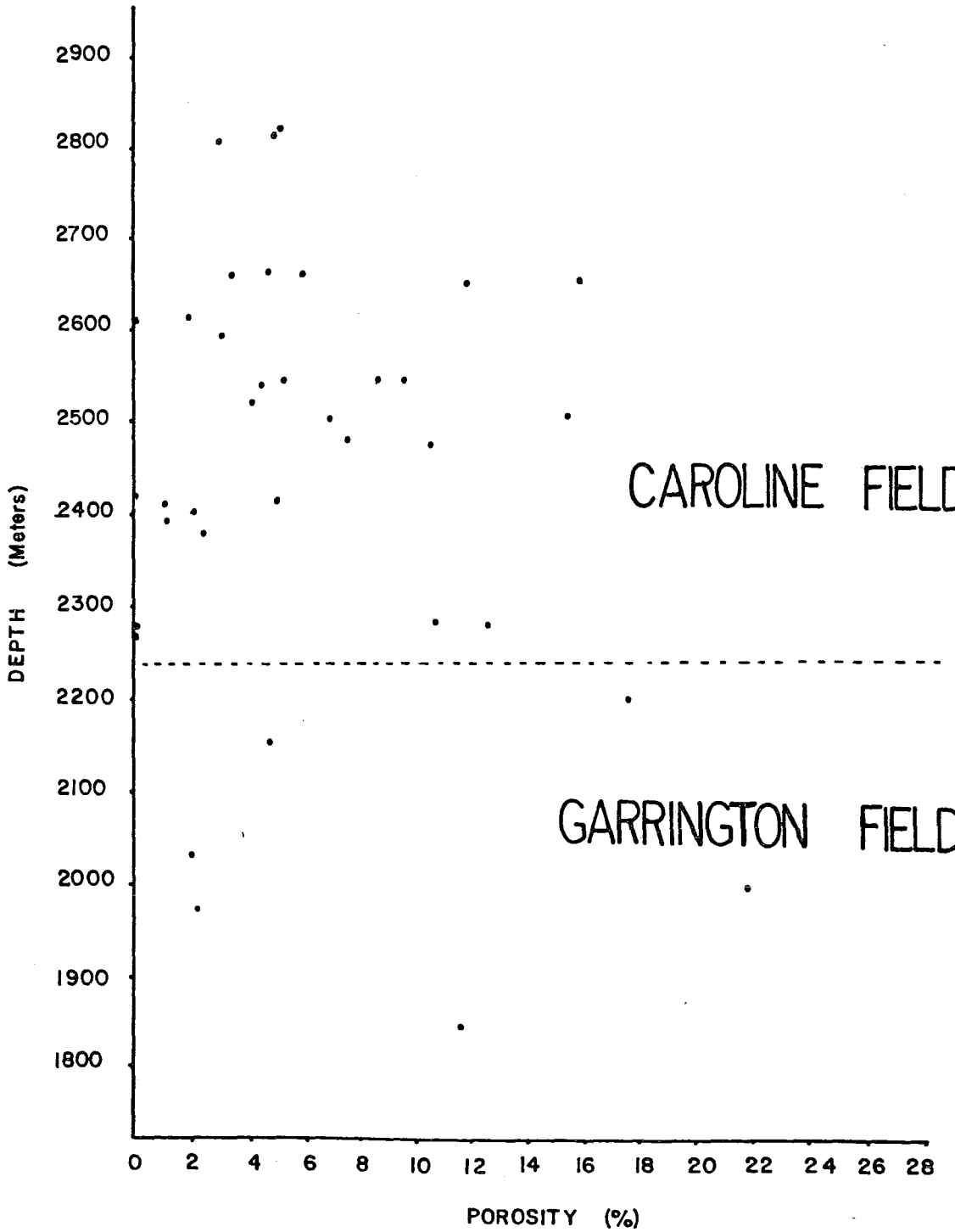
2900
2800
2700
2600
2500
2400
2300
2200
2100
2000
1900
1800
DEPTH (Meters)
CAROLINE FIELD
GARRINGTON FIELD
0 2 4 6 8 10 12 14 16 18 20 22 24 26 28
POROSITY (%)

SANDSTONE CLASSIFICATION

From the graphical analysis of grain size and mineralogy, two sandstone types can be defined as representative of the Ricinus, Caroline and Garrington fields. They are both sublitharenites (Folk, 1968), but may be distinguished as chert-enriched and chert-poor (Fig. 25). The chert-rich sublitharenites are generally found to be moderately to poorly sorted, sub-round to round, and coarse grained to conglomeratic in texture. The chert poor sublitharenites are generally extremely well sorted, very fine grained, and subangular in shape. It is probable that the two types of sandstone represent two different sources of clastic detrital sediment. The chert poor sublitharenites may have been weathered from a proximal igneous parent rock and hence small irregular grains of quartz are observed as the major component. The chert rich sublitharenites may have been derived from a more distal sedimentary environment, and hence the larger grain size, composite mineralogy, and well rounded shape.

FIGURE 25 : Ternary diagram illustrating the classification of the Ricinus, Caroline and Garrington sandstones (Folk, 1968). The Cardium sands composition is represented by the small square.

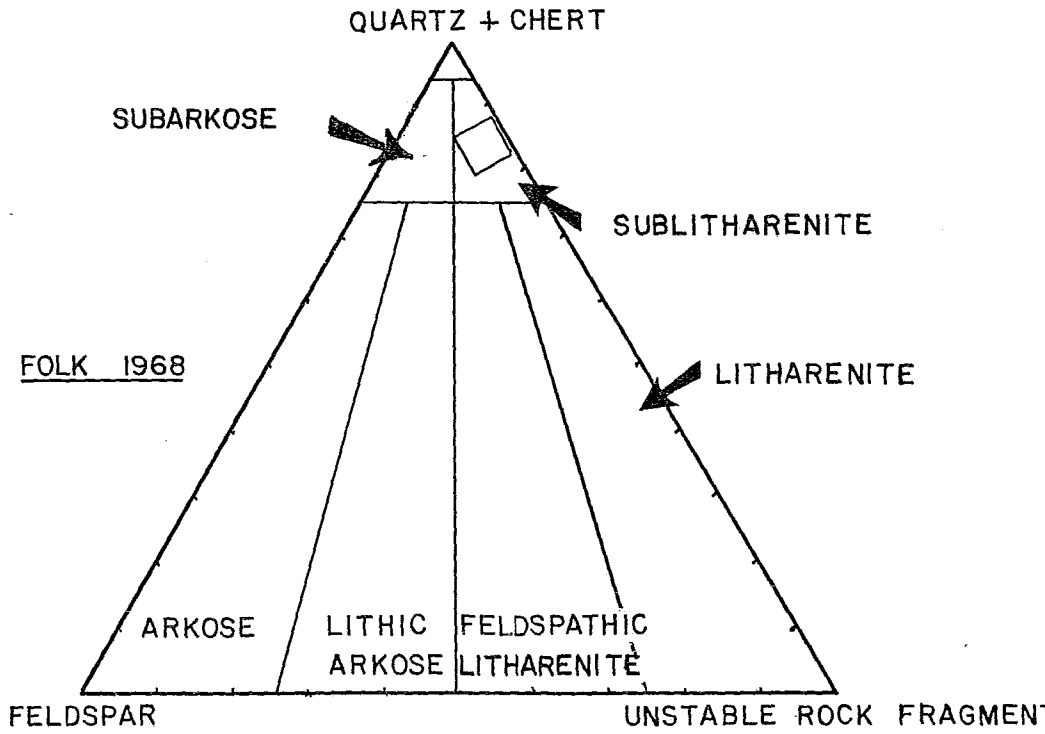
QUARTZ + CHERT
SUBARKOSE
SUBLITHARENITE
FOLK 1968
LITHARENITE
ARKOSE
LITHIC ARKOSE
FELDSPATHIC LITHARENITE
FELDSPAR
UNSTABLE ROCK FRAGMENT

HISTORY OF CEMENTS AND DIAGENESIS

The Ricinus, Caroline, and Garrington fields all share a similar cementing sequence, with common cementing agents. In order of abundance the cements were; siderite, calcite, silica, and pyrite. In the Ricinus field, multiple stages of both siderite and silica cement were observed. The first cement was siderite as it is found to line mineral grains with a thin prismatic envelope, and is observed to invade chert grains extensively. Calcite cement was next, as it was observed to pseudomorph prismatic siderite (Plate 8B), and replace siderite (Plate 5). Silica cement crystalized after siderite and calcite, as it is observed that siderite, calcite, and clays are all enveloped by the silica cement. Pyrite is found to be interstitial (Plate 23A), and in pore spaces (Plate 23B), but embays all other cements suggesting it was formed last.

However, inasmuch as these cements were observed in all fields, they varied in abundance, depending on the depth and grain size. The fields in order of depth of sands are Ricinus, Caroline and Garrington. In general, (excluding conglomeratic sandstone) the Ricinus sand contains by far the most silica cement, followed by the Caroline and the Garrington sands. The Garrington sands contain abundant carbonate cements, with lesser amounts being observed in the Caroline and Ricinus sands. Silica cement appears to increase in abundance, whereas carbonate

cements decrease in abundance with increasing depth.

The conglomeratic sandstones are all carbonate cemented to the exclusion of silica, regardless of depth. The carbonate cements appear to be particularly well established near large pore spaces and the larger grains, suggesting that the greater porosity and effective permeability is condusive to carbonate cementation. In this regard the Lower sands and the Upper sands of the Caroline and Garrington fields can be distinguished as the Lower sands are dominatly carbonate cemented, whereas the Upper sands tend to be silica cemented. This is probably related to the fact that the Lower sands are coarse grained to conglomeratic in texture.

Diagenesis In Other Cardium Finds

Several researchers working in other Cardium fields have established diagenetic sequences, both in agreement and disagreement with respect to the Ricinus, Caroline and Garrington cementing sequence.

In the Ferrier field siderite, calcite and silica have been observed in the conglomerates, and silica, calcite, and siderite observed in the fine grained sandstones (Griffith, 1982). Siderite, Kaclonite, illite, calcite and silica were observed within the Ricinus field (Amon, 1979).

In some disagreement, is the study of the Crossfield-Garrington fields (Berven, 1966). Siderite, Kaclonite, Wilkeite, and Silica are cited as the diagenetic sequence. In the Edson field, silica, dolomite, calcite and siderite are found to be the principle cementing agents (Sinha, 1970).

The main point of deliberation, is the time of crystalization of the silica cement. As many fields have silica cement forming first, as forming last in the cementing sequence. In addition to this, the Cardium sandstones are characterized by diverse cementing agents, complicated by cyclic sequences, and multiple stages of some cements.

DISCUSSION

The most effective and concise method of comparing the Ricinus, Caroline and Garrington sands is by superimposing the four ternary diagrams previously described (Fig. 26). From this illustration it is evident that certain sands can be distinguished from other sands on the basis that they are situated in different regions of the ternary diagram. The "base" diagram represents the Ricinus sand population. Overlain on this diagram is a second ternary diagram with two populations representing the Upper and Lower sands of the Caroline and Garrington fields.

The most striking relationship are the apparent differences between the Upper and Lower sands. The Upper sands tend to be chert poor, compared to the Lower sands which tend to be more chert rich. In addition to this, distinctions can be made on the basis of grain size. The Upper sands are composed of grains which are very fine grained and well sorted, and vary from subangular to angular in sphericity. The Lower sands are generally coarse to conglomeratic in grain size, poorly sorted, and vary from subround to round in sphericity.

Nearly all the Upper sands fall within the Ricinus sands population, and therefore cannot be distinguished on the basis of bulk mineralogy. Such is not the case for the Lower sands, as a significant pro-

portion of the Lower sands population is not enveloped by the Ricinus population.

In particular, those Lower sand thin sections rich in chert remain outside the Ricinus sand population. Furthermore, the Lower Garrington sand can be distinguished from the Lower Caroline sand, on the same basis - the Lower Garrington sand is distinctly enriched with respect to chert. The Upper Garrington and Upper Caroline sand populations tend not to be so distinct as in the case of the Lower sands.

This is intriguing, as the Upper sands have been confirmed as continuous between the Caroline and the Garrington fields by well logs, whereas the same is not true for the Lower sands. The possibility arises therefore, that the two Lower sands may represent two distinct pulses of clastic sediment with varying provenances, and hence the varying bulk mineralogies.

One important consideration, is that the observed differences within the Lower sand mineralogies are based upon a limited number of thin sections within the Lower Garrington, and on this basis are hardly conclusive. Additional research in the Garrington field is suggested, especially in the Lower sand. Additional data may reveal that the Lower Garrington population merges with the Lower Caroline sand population, or that they remain distinct.

In either instance, it is fair to say that one population is concentrated in a region of the ternary diagram not occupied by the other.

FIGURE 26 : Ternary diagram comparing the different mineralogies of the Pininus, Caroline, and Garrington sands.

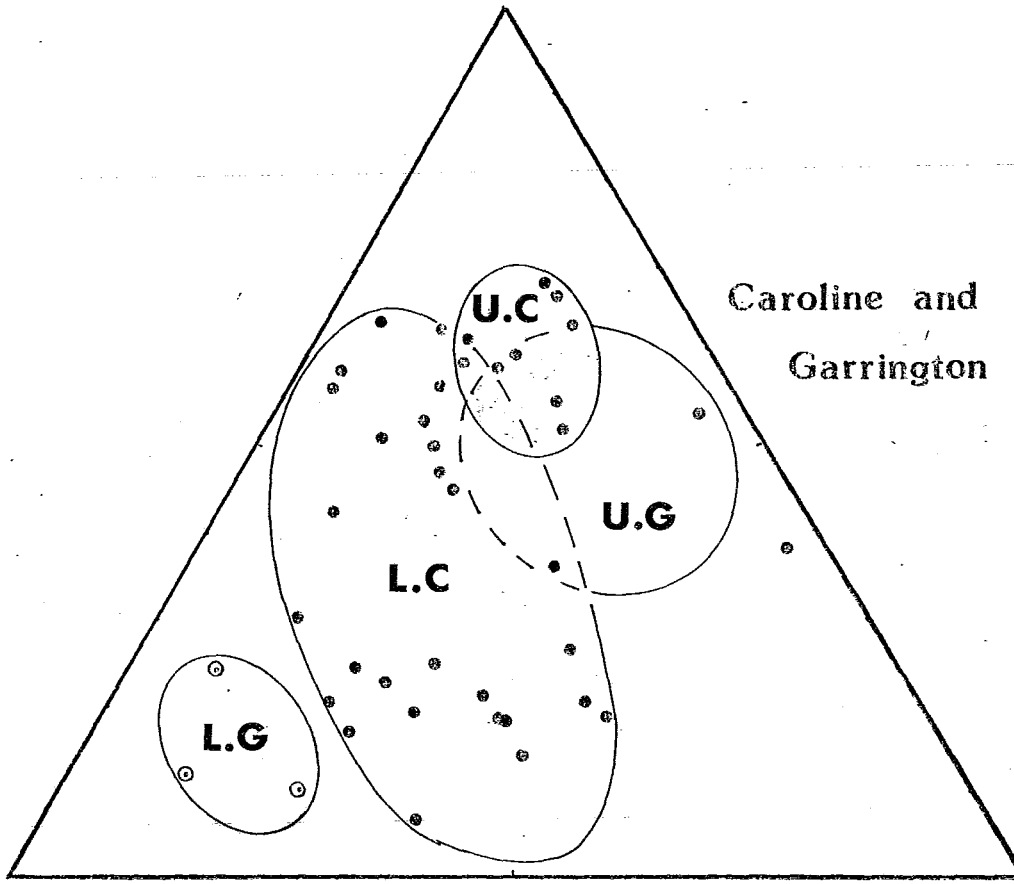

Caroline and Garrington

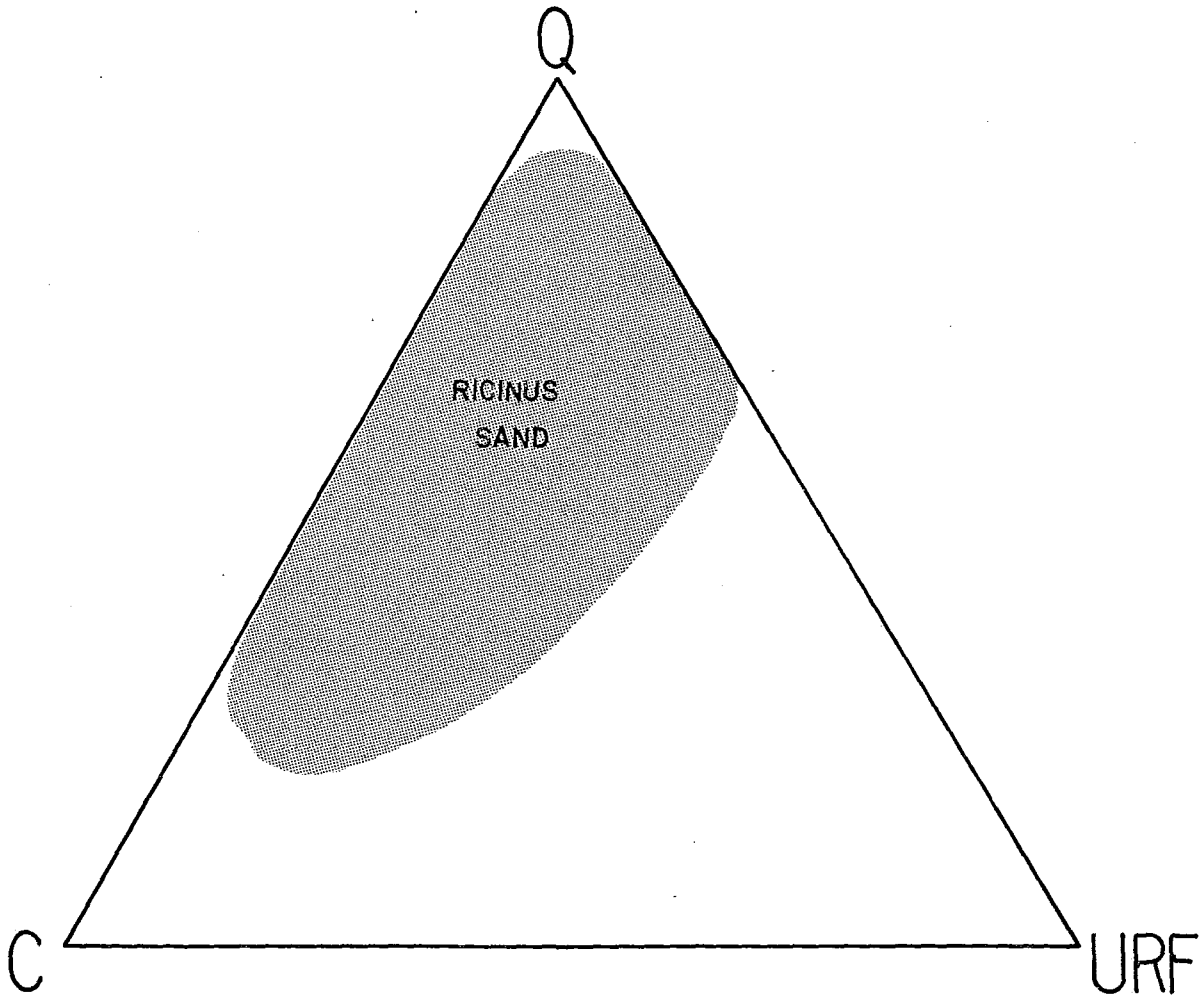
Q
RICINUS
SAND
C
URF

CHAPTER THREE

CONCLUSIONS

1. The Upper (A) and the Lower (B) sands of the Caroline and Garrington fields can be distinguished on the basis of petrography.

2. The Ricinus sand and the Lower sands of the Caroline and Garrington fields can be distinguished on the basis of petrography.

3. The Lower Garrington sand and the Lower Caroline sand can be distinguished on the basis of petrography, in the context of the amount of data available. It is therefore suggested that the Garrington field be considered an area for further research.

4. Mineralogy of the Ricinus, Caroline and Garrington fields are controlled by the nature of their transport as well as their sources. Two sandstone types are evident within these fields. They are chert rich and chert poor sublitharenites. The former is fine grained and angular suggesting a proximal igneous source. The latter are more rounded and occur as coarse composite clasts suggesting a distal sedimentary source. Grain size, shape and sorting can be related to mineralogy in these sandstone types.

5. The Ricinus, Caroline and Garrington fields all share a common cementing history. The cementing agents observed, in order of their occurence were; siderite, calcite and silica, with pyrite occuring very rarely.

6. The abundance of cements observed within the sands of the Ricinus, Caroline and Garrington fields are controlled by the depth of the sand, and the grain size of the sand.

7. From the literature published by other researchers working in different Cardium fields, it is evident that the cementing sequence within the sandstones is variable, with respect to the order, type and the relative proportions of cementing agents.

PLATE 0 : A visual aid to establish scale for all photographs taken under cathode luminescence. One square represents 1 mm, therefore magnification is about 50x.

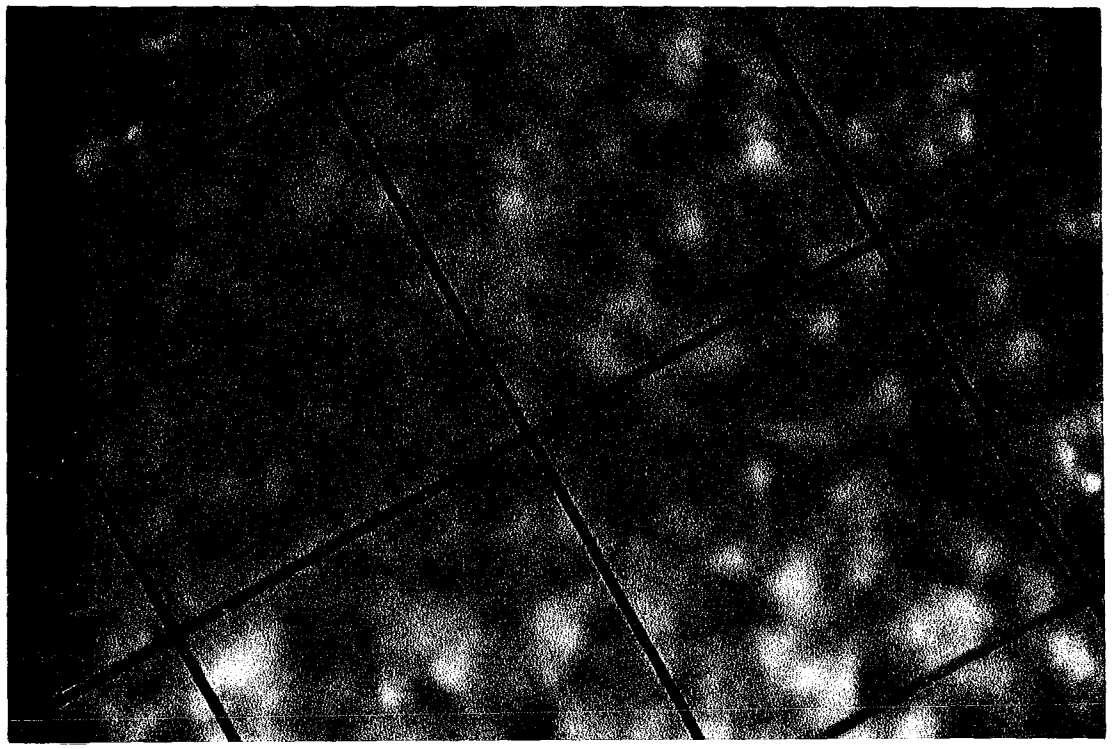

PLATE 1A : Thin Section 11-17-35-8W5 9267.5 ft Caroline Field, magnification 50x. Plain light photograph of a silica cemented sandstone. Note the blade of muscovite bent around biogenic chert.

PLATE 1B : Same as above, but under cathode luminescence.

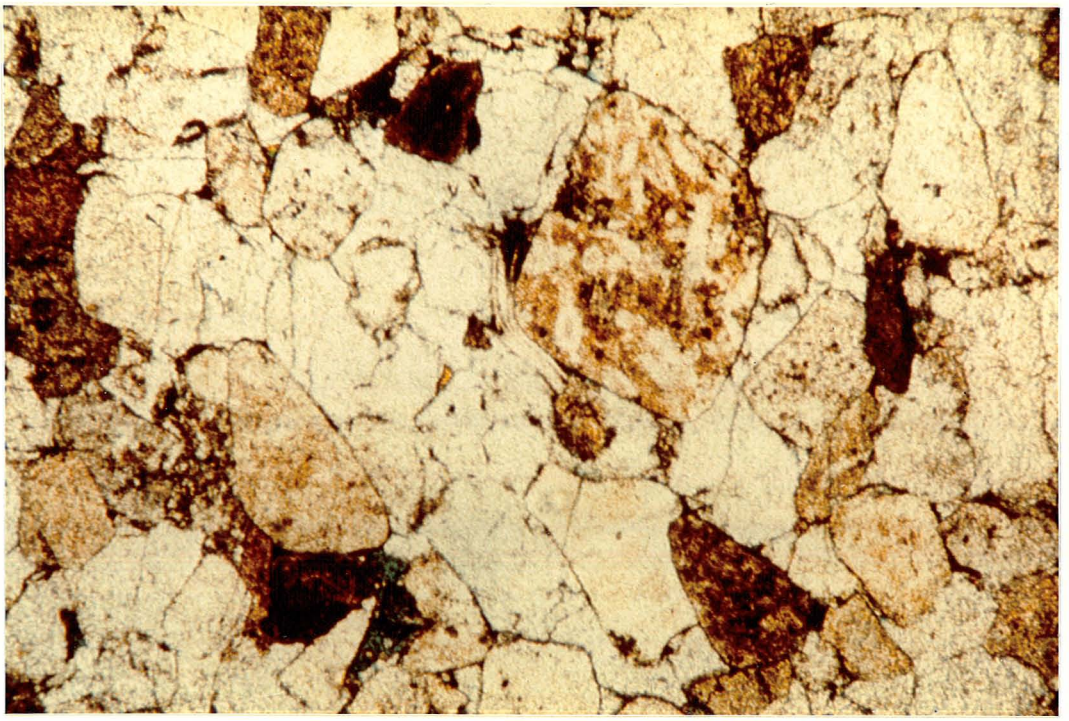

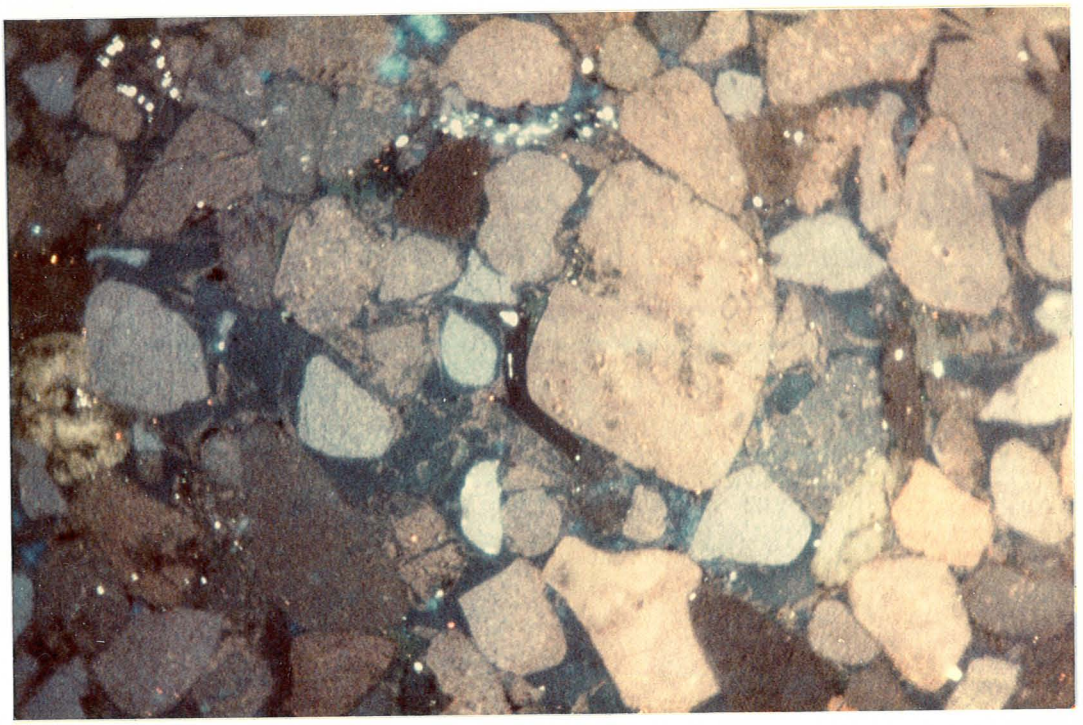

PLATE 2A : Thin Section 7-9-33-7W5 6565.0 Ft Ricinus Field, magnification 50x. Crossed nicols photograph of silica cemented sandstone. Note the multiple stages of blue-black, and chocolate brown cements.

PLATE 2B : Same as above, only under cathode luminescence.

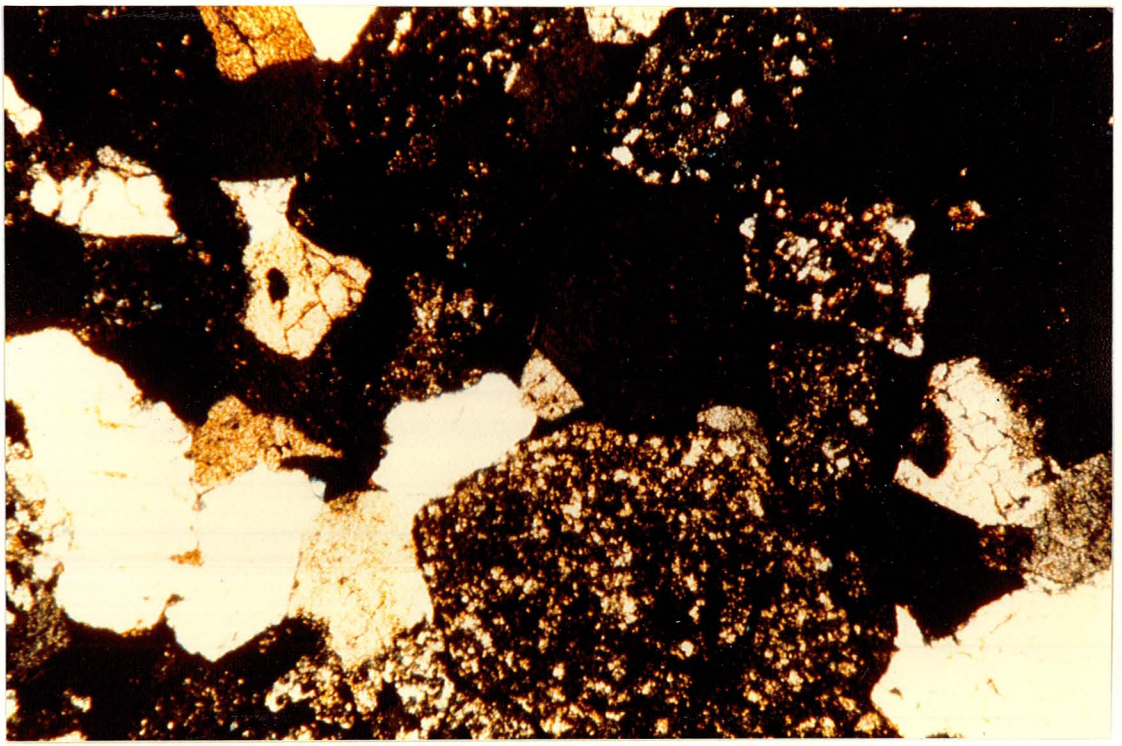

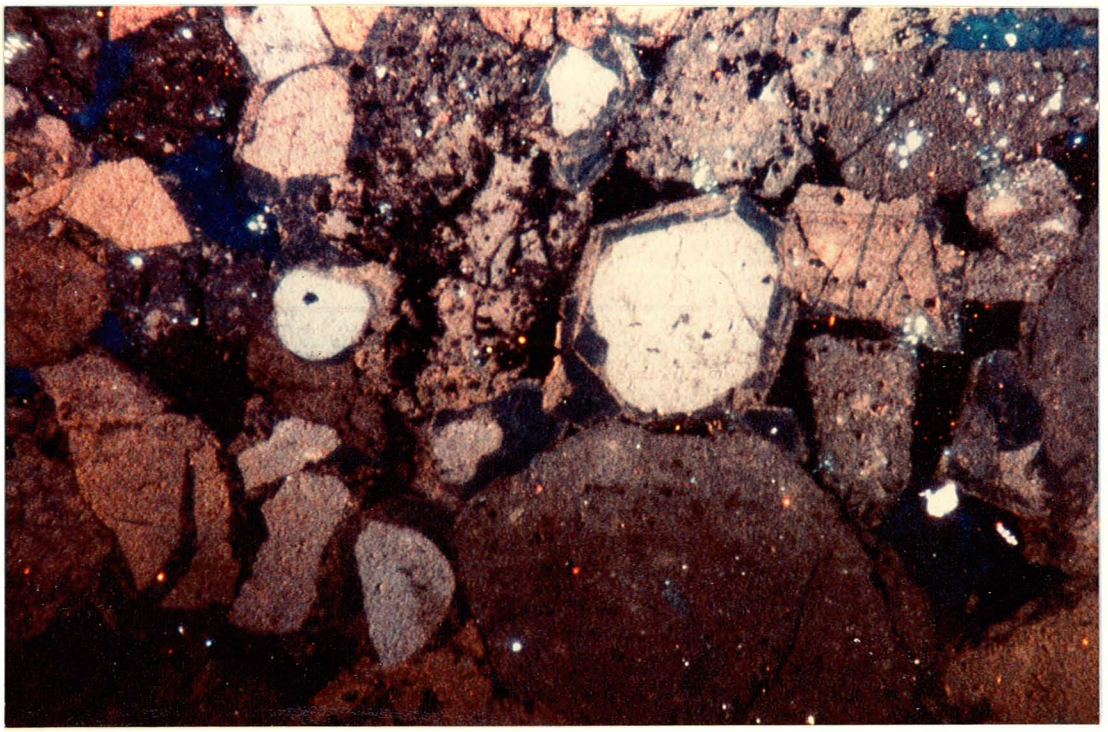

PLATE 3A : Thin Section 7-9-33-7W5 6565.0 ft Ricinus Field, magnification 50x. Plain light photograph of a silica cemented fine grained sandstone. Note the silica cement has filled fractures within the quartz grains.

PLATE 3B : Same as above, but under cathode luminoscope.

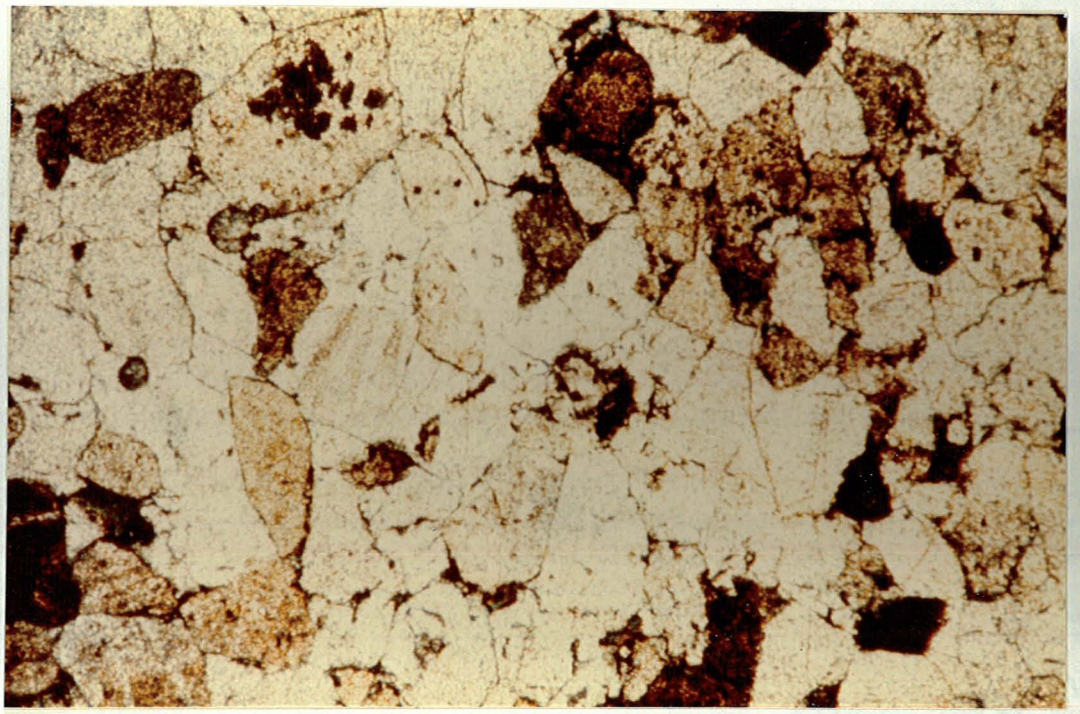

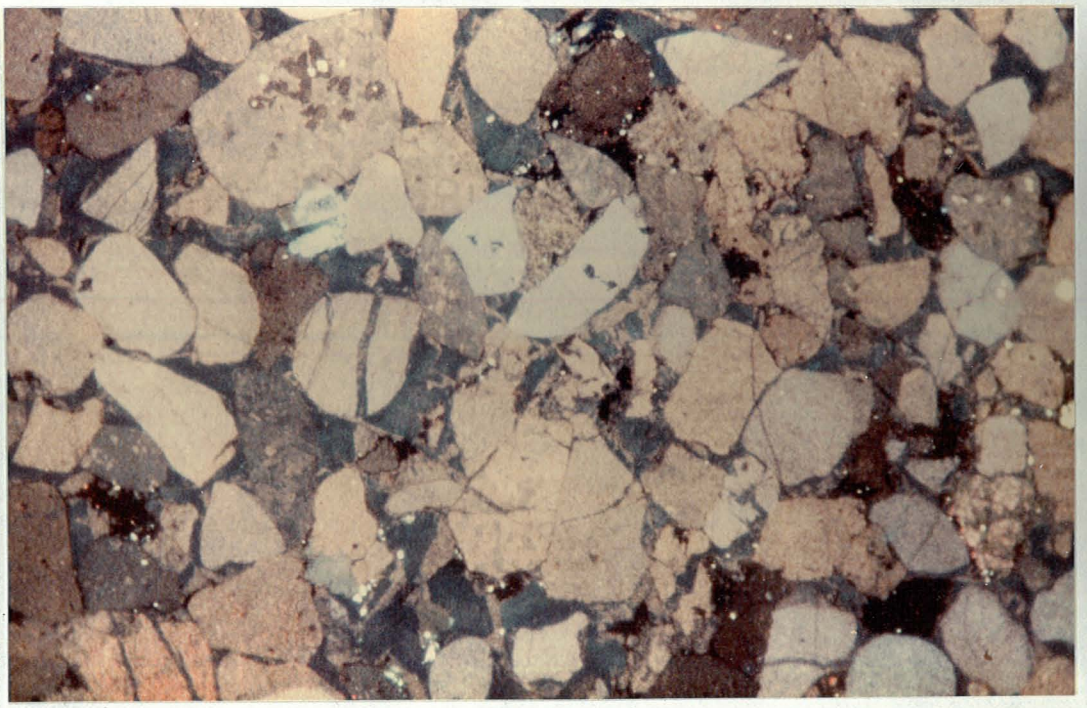

PLATE 4A : Thin Section 7-9-33-7W5 6555.0 ft Ricinus Field, magnification 50x. Crossed nicols photograph of a dominantly silica cemented, very fine grained sandstone. Note the patchy distribution of the calcite cement (lime yellow color).

PLATE 4B : Same as above, but under cathode luminoscope. Calcite luminesces the vivid red-orange color.

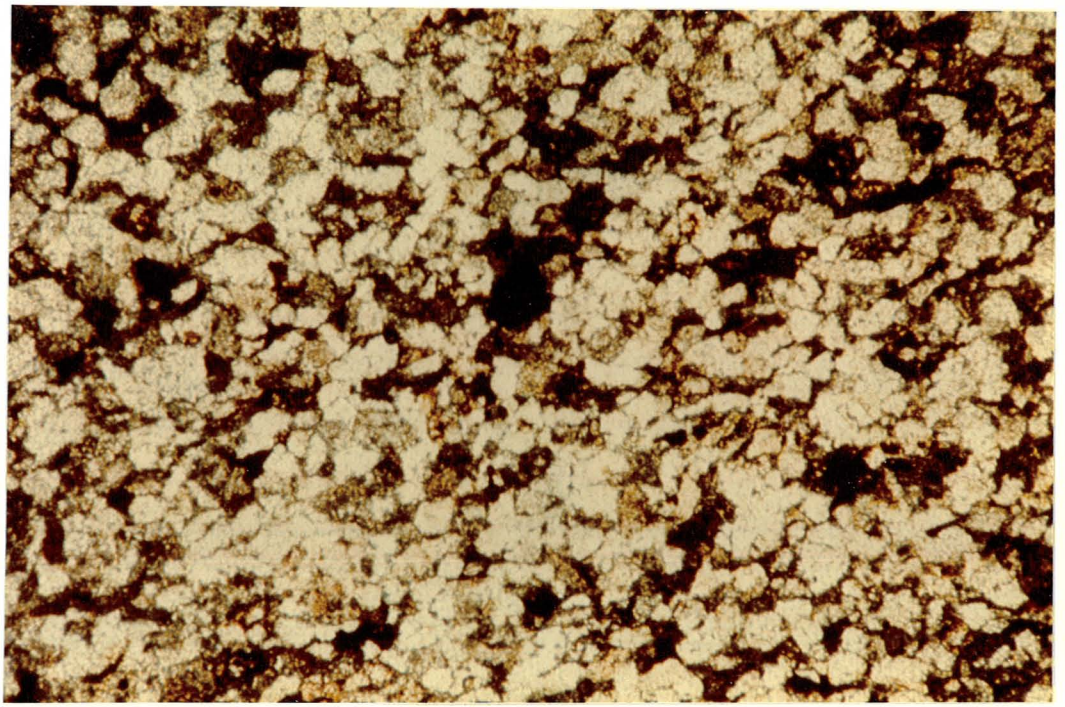

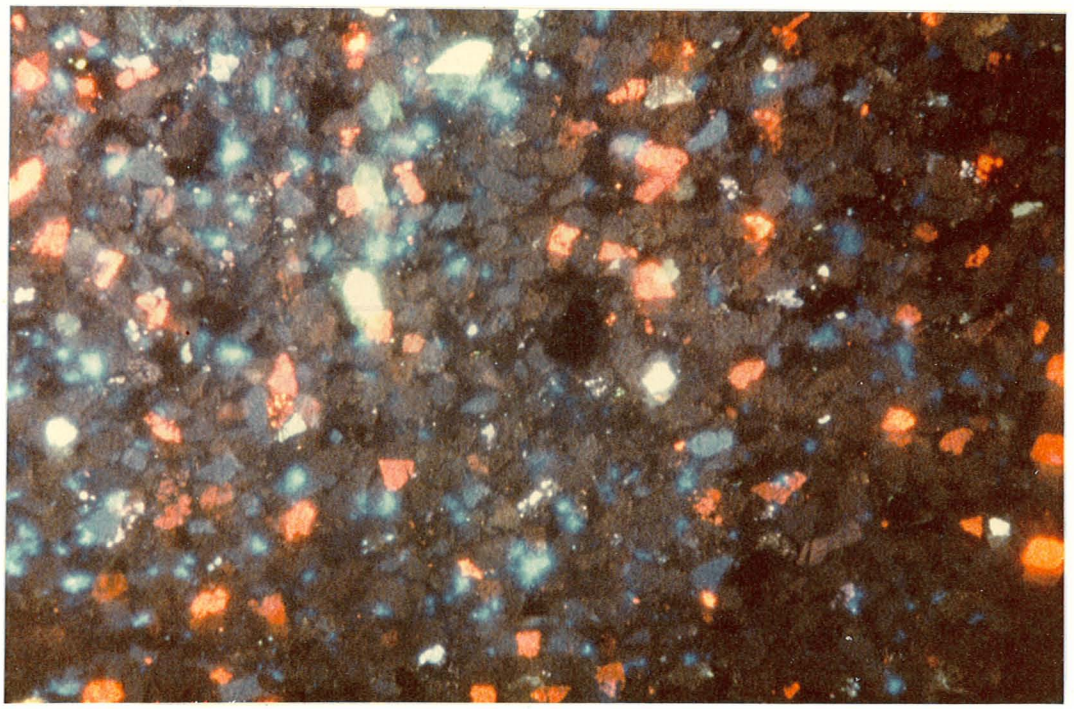

PLATE 5A : Thin Section 11-17-35-8W5 9267.5 ft Caroline Field, magnification 50x. Crossed nicols photograph of a calcite cemented, conglomeratic sandstone. Note that the calcite cement (yellow) is replacing the siderite cement (brown), which in turn encases the grains.

PLATE 5B : Same as above, but under cathode luminescence. Calcite luminesces a vivid orange-red.

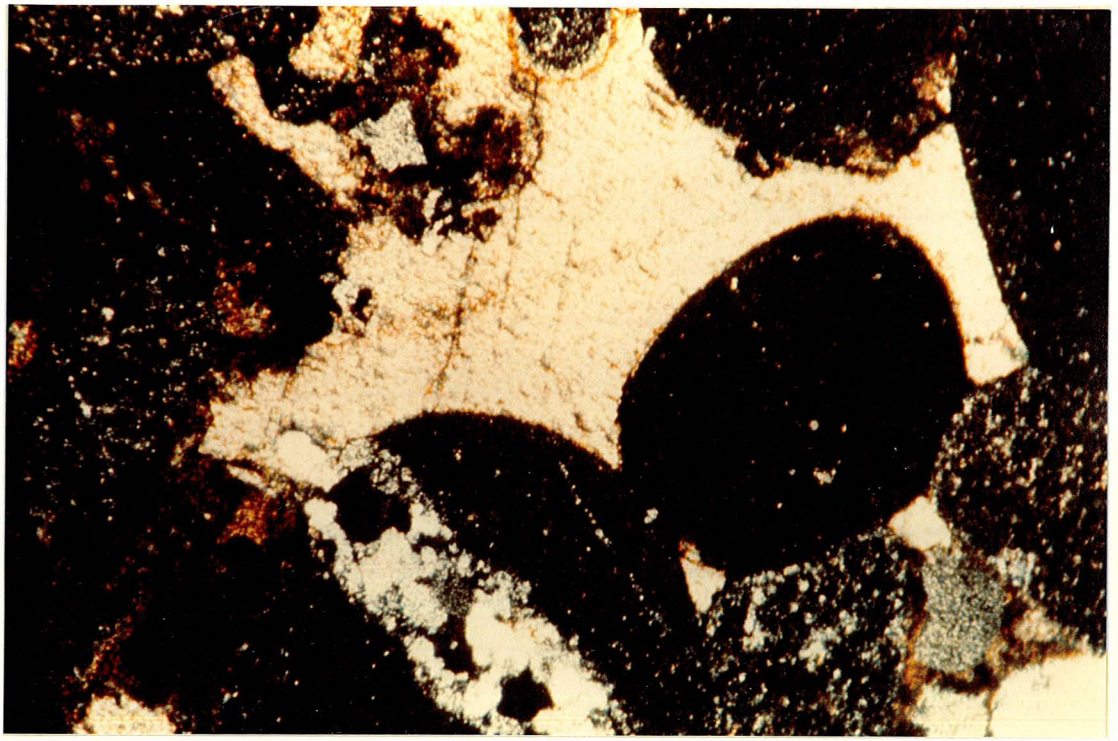

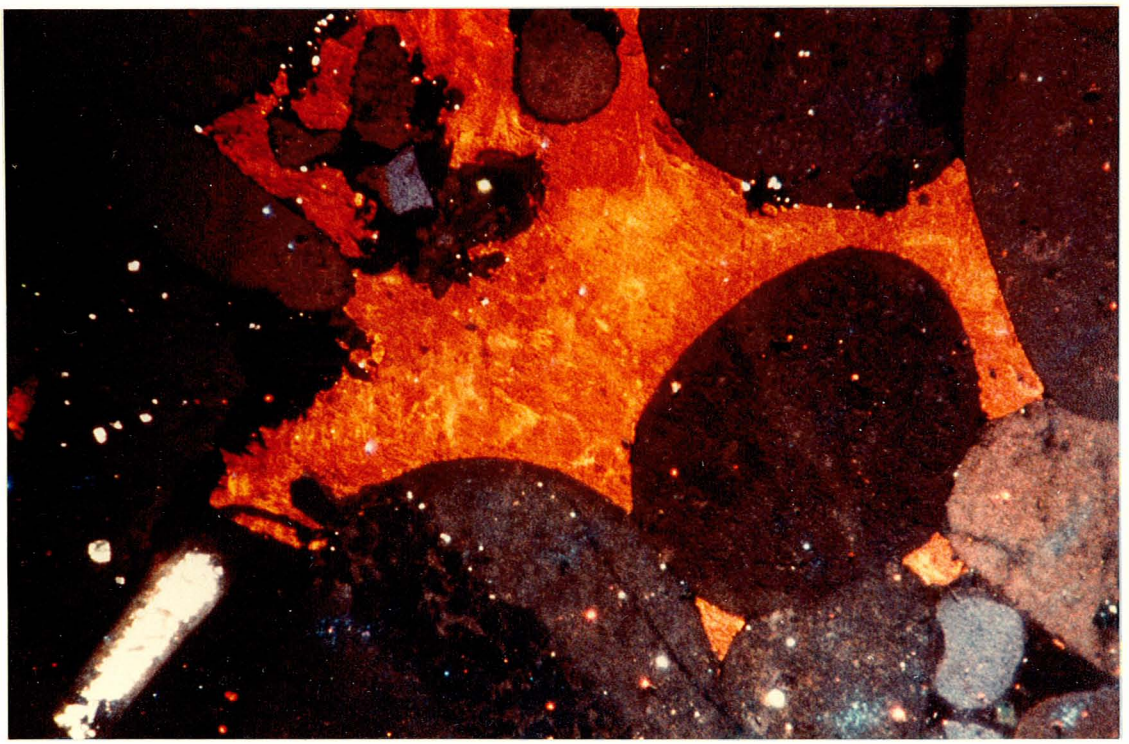

PLATE 6A : Thin Section 11-17-35-8W5 9267.5 ft Caroline Field, magnification 50x. Crossed nicols photograph of calcite cemented sandstone. Note that the calcite has exploited weaknesses and fractures within the composite clasts.

PLATE 6B : Same as above, but under cathode luminescence.

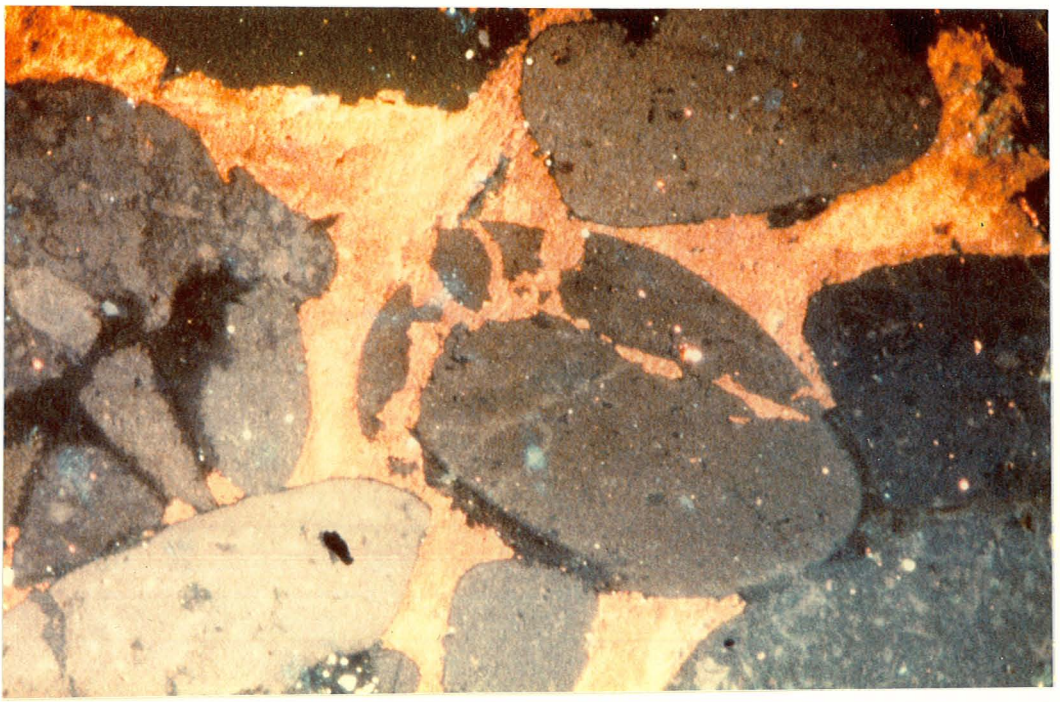

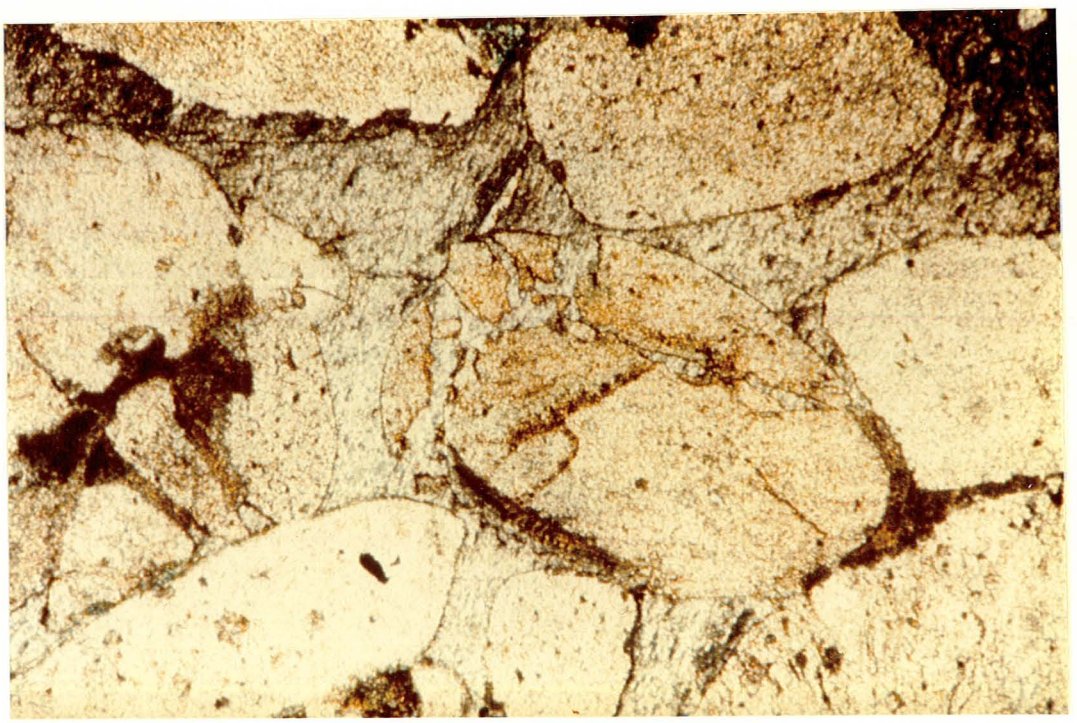

PLATE 7A : Thin Section 16-9-35-6W5 7742.01 ft Caroline Field, magnification 50x. Crossed nicols photograph of silica and calcite cemented, fine grained sandstone. Calcite is the most abundant, with minor amounts of silica replacing it along grain boundaries.

PLATE 7B : Same as above, but under cathode luminoscope.

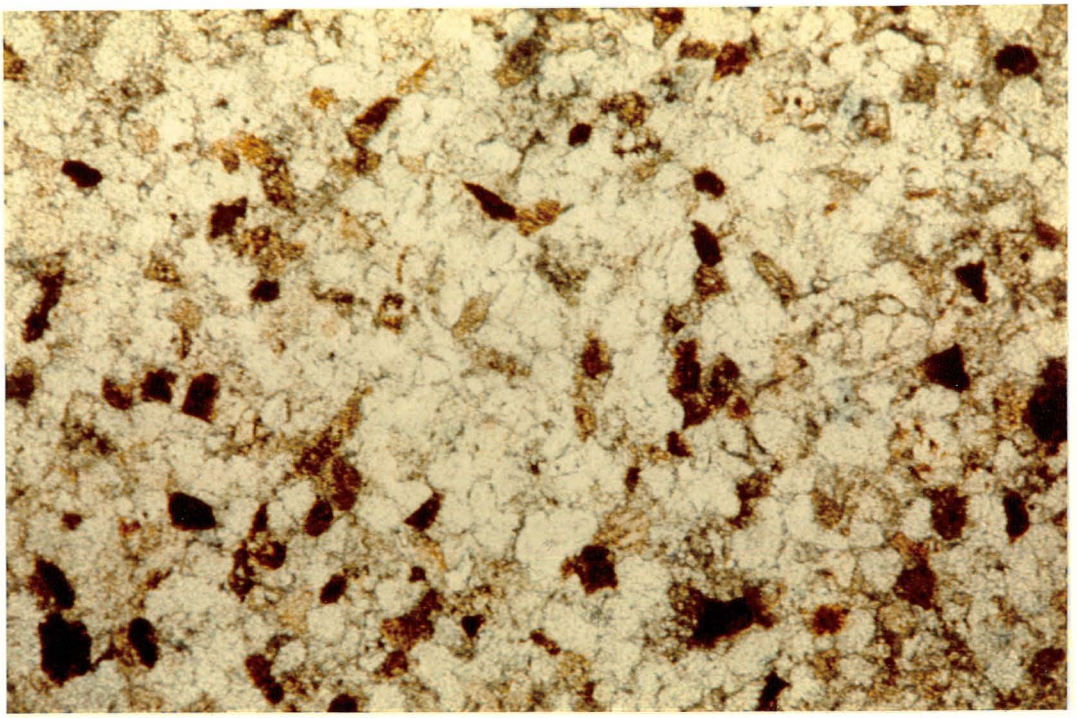

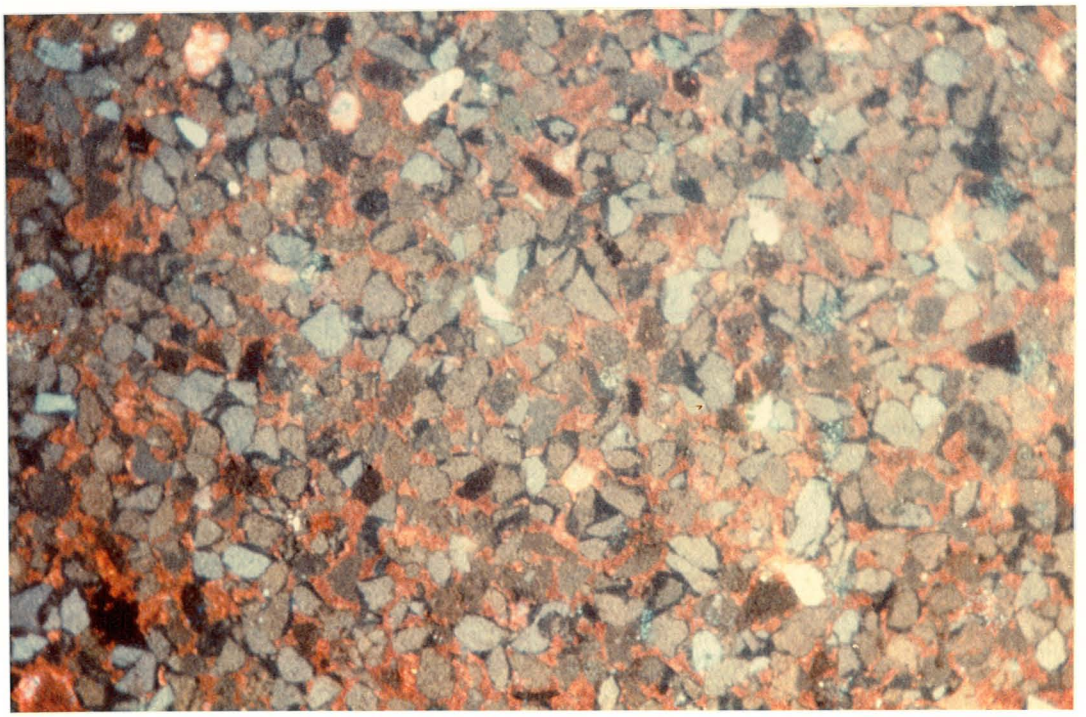

PLATE 8A : Thin Section 16-9-35-6W5 7742.1 ft
Caroline Field, magnification 63x.
Crossed nicols photograph of calcite cemented fine grained sandstone. Note the alternating dark and light growth twinning.

PLATE 8B : Thin Section 4-21-37-6W5 7174.0 ft
Garrington Field, magnification 63x
Crossed nicols photograph of calcite cement pseudomorphing siderite cement.

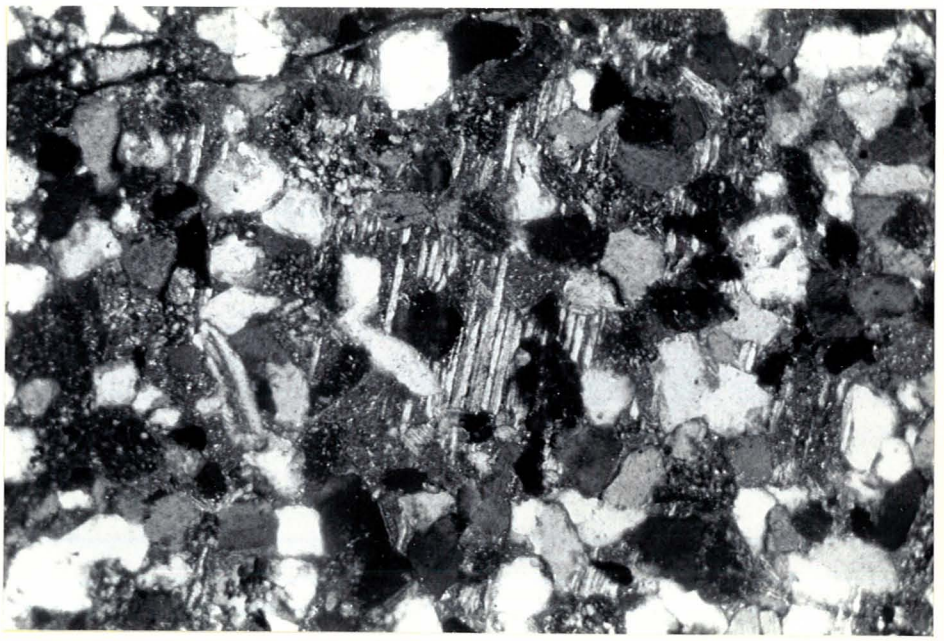

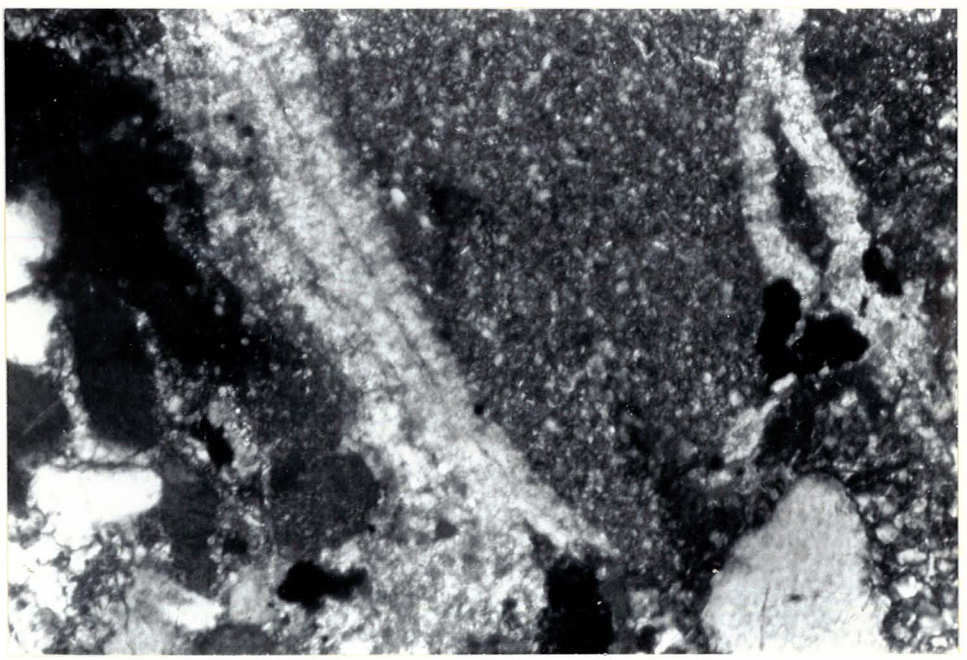

PLATE 9A : Thin Section 10-22-36-8W5 8665.5 (T/4)
Caroline Field, magnification 63x.
Crossed nicols photograph of siderite cemented, conglomeratic sandstone. Note the distinct "spherulitic" texture of siderite (yellow-gold color).

PLATE 9B : Thin Section 10-35-31-2W5 5976.0 ft
Garrington Field, magnification 63x.
Crossed nicols photograph of siderite cemented, conglomeratic sandstone. Note the manner in which the spherules grow around a clay or shale fragment nucleus.

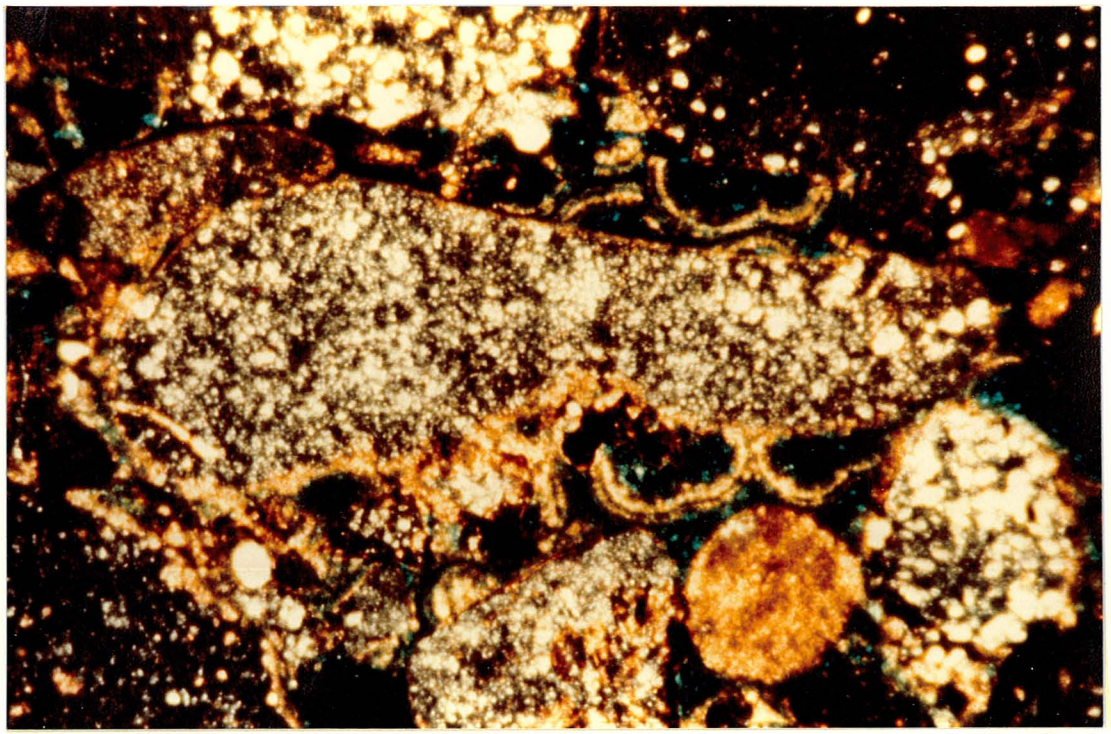

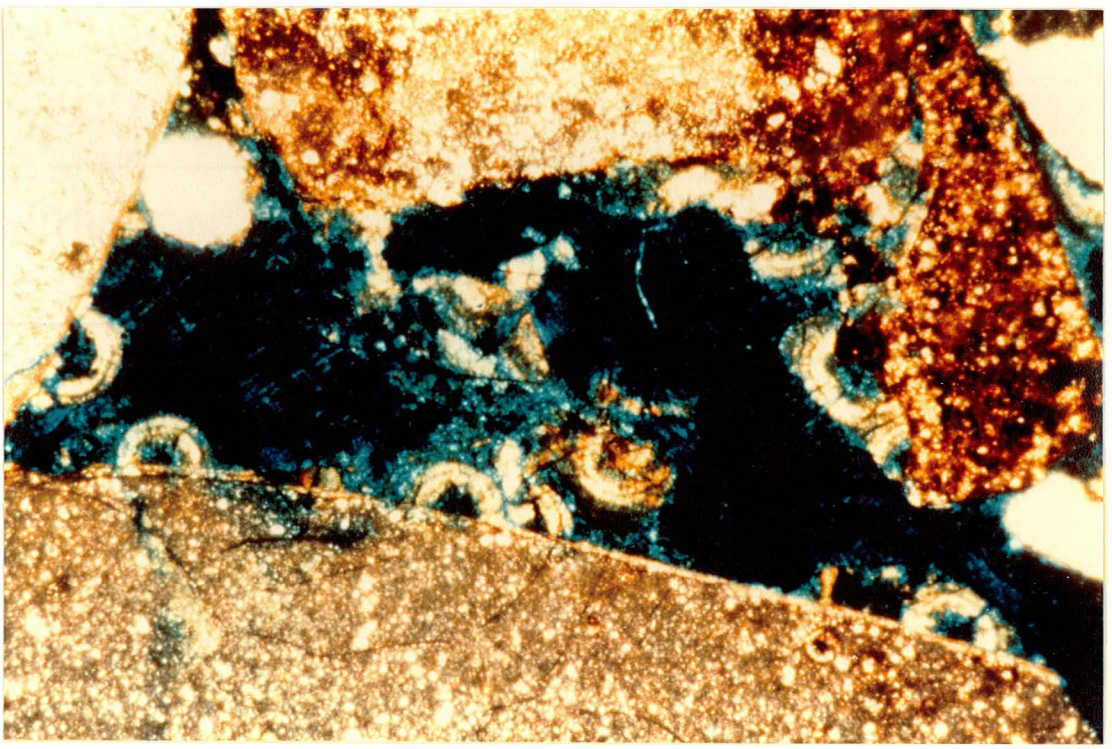

PLATE 10A : Thin Section 10-33-34-6W5 7880.0 ft
Caroline Field, magnification 63x.
Crossed nicols photograph of siderite cemented fine grained sandstone. Note the abundant spherules, some of which may be composed of phosphate.

PLATE 10B : Same as above, but with increased magnification 160x.

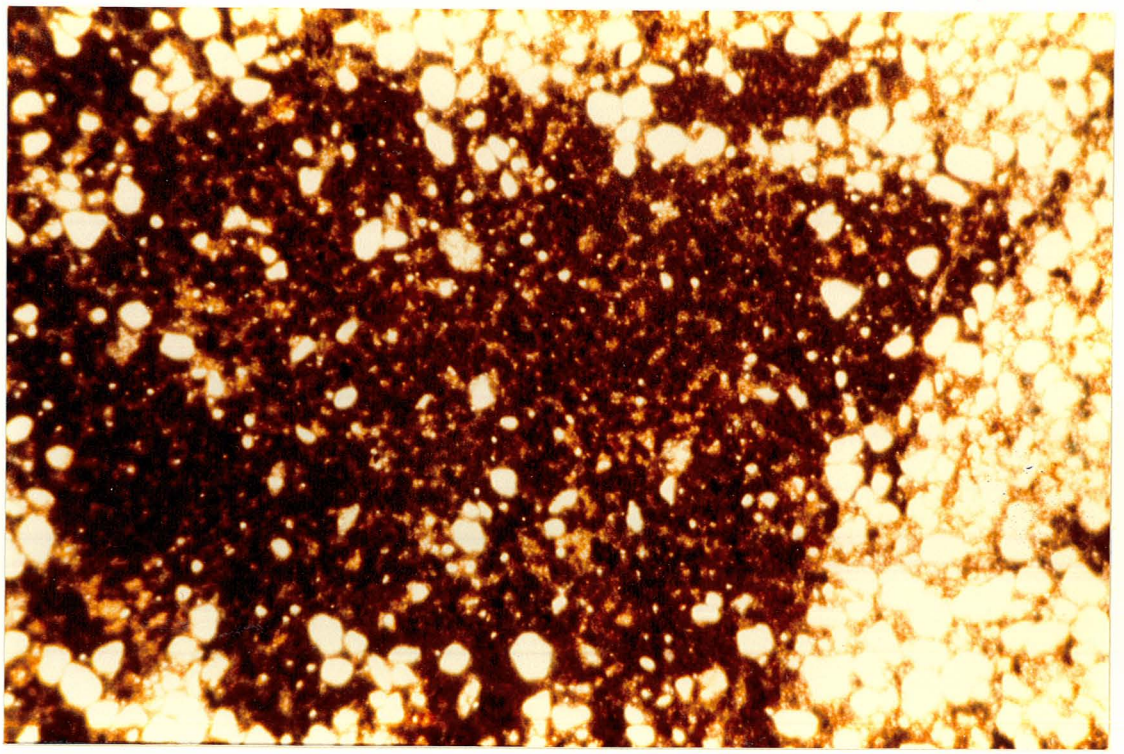

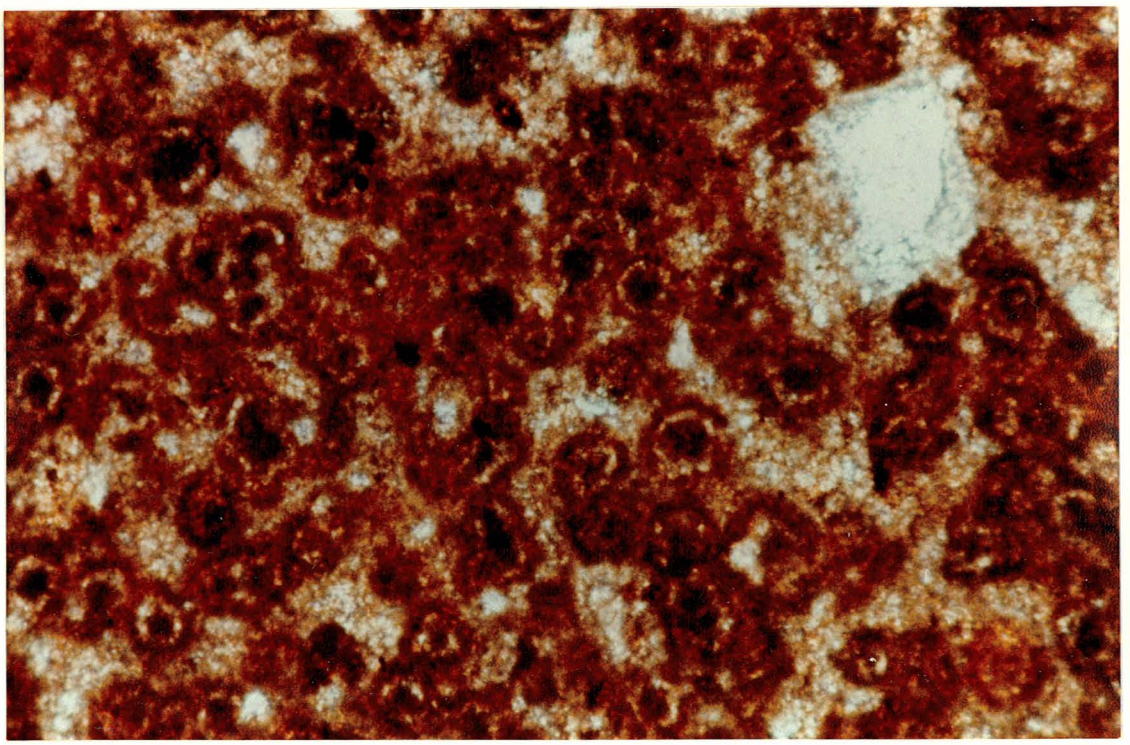

PLATE 11A : Thin Section 2-34-36-9W5 9254.0 ft Ricinus Field, magnification 50x. Crossed nicols photograph of silica cemented sandstone, with some chert clasts containing euhedral siderite rhombohedrons.

PLATE 11B : Same as above, but under the cathode luminoscope. Note also, the multiple stages of silica cement.

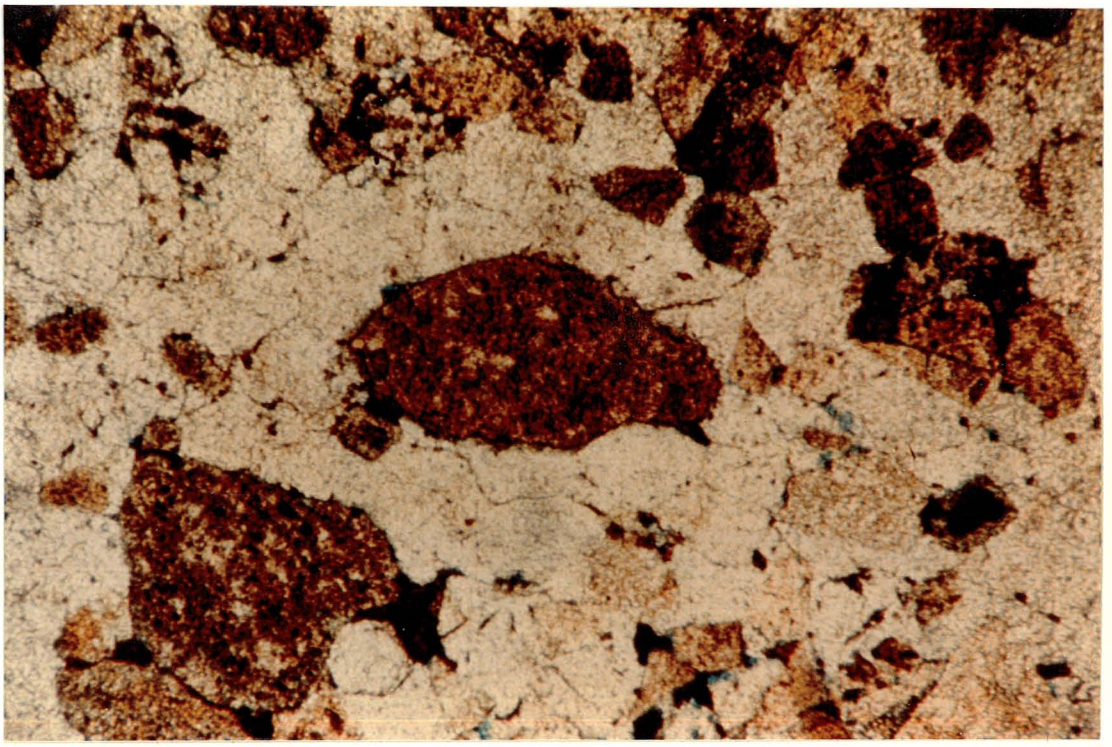

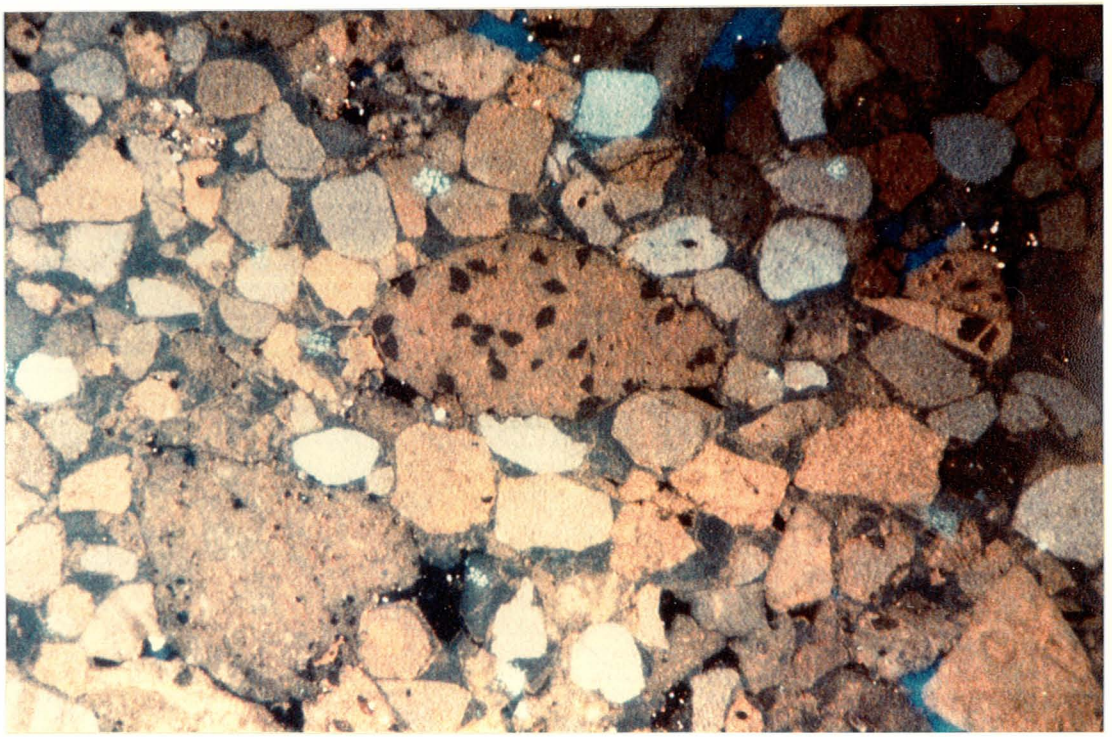

PLATE 12A : Thin Section 2-34-36-9W5 9226.0 ft
Ricinus Field, magnification 63x.
Crossed nicols photograph of a very
rounded chert grains containing good
euhedral "rhombs" of siderite, and
grains of chert altering to chalcedony.

PLATE 12B : Thin Section 2-34-36-9W5 9226.0 ft
Ricinus Field, magnification 160x.
Crossed nicols photograph of chert
containing euhedral "rhombs" of
siderite.

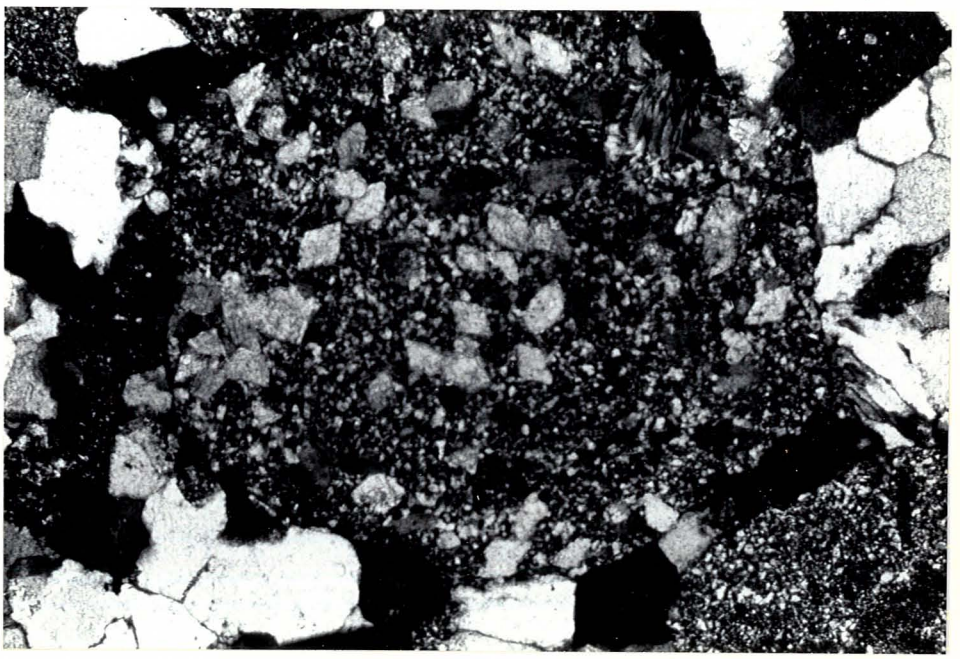

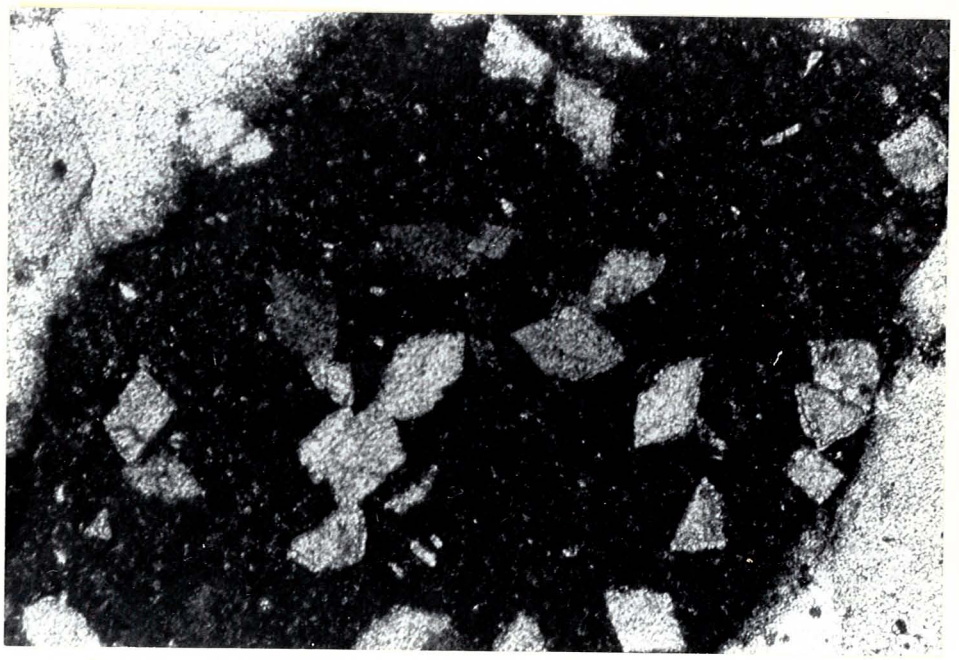

PLATE 13A : Thin Section 11-31-34-6W5 8171.0 ft Caroline Field, magnification 63x. Plane light photograph of siderite cement filling in pore space, and binding chert grains interstitially. Note also the black organic matter found within the pore spaces (blue).

PLATE 13B : Same as above, but under the cathode microscope. Note the characteristic iron cross extinction of the siderite.

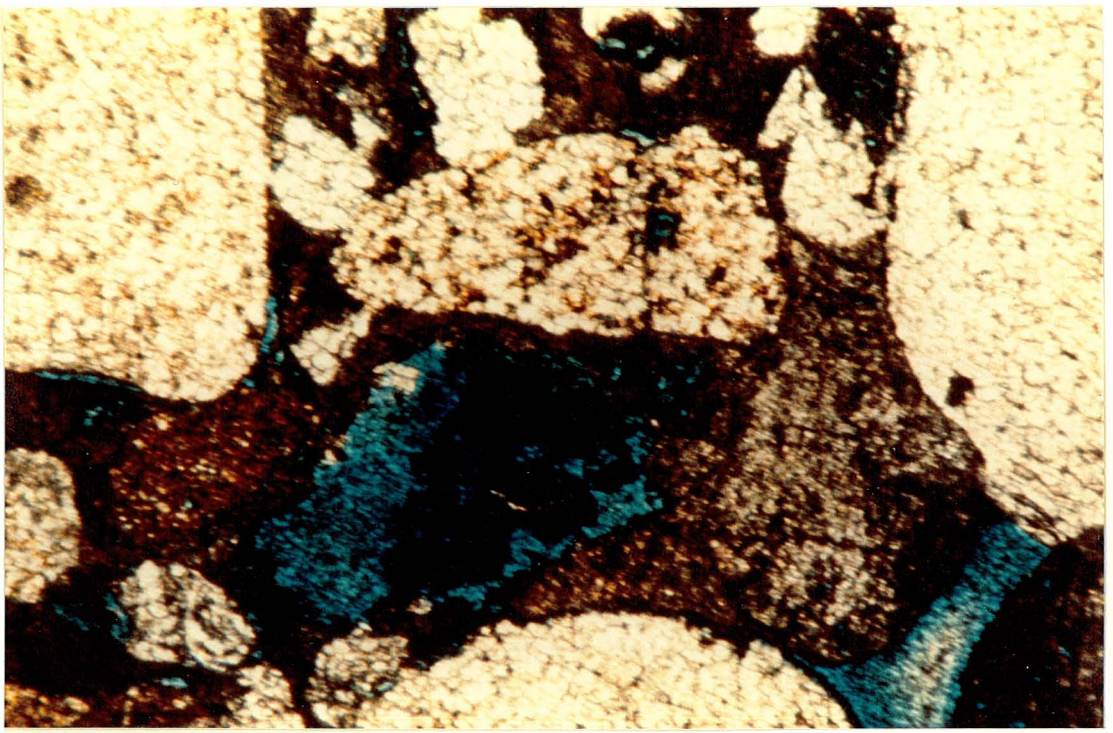

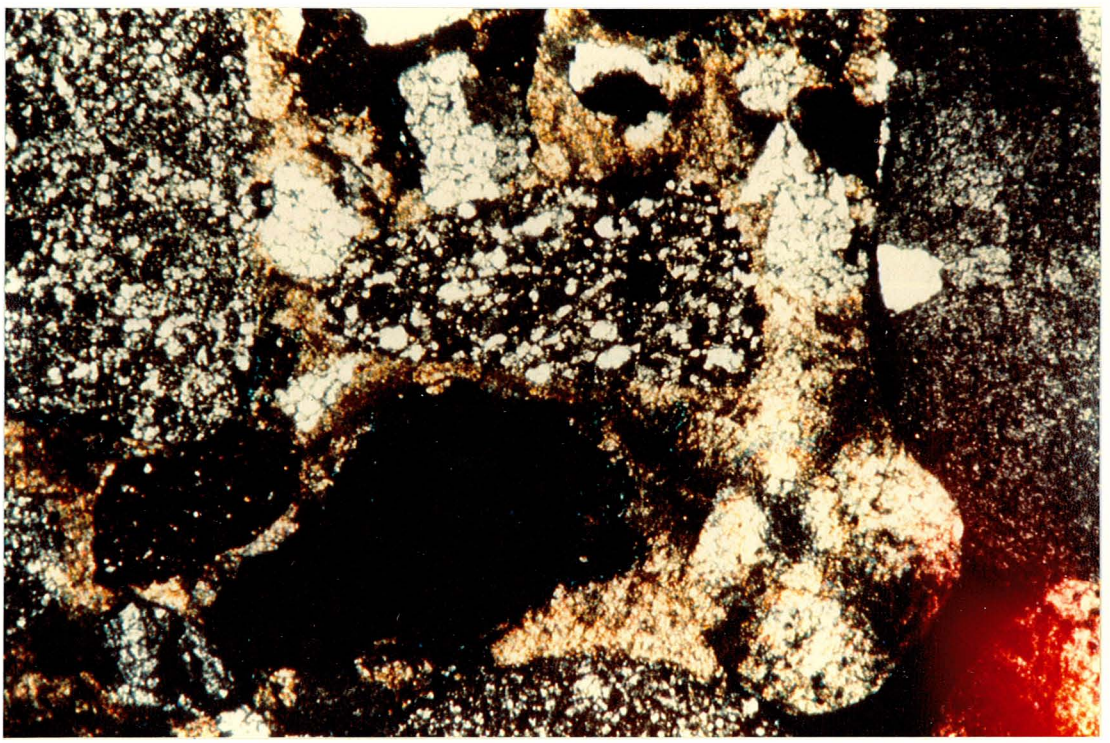

PLATE 14A : Thin Section 10-22-36-8W5 8660.5 ft
Caroline Field, magnification 63x.
Plain light photograph of siderite
cemented conglomeratic sandstone.
Note the three blades of muscovite
wedged between two chert clasts.

PLATE 14B : Same as above, but with crossed
nicols. Note the high pinkish
yellow birefringence of muscovite.

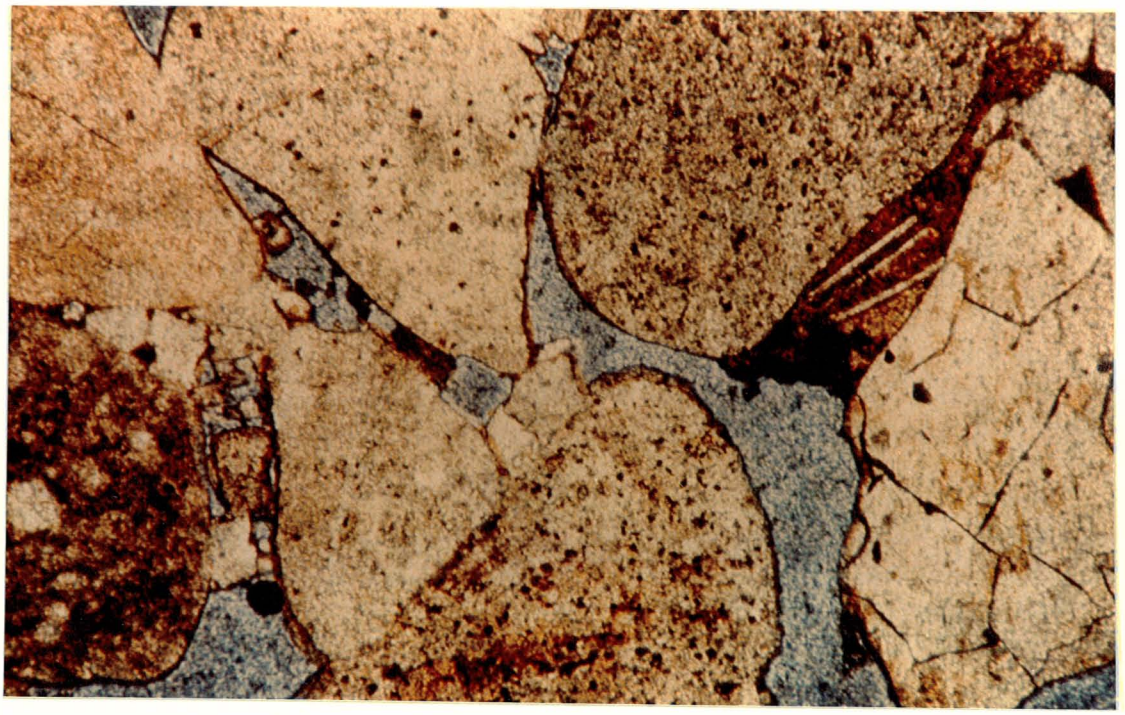

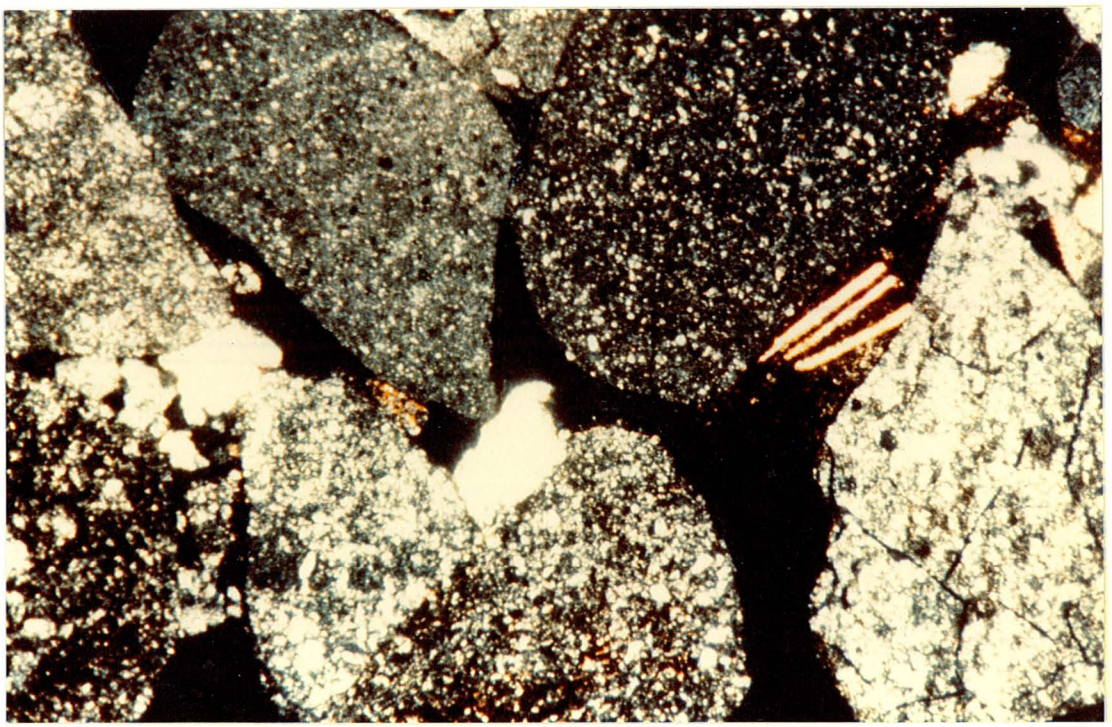

PLATE 15A : Thin Section 16-26-36-9W5 8889.0 ft Ricinus Field, magnification 160x. Crossed nicols photograph of plagioclase feldspar. Note that it is in equilibrium with the quartz and chert, but is being replaced by the siderite.

PLATE 15B : Thin Section 11-33-36-9W5 9442.0 ft Ricinus Field, magnification 160x. Crossed nicols photograph of silica cemented sandstone, containing a single blade of undeformed muscovite. Note the perfect cleavage parallel to the grain boundary.

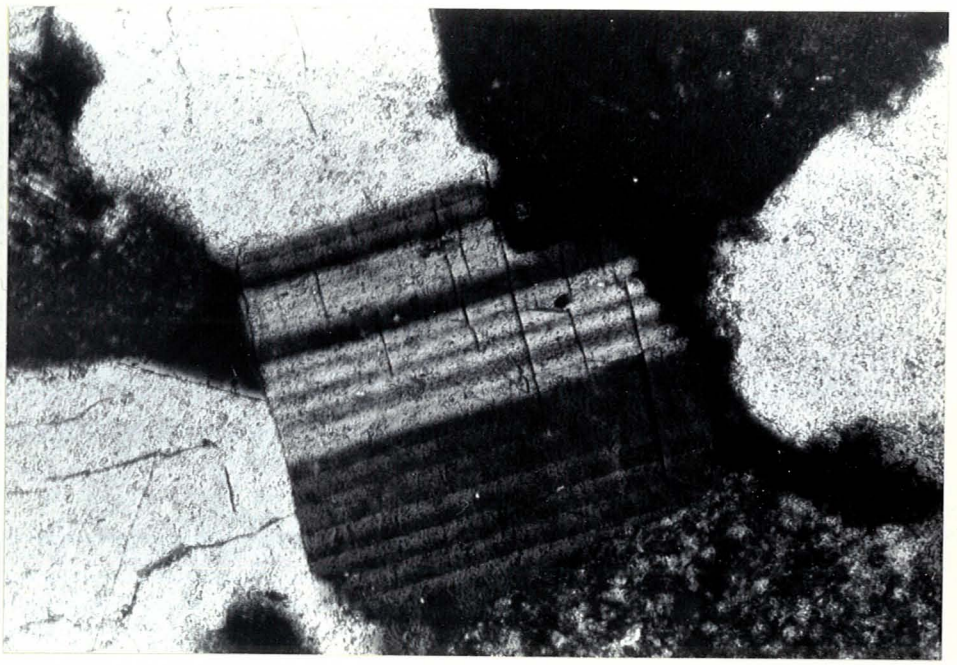

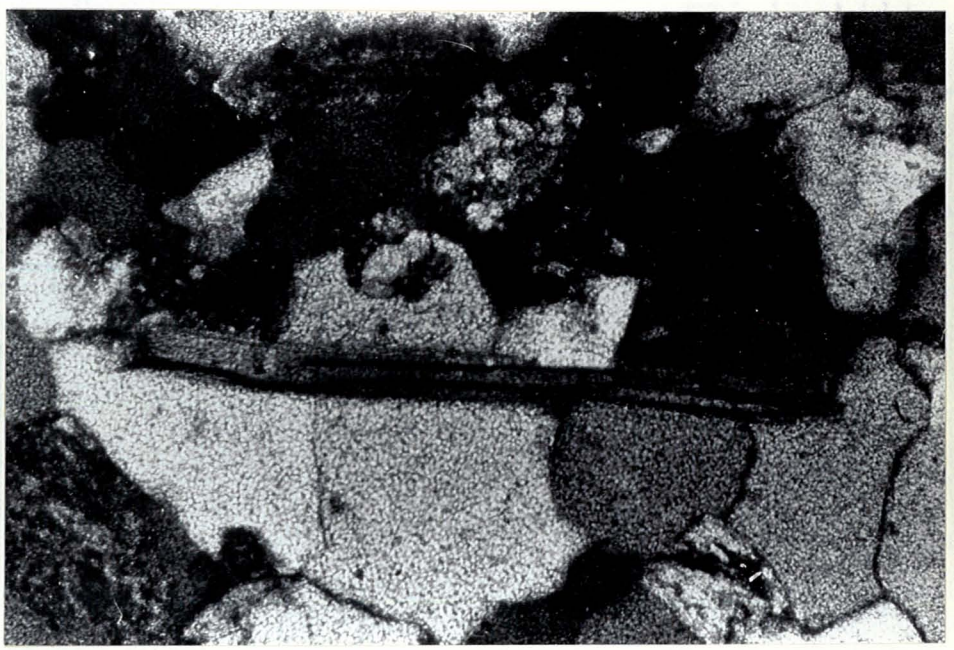

PLATE 16A : Thin Section 7-9-33-7W5 6555.0 ft
Ricinus Field, magnification 160x.
Crossed nicols photograph of chert
altering to radially fibrous
chalcedony.

PLATE 16B : Thin Section 7-9-33-7W5 6555.0 ft
Ricinus Field, magnification 160x.
Crossed nicols photograph of chert
altering to "zebraic" chalcedony.

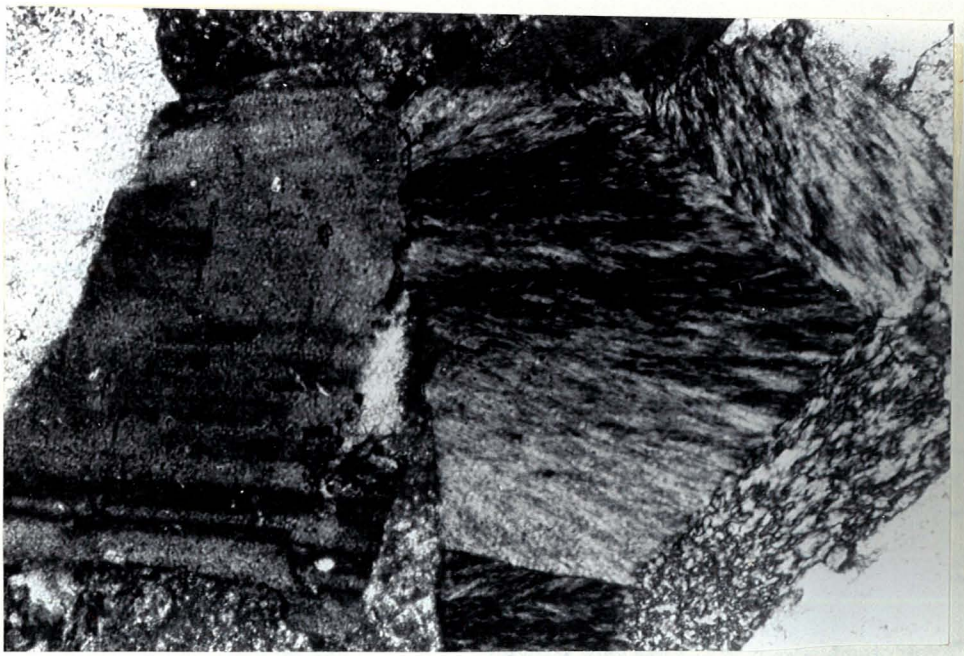

PLATE 17A : Thin Section 7-28-34-8W5 5855.0 ft Ricinus Field, magnification 50x. Plain light photograph of chert filling a void. The void was first lined with several generations of chert alternating with hematite or siderite invaded chert, as pore fluids changed compositions.

PLATE 17B : Same as above, but under crossed nicols. Note how chert has altered to chalcedony, oriented normal to what must have been the original cavity wall.

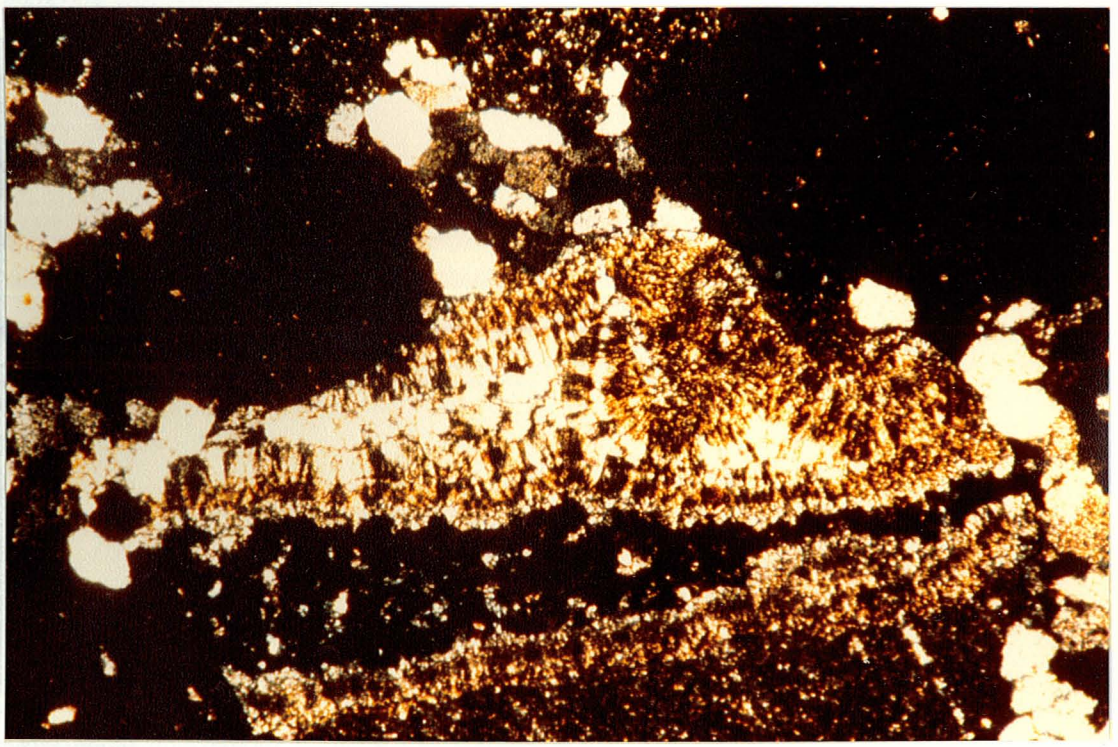

PLATE 18A : Same as previous photograph, but under cathode luminescence. Note that the fragment contains zones which have been truncated, indicating its allochthonous nature.

PLATE 18B : Thin Section 16-9-35-6W5 7742.01 ft Caroline Field, magnification 50x. Plain light photograph of a composite clast of chert being invaded by the pore fluids and removing impurities.

PLATE 19A : Thin Section 16-9-35-6W5 7742.01 ft Caroline field, magnification 50x. Crossed nicols photograph of composite chert clast being invaded by pore fluids. Note in particular the characteristic pinhead extinction of chert.

PLATE 19B : Same as above, but under cathode luminescence. Again, note multiple stages of silica cements, as well as the infrequent grain embayments.

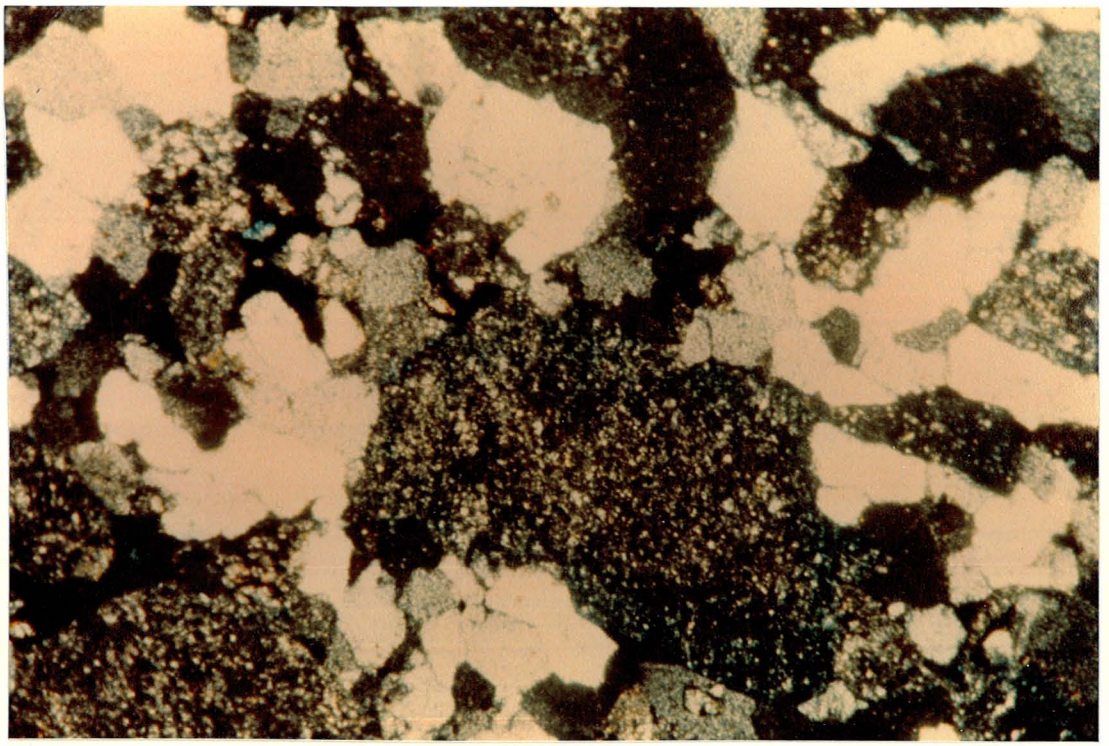

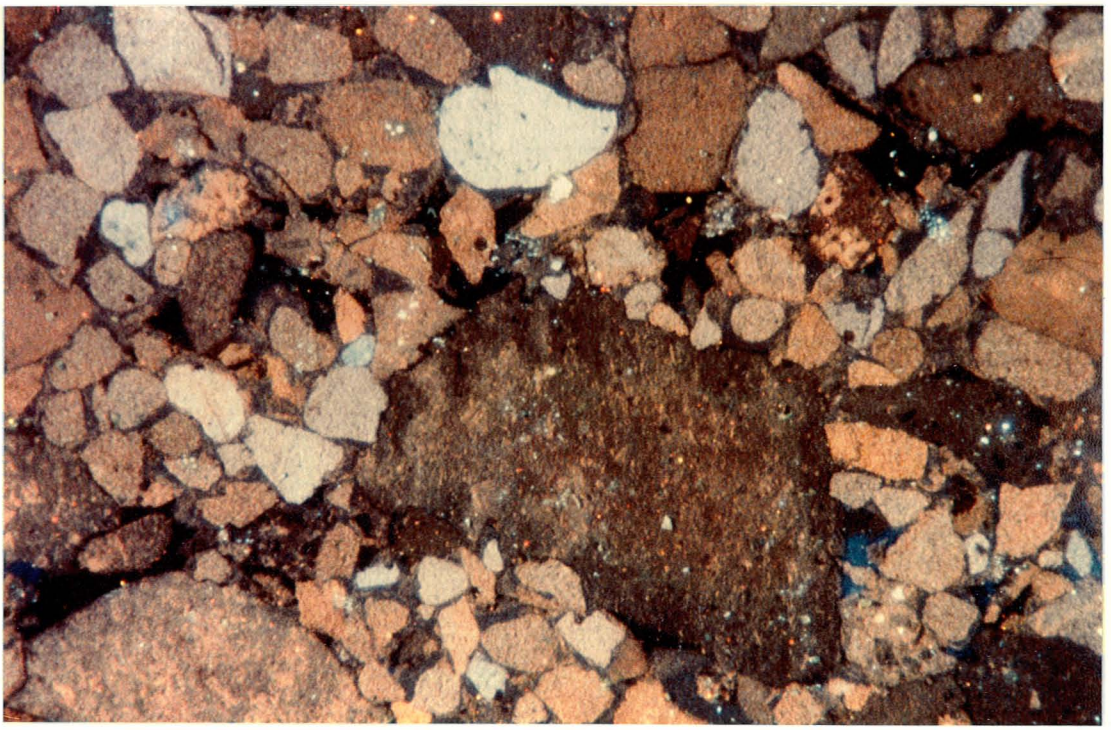

PLATE 20A : Thin Section 16-12-34-4W5 6611.0 ft
Garrington Field, magnification 63x.
Crossed nicols photograph of a grain
of metamorphic quart. Note the drawn
out texture of the subgrains.

PLATE 20B : Thin Section 7-9-33-7W5 6565.0 ft
Ricinus Field, magnification 63x.
Crossed nicols photograph of a fine
grained sandstone containing a small
pelecypod fragment.

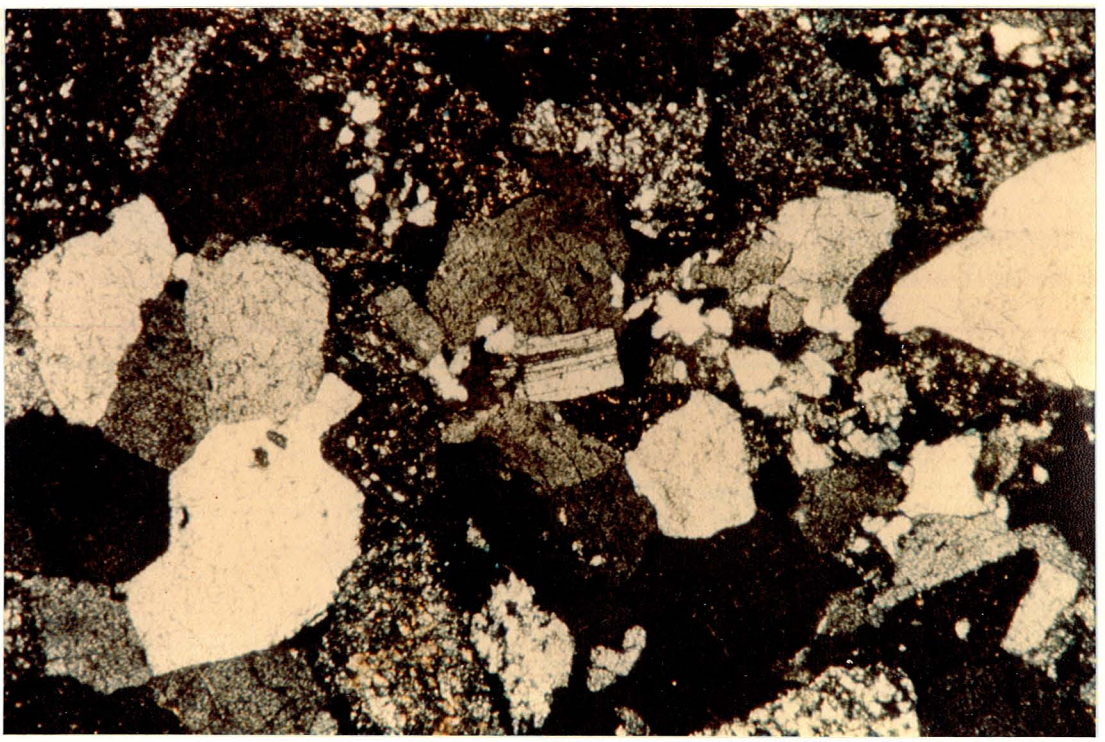

PLATE 21A : Thin Section 16-12-34-4W5 6611.0 ft Garrington Field, magnification 50x. Plain light photograph of a composite chert clast containing rock fragment and siderite inclusions.

PLATE 21B : Same as above, but under cathode luminescence. An unknown mineral associated with rock fragments gives off a bright yellow-white luminescence. Note extensive fracturing extending beyond individual grain boundaries.

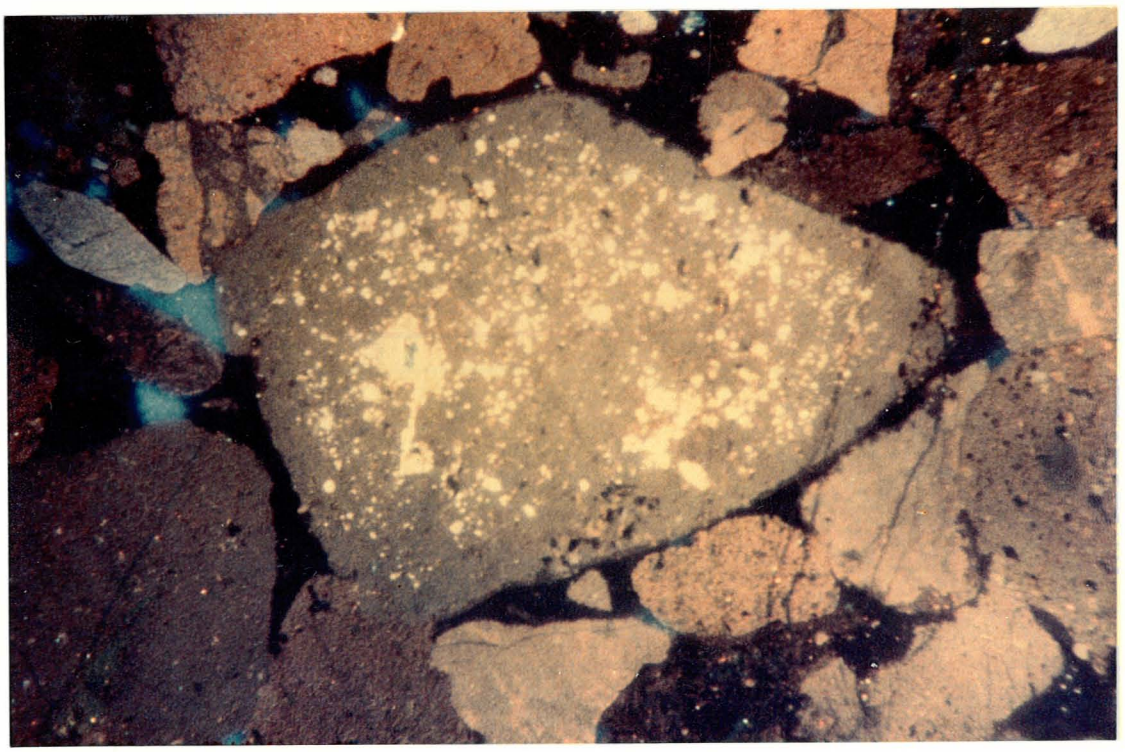

PLATE 22A : Thin Section 16-6-34-3W5 6538.0 ft Garrington Field, magnification 63x. Plain light photograph of a silica cemented quartz grain. Note the dust rims denoting the original grain boundary.

PLATE 22B : Thin Section 11-17-35-8W5 9274.0 ft Caroline Field, magnification 160x. Plain light photograph of a silica cemented quartz grain. Note the dust rim and the sutured contacts between cemented grains.

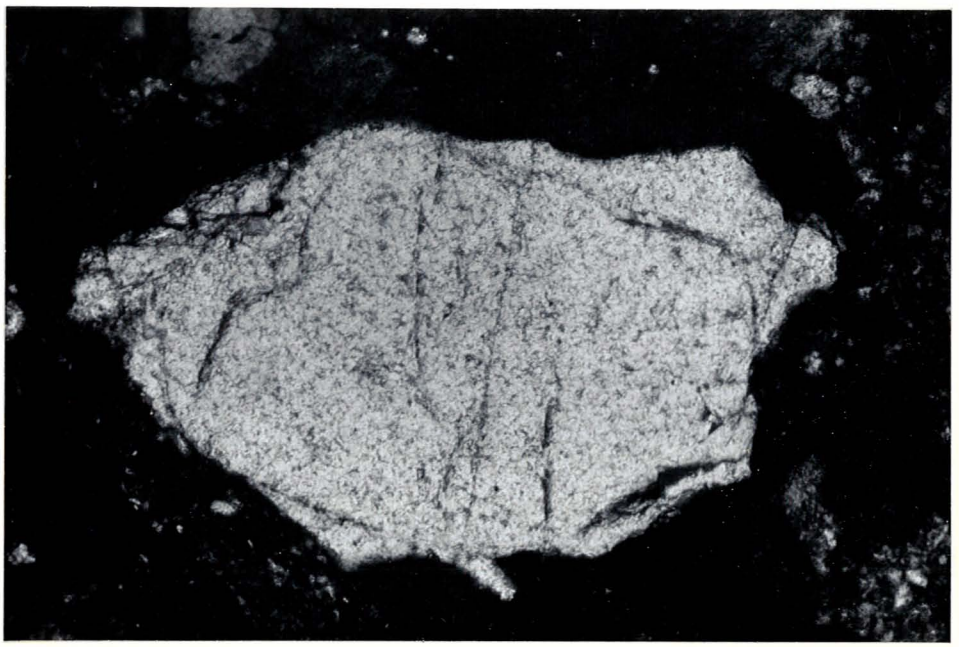

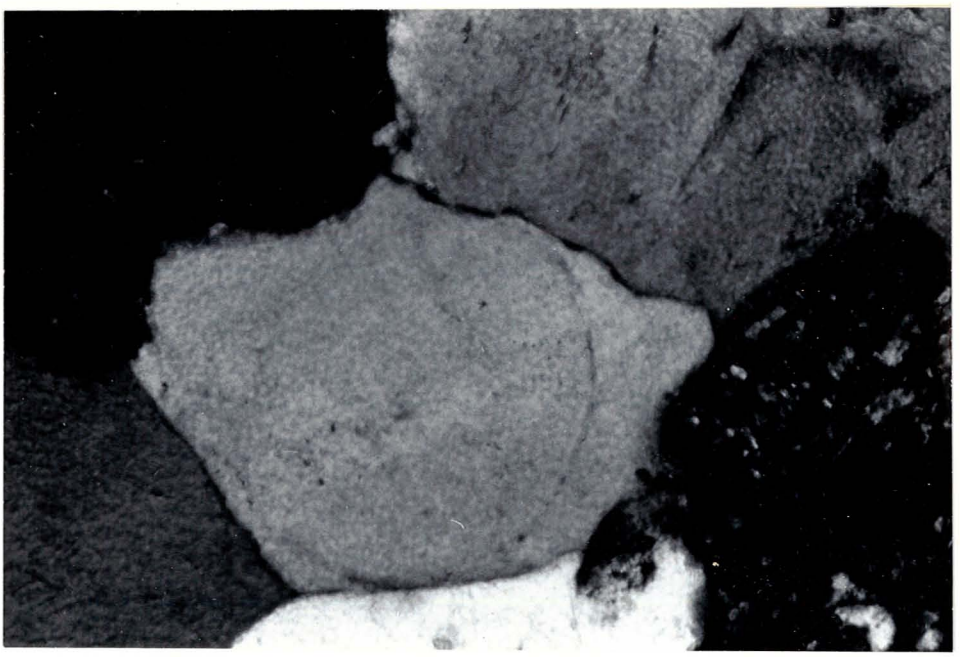

PLATE 23A : Thin Section 11-21-34-8W5 7081.0 ft Ricinus Field, magnification 63x. Crossed nicols photograph of authigenic pyrite. Note the euhedral cubic habit of the crystals.

PLATE 23B : Thin Section 11-21-34-8W5 7081.0 ft Ricinus Field, magnification 63x. Crossed nicols photograph of authigenic pyrite replacing pyrite, and filling pore space.

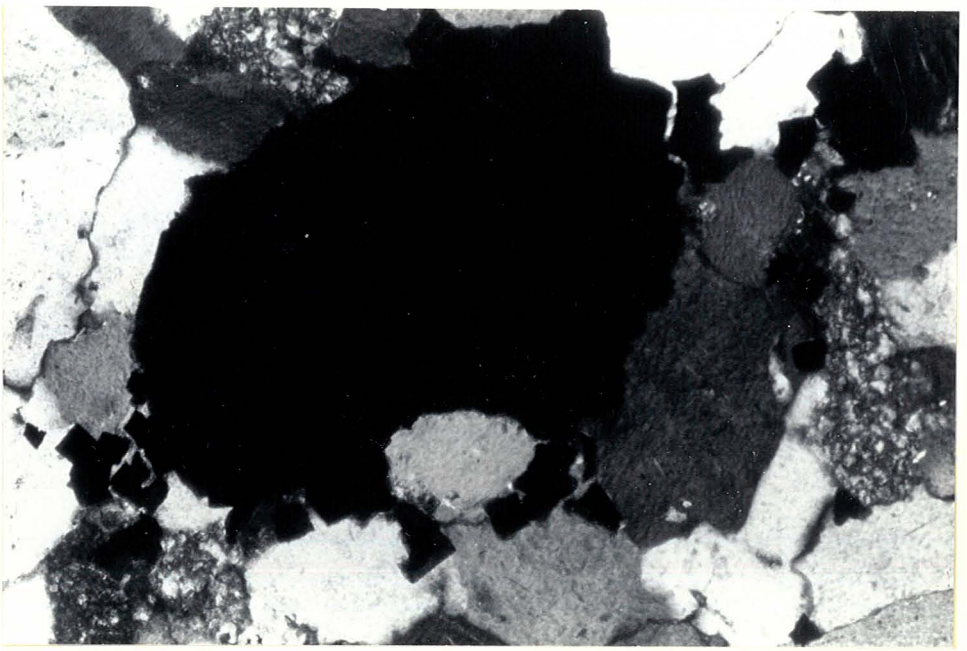

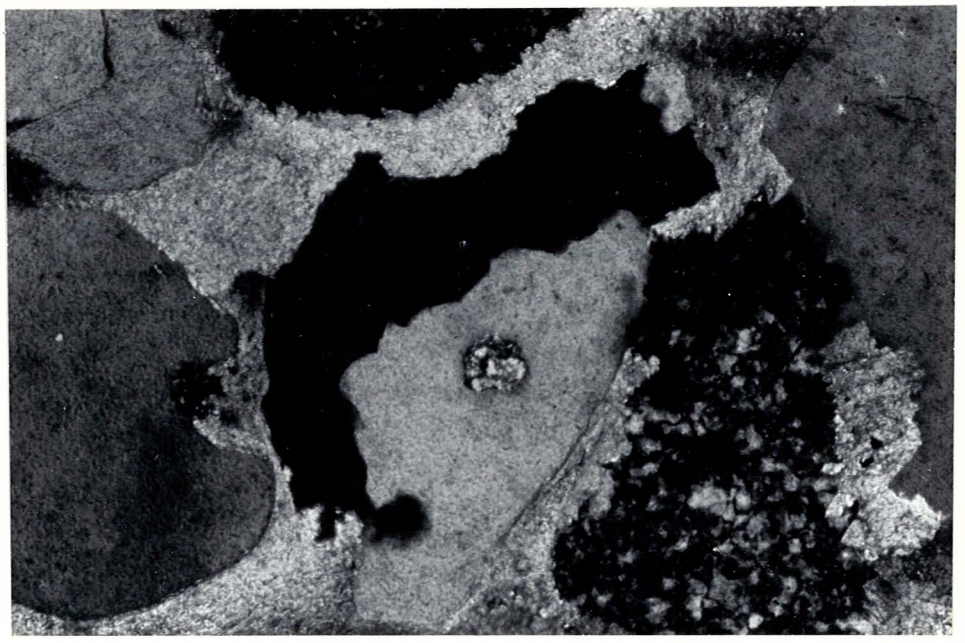

PLATE 24A : Thin Section 7-28-34-8W5 5802.0 ft
Ricinus Field, magnification 160x.
Plain light photograph of concentric fractures in calcite cement. The chert fragment may be recrystalizing to chalcedony and stressing the tightly binding cement.

PLATE 24B : Thin Section 4-21-37-6W5 7174.0 ft
Garrington Field, manification 160x.
Crossed nicols photograph of the formation of styloliths, a pressure solution phenomenon.

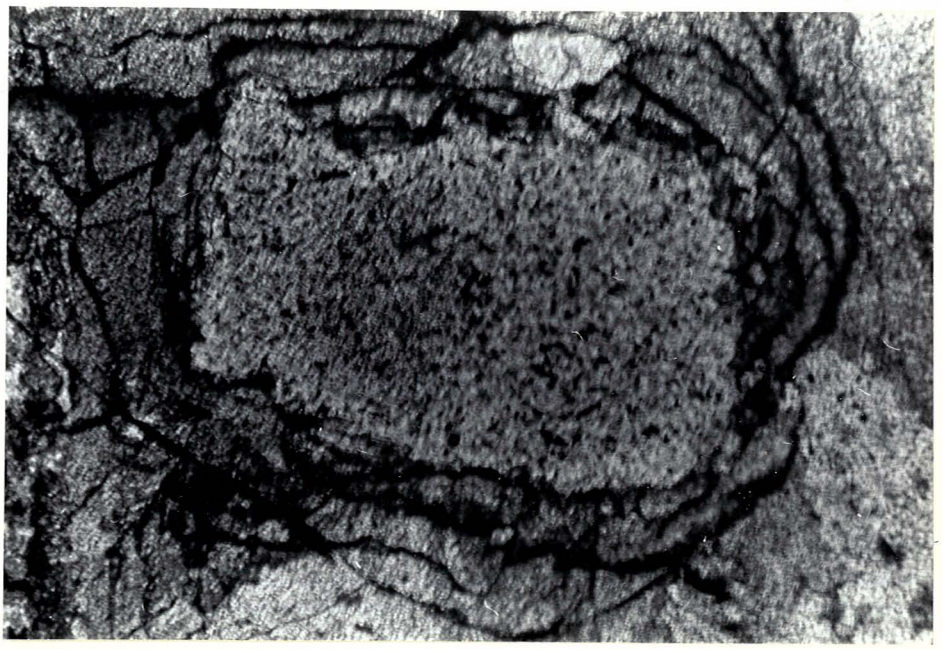

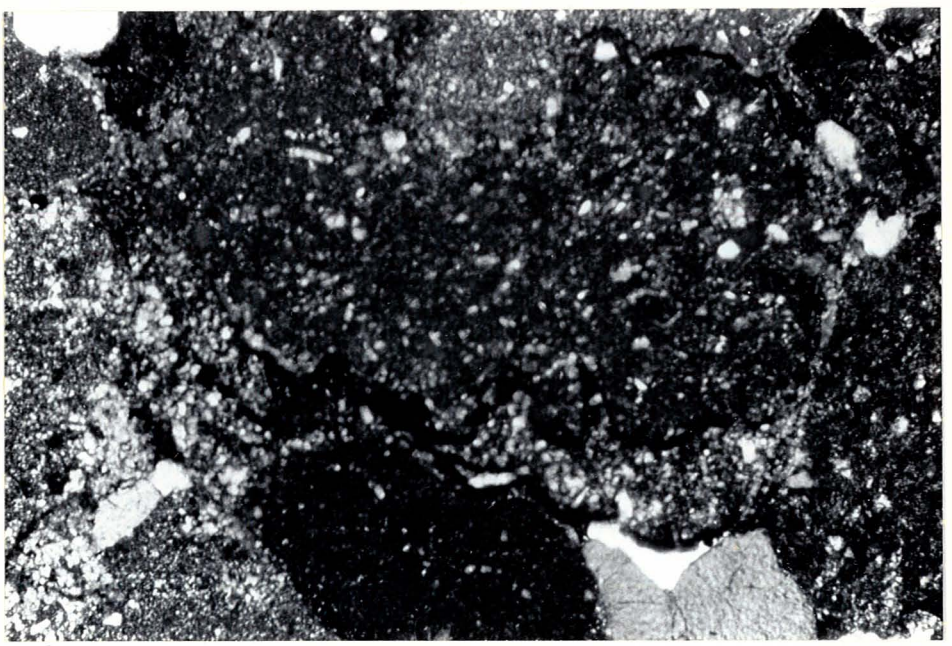

PLATE 25A : Thin Section 11-17-35-8W5 9267.5 ft
Ricinus Field, magnification 63x.
Plain light photograph of a siderite invaded chert clast, containing intersecting fractures, infilled by quartz.

PLATE 25B : Same as above, but with crossed nicols.

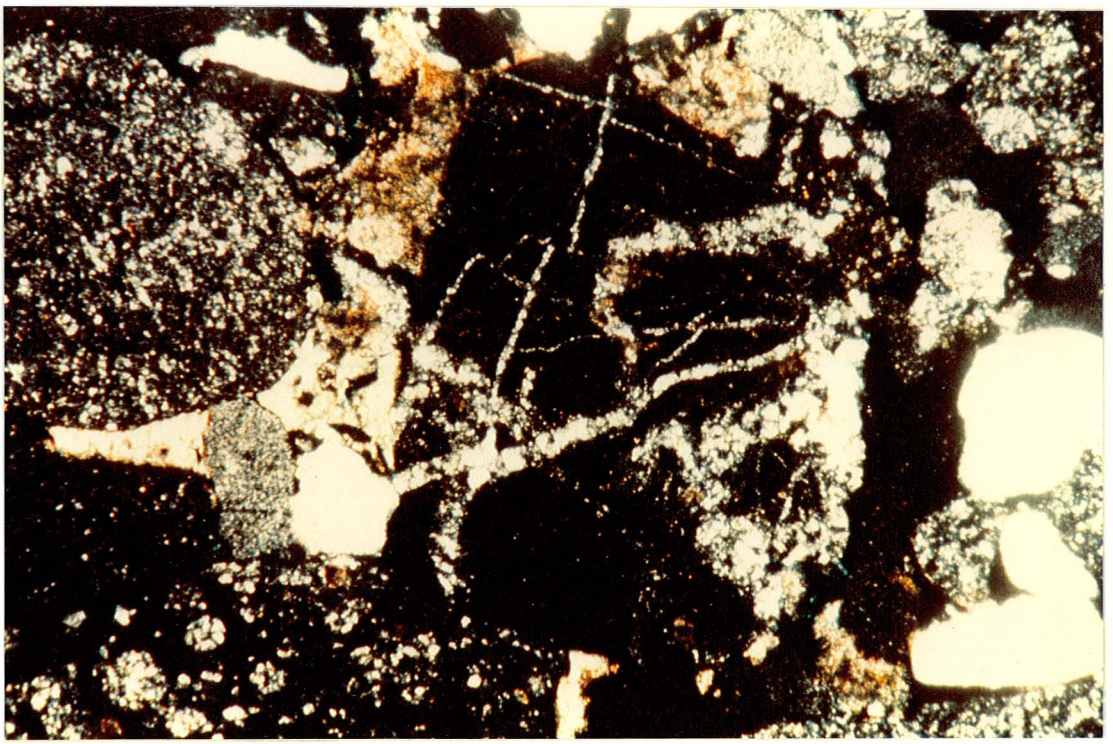

PLATE 26A : Thin Section 7-28-34-8W5 5855.0 ft Ricinus Field, magnification 50x. Crossed nicols photograph of a siderite invaded chert clast, containing linear fractures with sub-parallel orientations. "Combstooth" quartz fills these fractures.

PLATE 26B : Same as above, but under cathode luminescence. Note that the fractures show the characteristic blue-black luminesce of silica cement. Also evident are sutured contacts between the composite chert clasts.

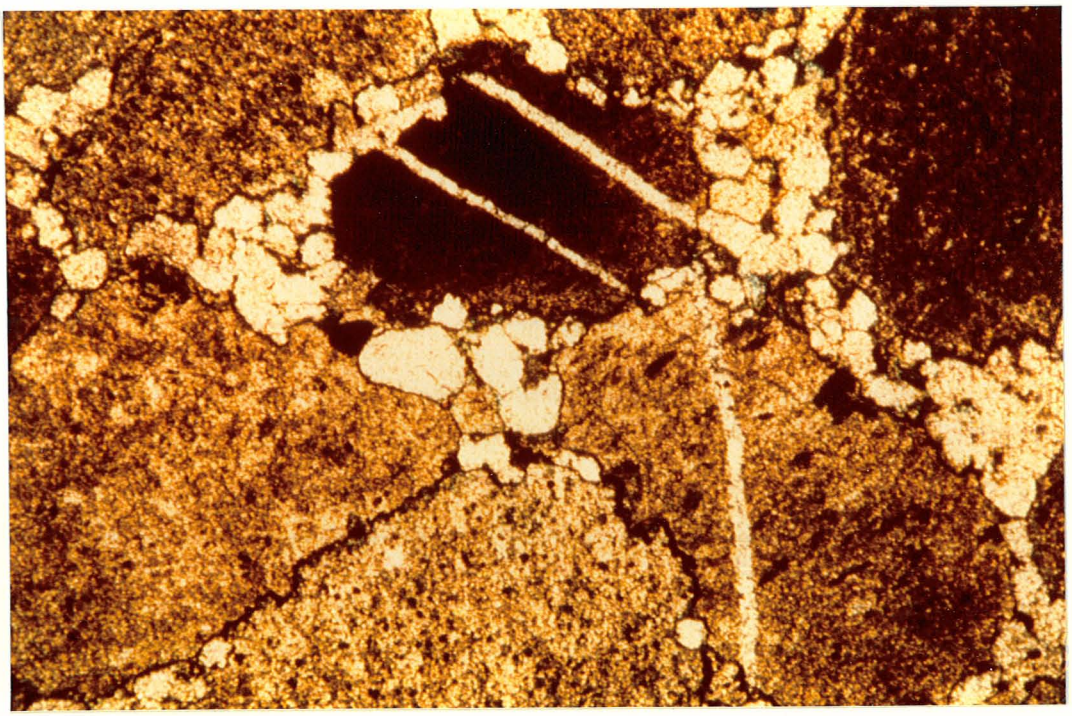

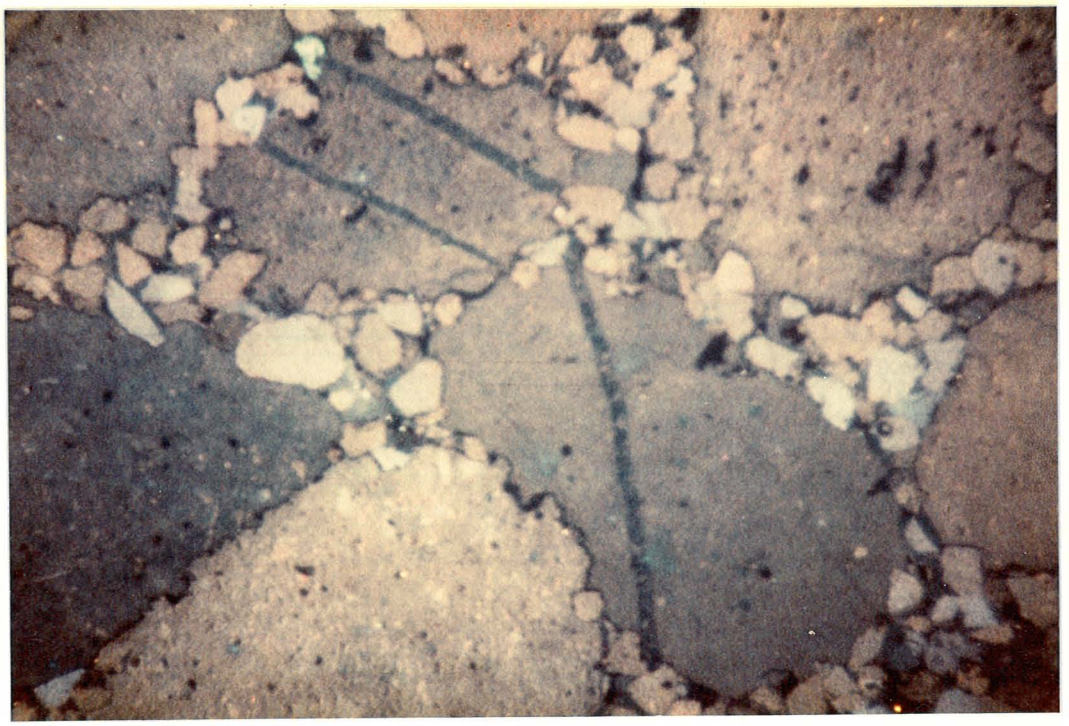

PLATE 27A : Thin Section 16-12-34-4W5 6611.01 ft Garrington Field, magnification 63x. Plain light photograph of fluids exploiting fractures in a chert clast. This is one of several type of secondary porosity.

PLATE 27B : Same as above, but with crossed nicols.

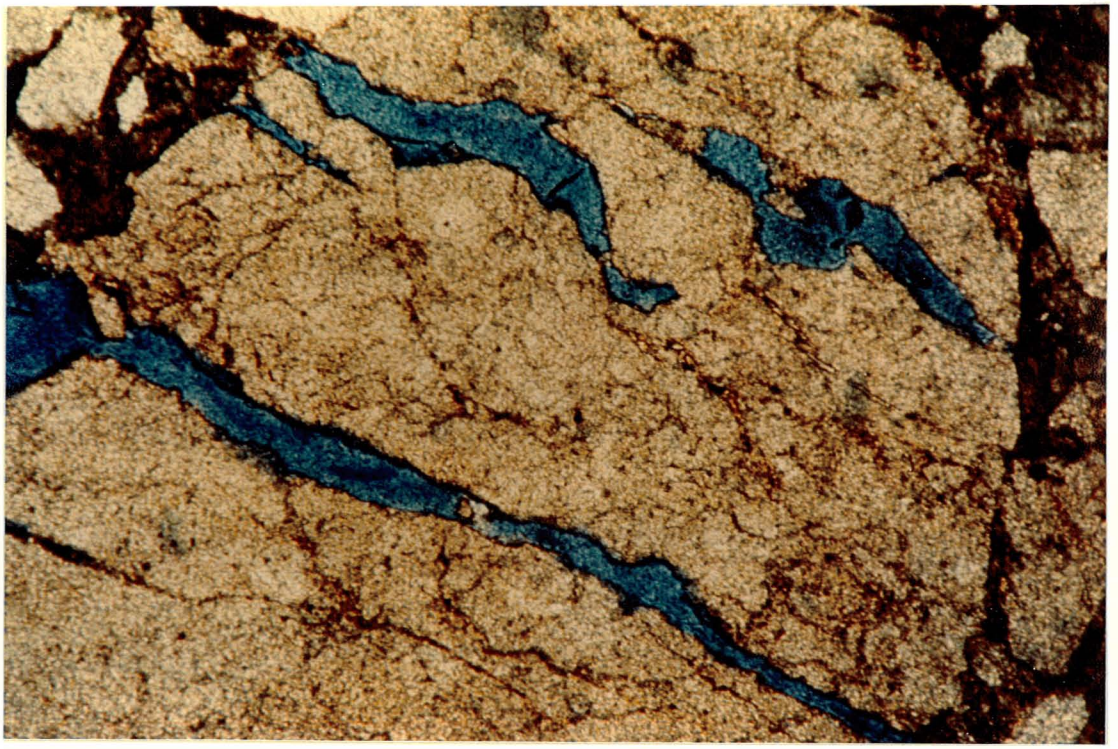

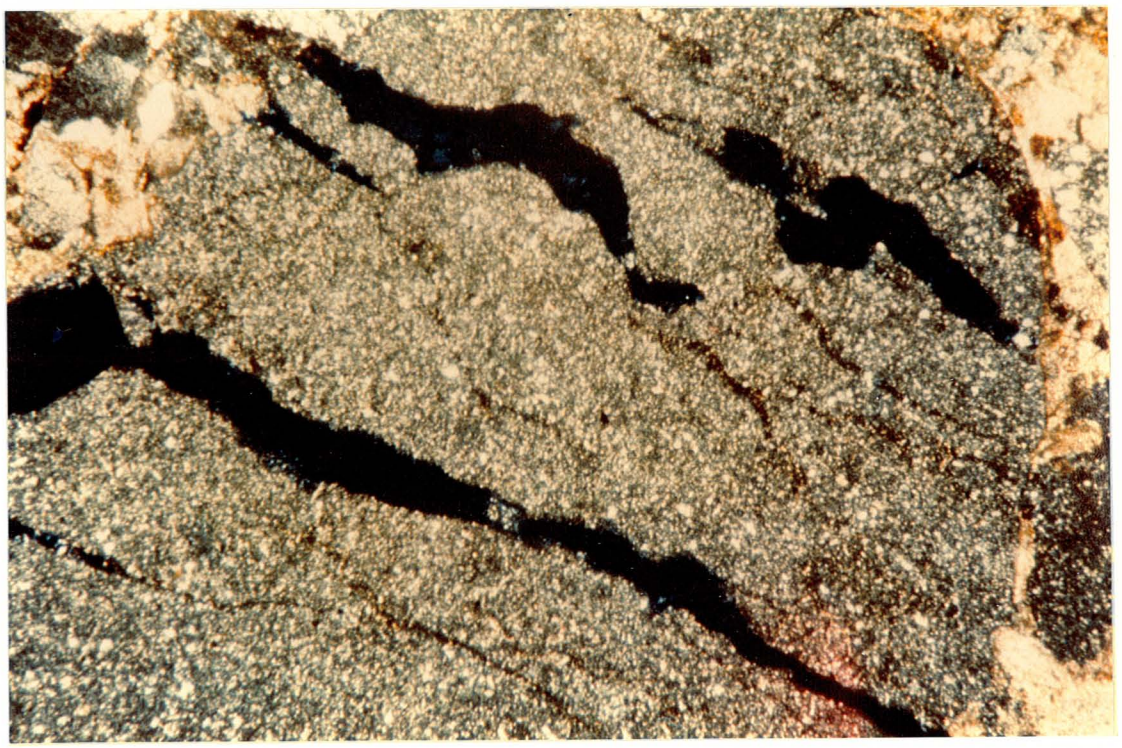

PLATE 28A : Thin Section 3-23-36-8W5 8535.5 ft
Caroline Field, magnification 50x.
Plain light photograph of a composite chert clast containing biogenic remains. Sponge spicules and crinoid stems are most evident.

PLATE 28B : Thin Section 16-12-34-4W5 6611.0 ft
Garrington Field, magnification 63x.
Crossed nicols photograph of siderite invaded chert, containing silicified foraminifera remains.

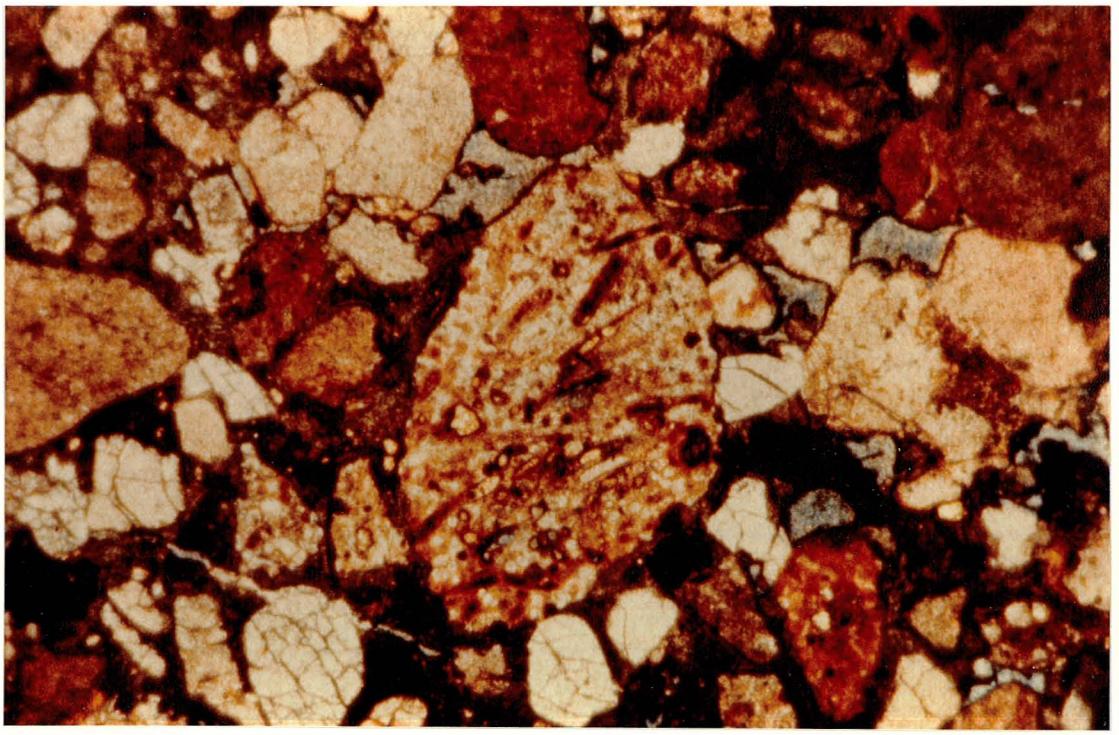

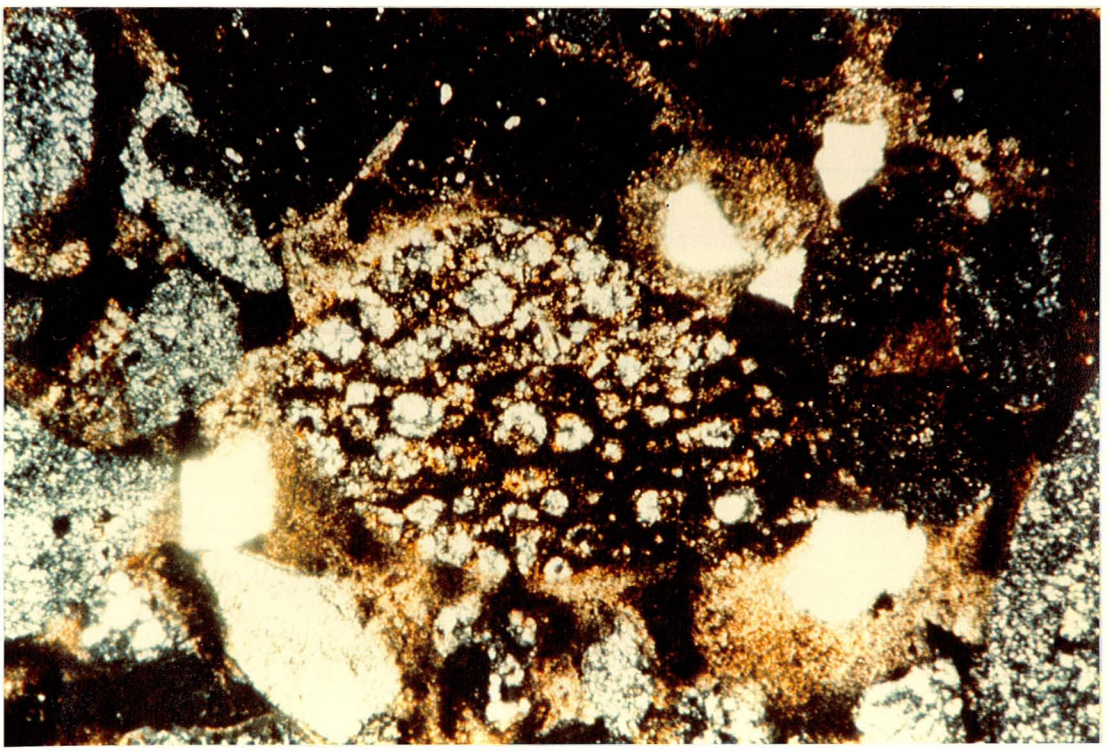

PLATE 29A : Thin Section 7-9-33-7W5 6565.0 ft Ricinus Field, magnification 50x. Plain light photograph of siderite invaded chert containing bryozoan and crinoid remains.

PLATE 29B : Same as above, but under crossed nicols.

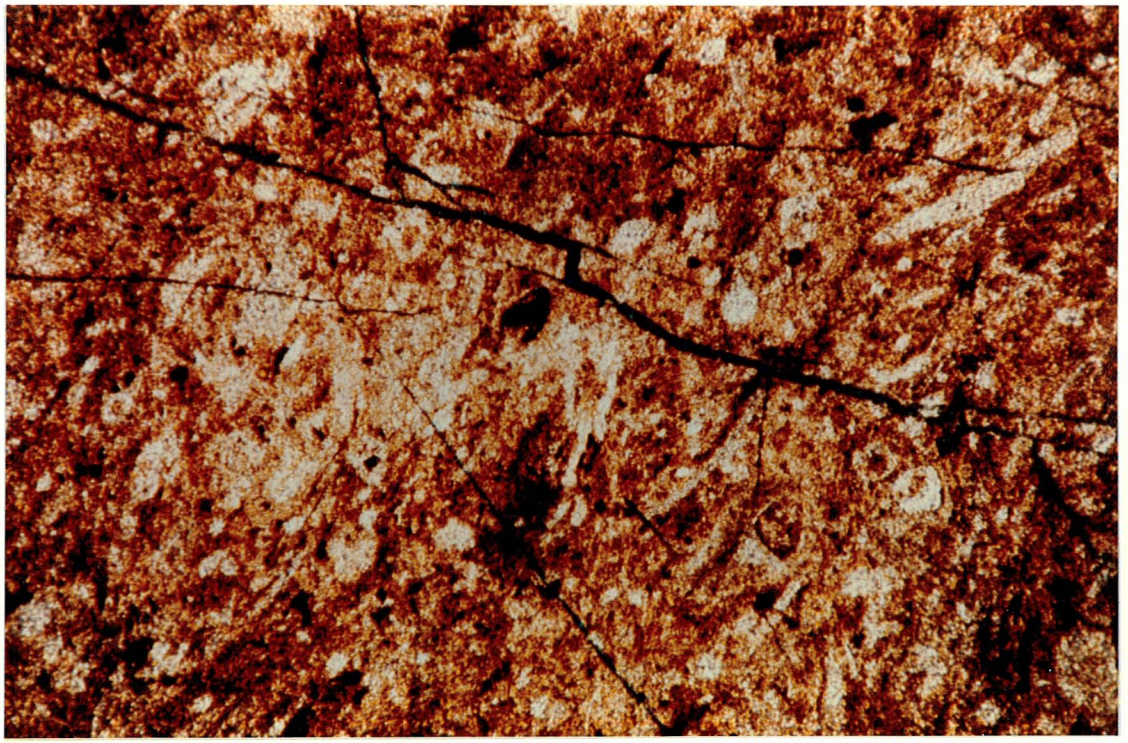

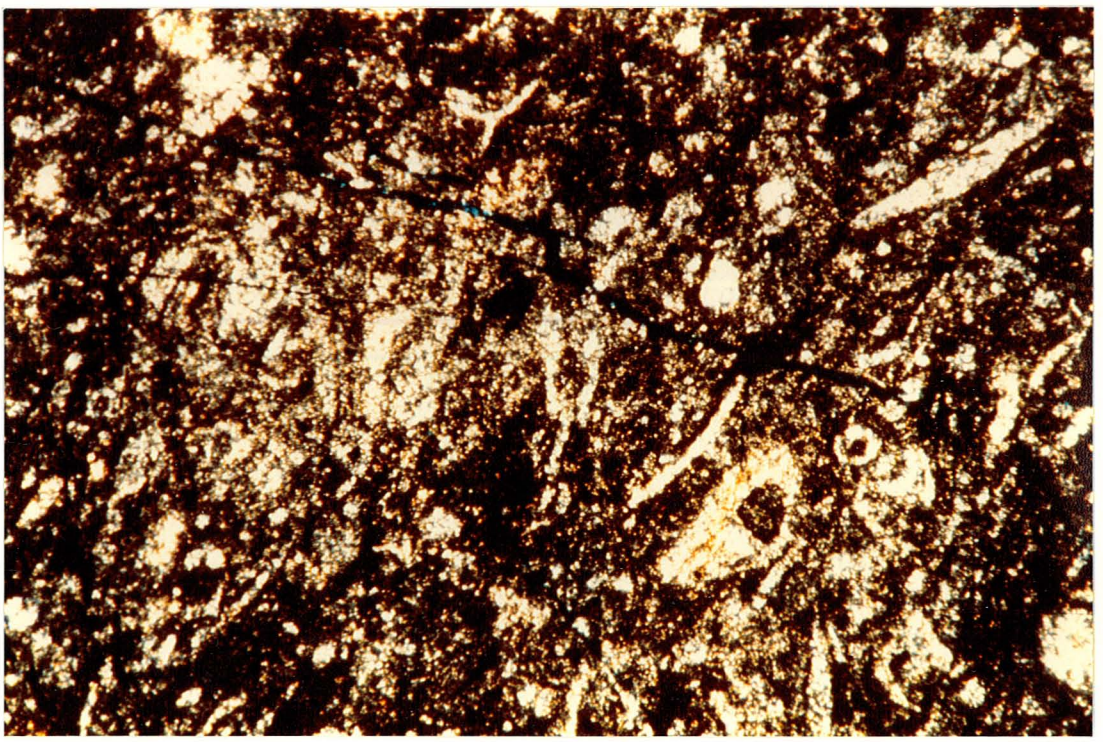

PLATE 30A : Thin Section 10-11-35-8W5 8378.0 ft Ricinus Field, magnification 63x. Crossed polars photograph of a chert clast containing silicified bryozoan remains.

PLATE 30B : Thin Section 10-22-36-8W5 8660.5 ft Caroline Field, magnification 50x. Crossed nicols photograph of a chert clast containing silicified crinoid and foraminifera remains. Note the radially fibrous siderite surrounding the chert clast.

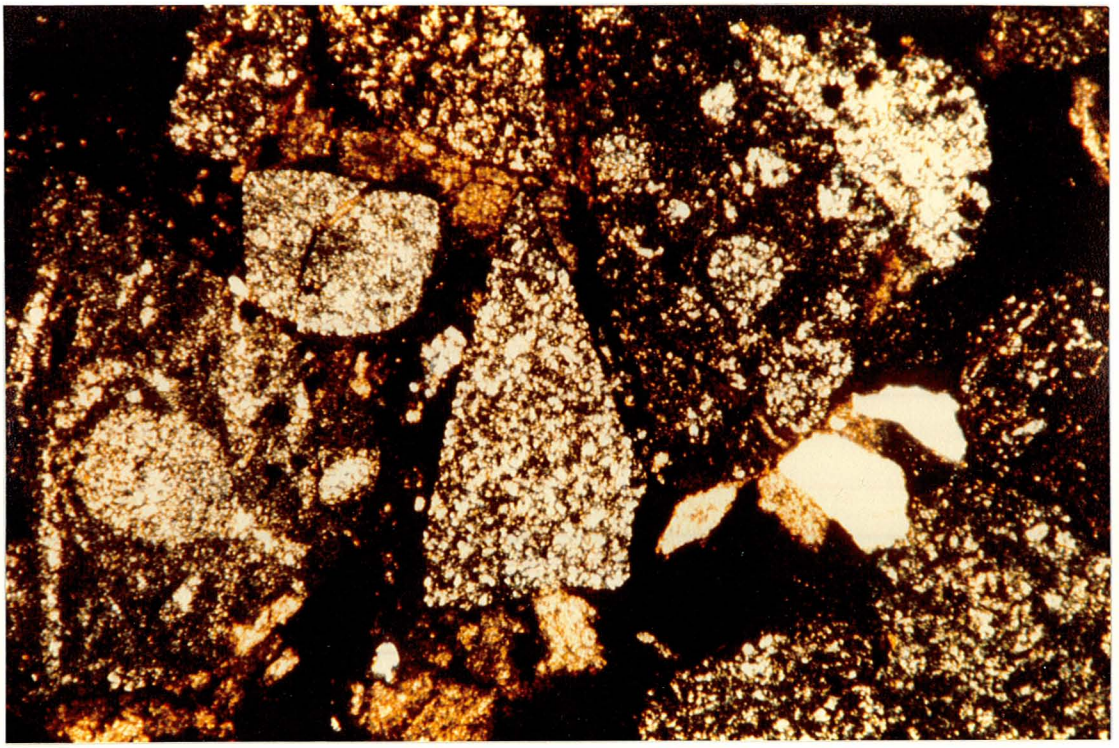

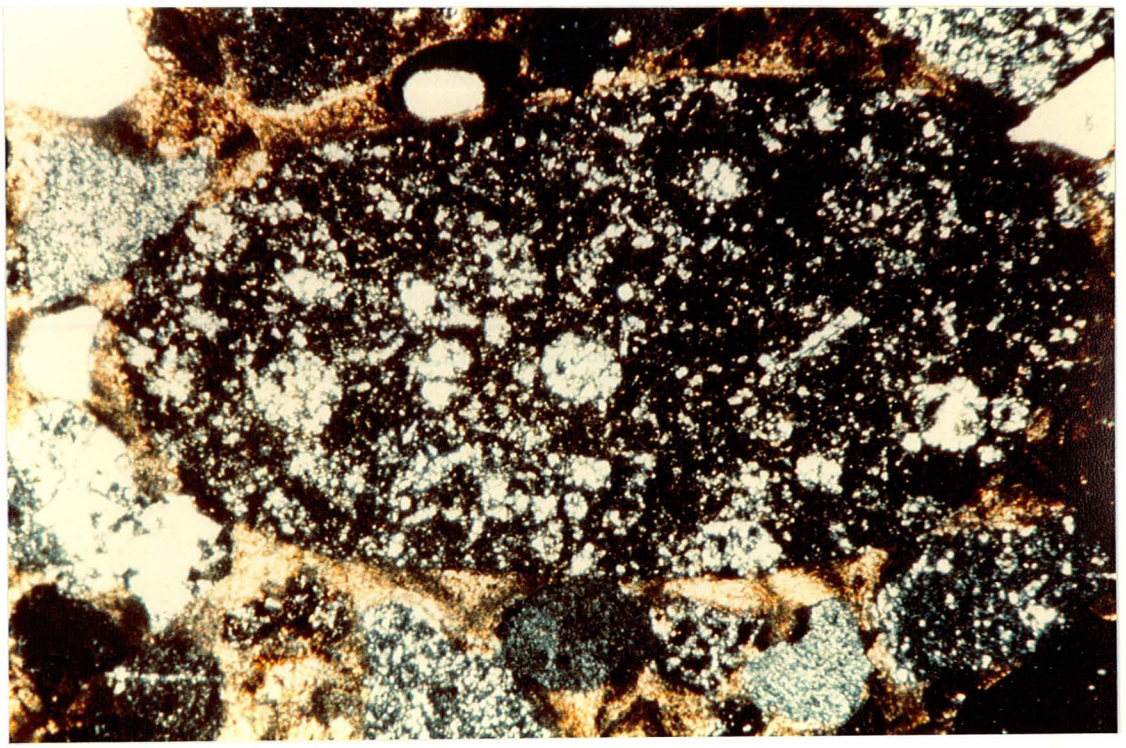

PLATE 31A : Thin Section 7-9-33-7W5 6565.0 ft
Ricinus Field, magnification 50x.
Crossed nicols photograph of a euhedral crystal of siderite having been replaced by pore fluids. Note that this has taken place in a lithifed chert clast, suggesting permiability. This is another example of secondary porosity.

PLATE 31B : Thin Section 10-11-35-8W5 8378.0 ft
Ricinus Field, magnification 50x.
Photograph under cathode luminescence, of a chert clasts containing abundant biogenic material. Sponge spicules and diatom remains are most apparent.

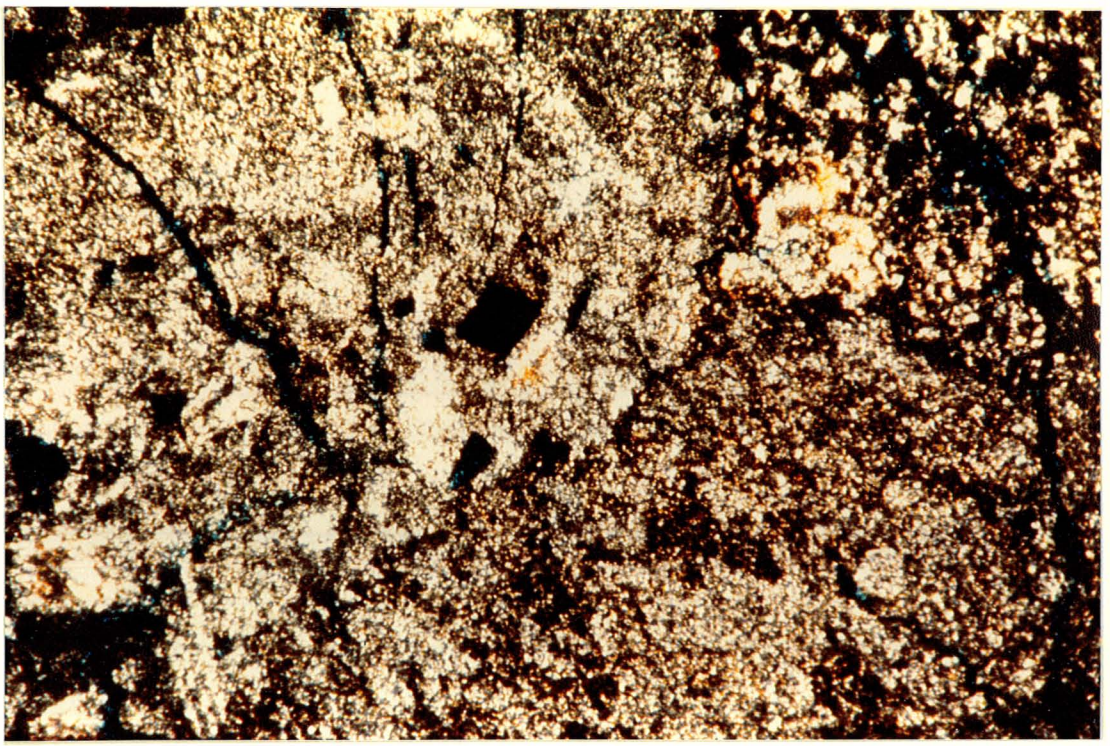

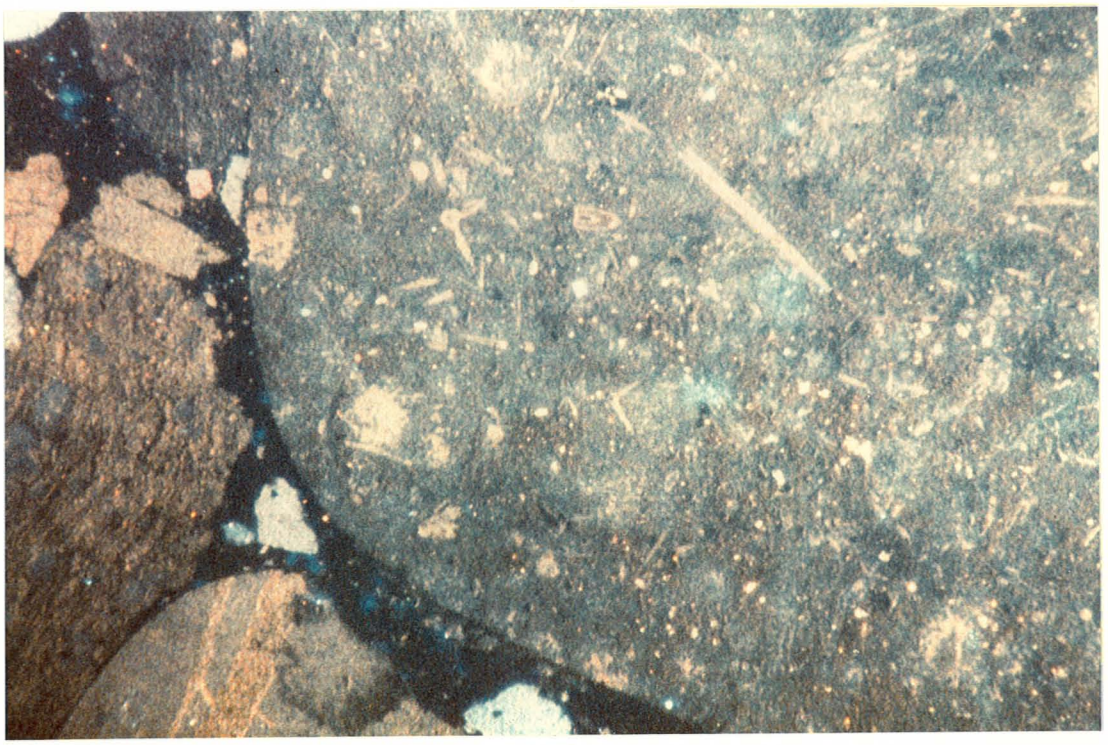

PLATE 32A : Thin Section 16-31-35-7W5 2540.79 m
Caroline Field, magnification 50x.
Plain light photograph of coarse sandstone, containing a poorly preserved plant fragment.

PLATE 32B : Same as above, but under cathode luminescence.

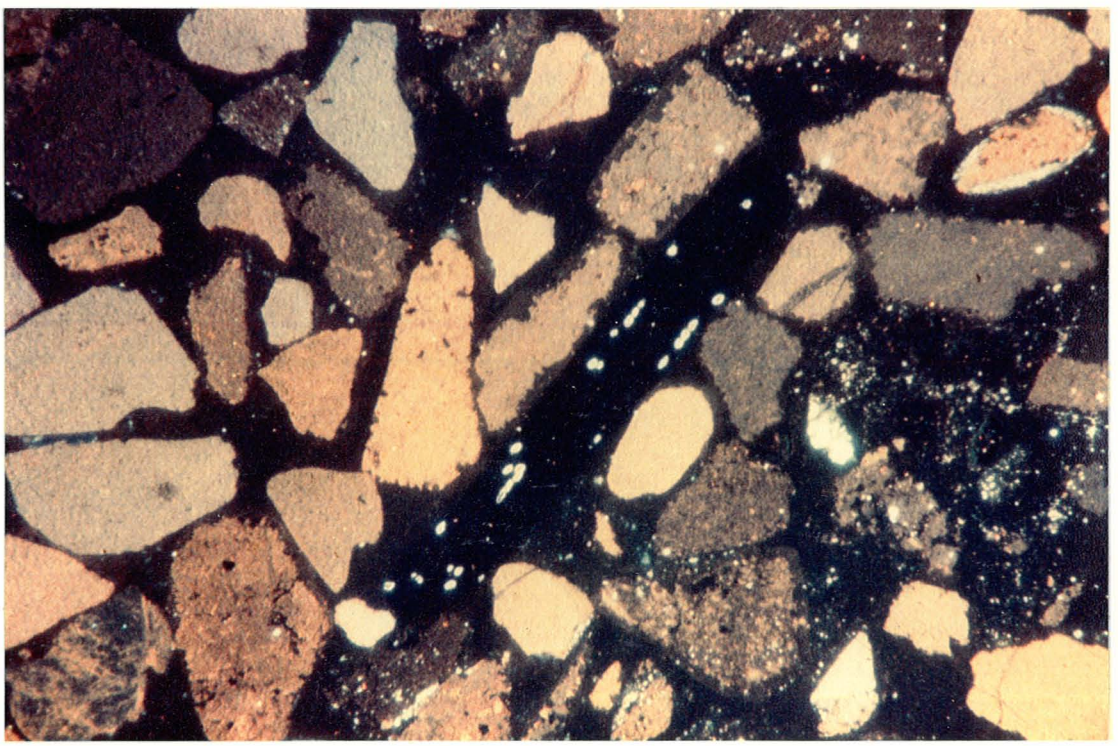

PLATE 33A : Thin Section 7-28-34-8W5 5855.0 ft Ricinus Field, magnification 50x. Crossed nicols photograph of silica cemented, coarse grained sandstone, containing a calcite pelecypod fragment. Note the growth laminations within the shell fragment.

PLATE 33B : Same as above, but under cathode luminescence.

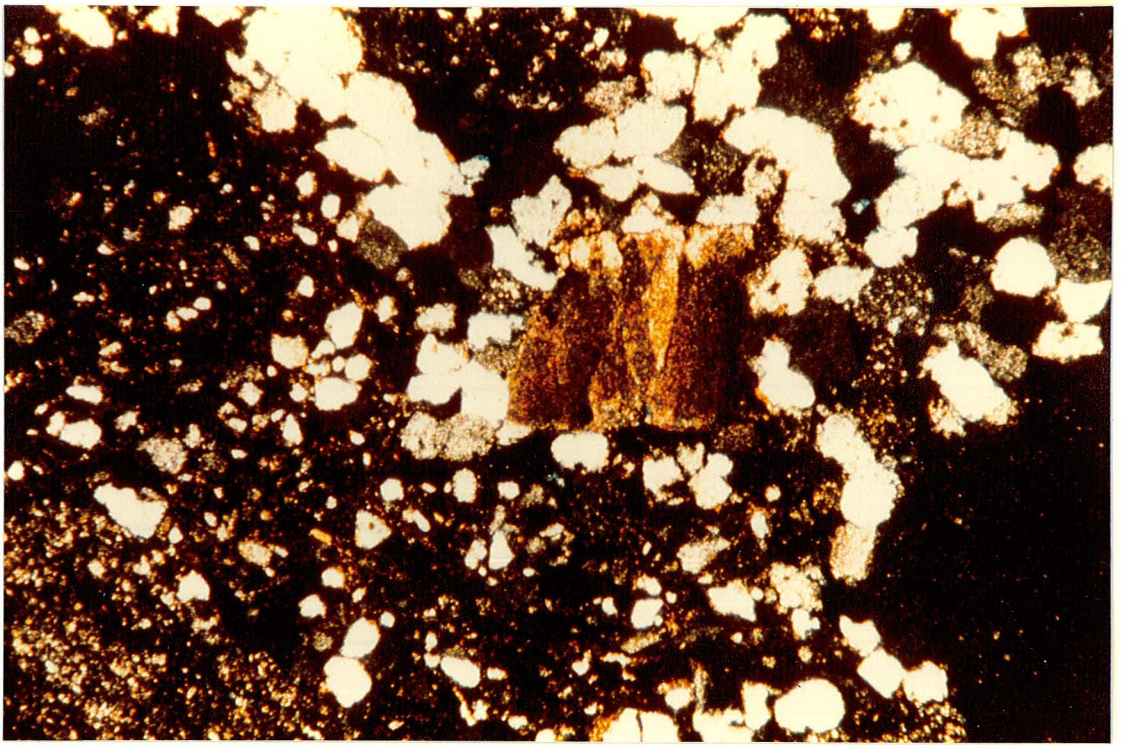

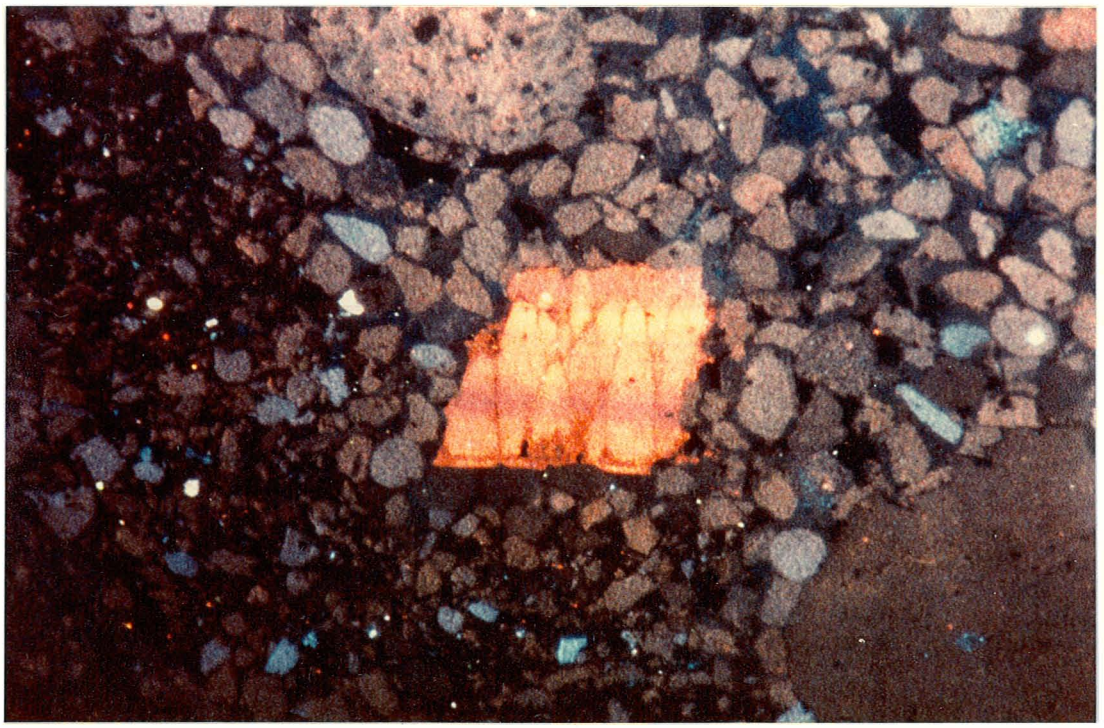

PLATE 34A : Thin Section 10-11-35-8W5 8378.0 ft
Ricinus Field, magnification 63x.
Plain light photograph of a silicified
pelecypod shell fragment.

PLATE 34B : Same as above, but under crossed
nicols.

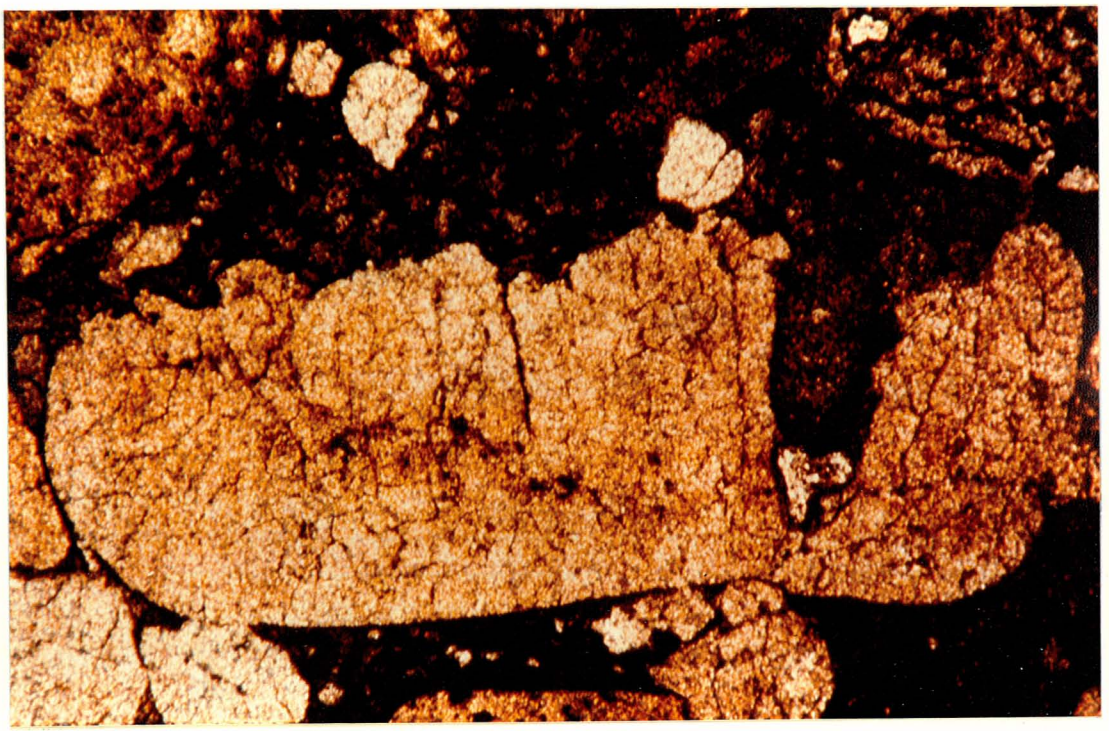

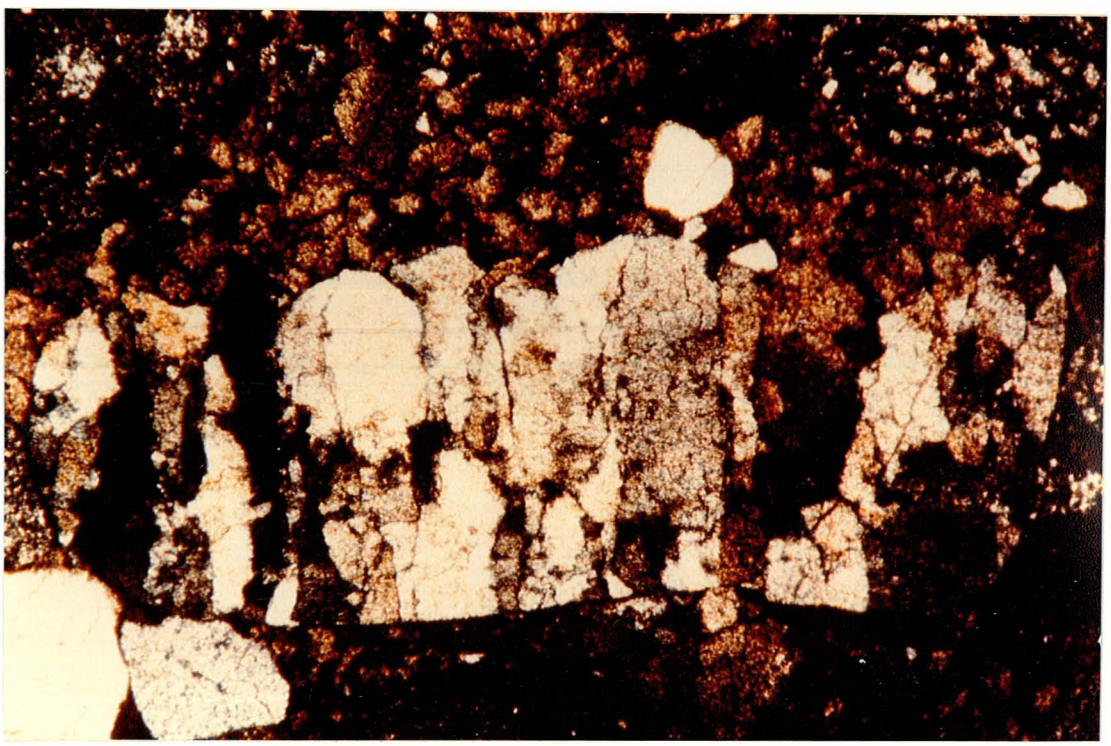

PLATE 35A : Thin Section 3-23-36-8W5 8535.5 ft (T/3) Caroline Field, magnification 63x. Plain light photograph of a composite chert clast composed of 80% chert, and 20% quartz grains.

PLATE 35B : Same as above, but under crossed nicols.

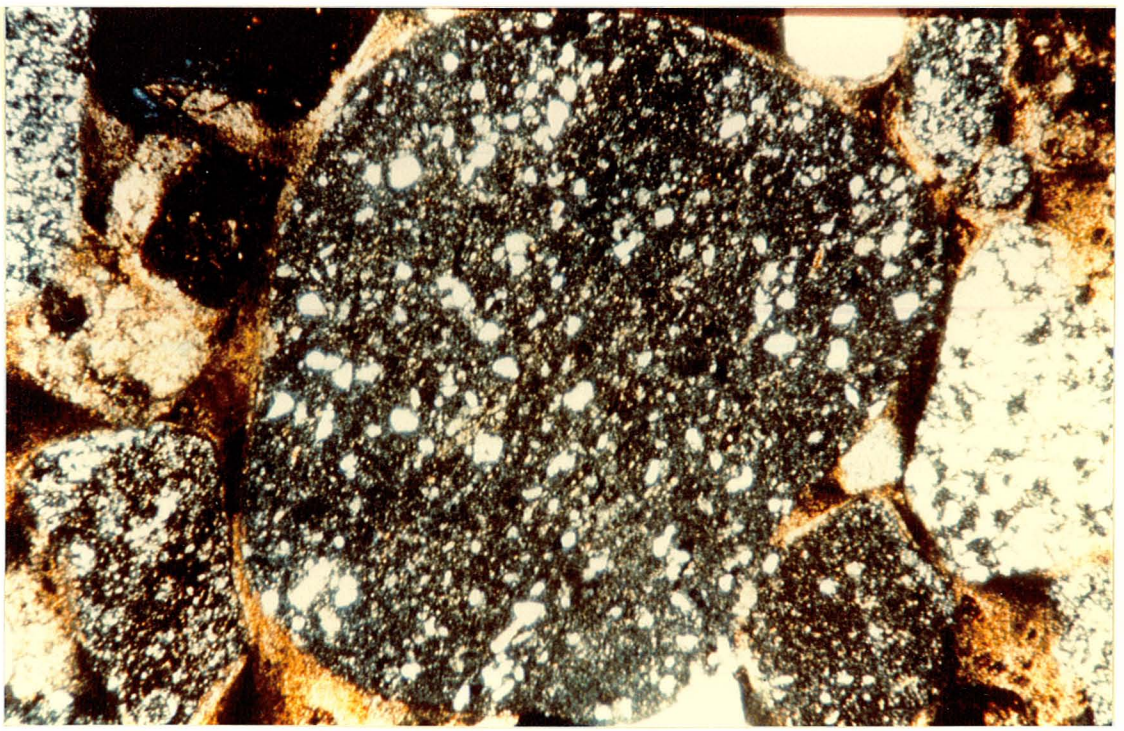

PLATE 36A : Thin Section 16-6-34-3W5 6538.0 ft
Garrington Field, magnification 63x.
Plain light photograph of a composite
chert clast composed of 60% chert and
40% quartz and rock fragments.

PLATE 36B : Same as above, but under crossed
nicols.

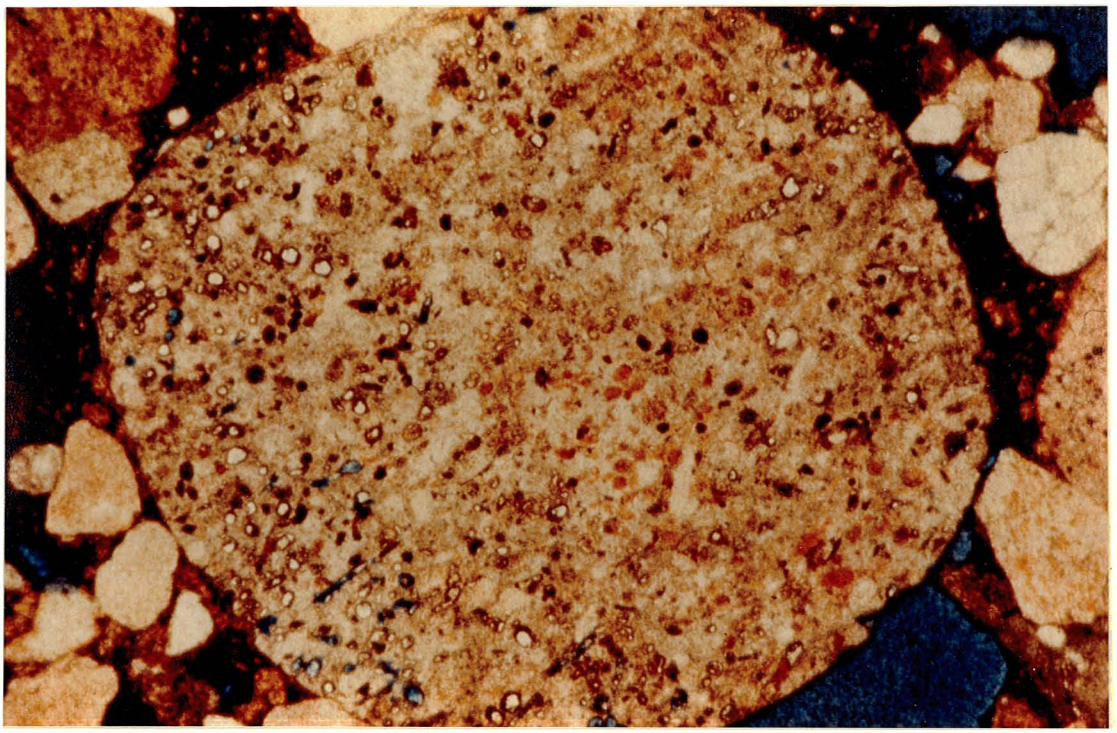

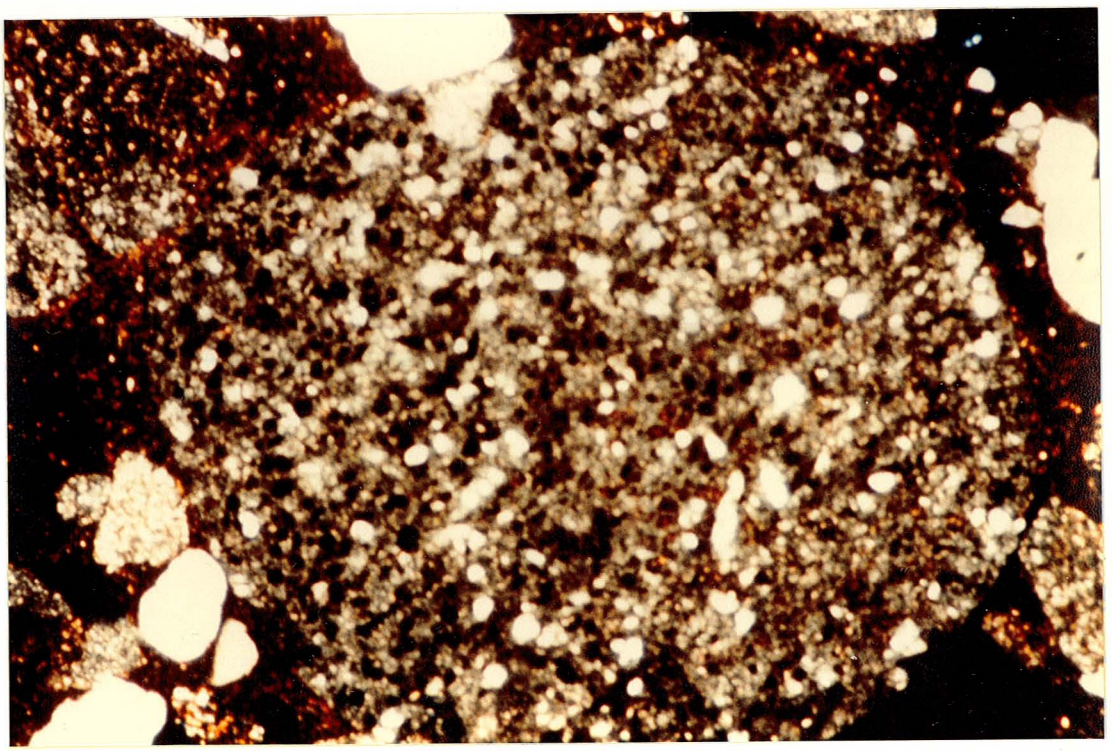

PLATE 37A : Thin Section 3-23-36-8W5 8535.5 ft
Caroline Field, magnification 63x.
Plain light photograph of a composite chert clast composed of 40% chert, and 60% quartz grains.

PLATE 37B: Same as above, but under crossed nicols.

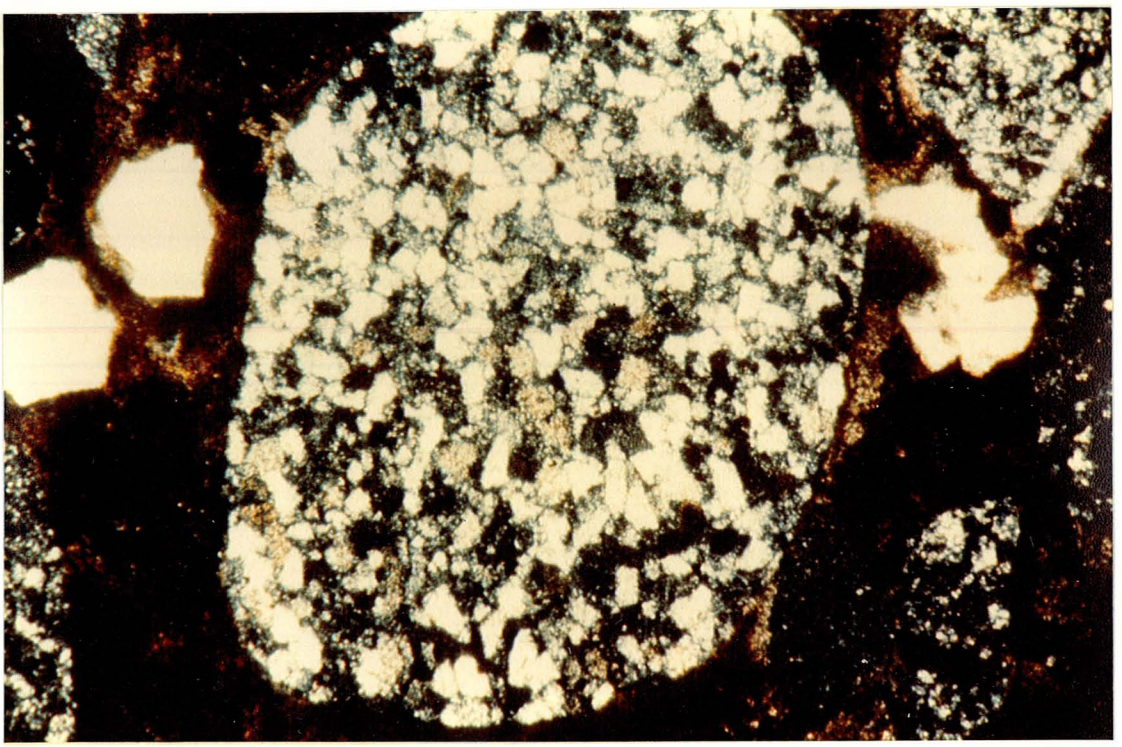

PLATE 38A : Thin Section 5-22-35-7W5 8250.0 ft
Caroline Field, magnification 63x.
Plain light photograph of a composite
chert clast composed of 20% chert,
and 80% siderite.

PLATE 38B : Same as above, but under crossed
nicols.

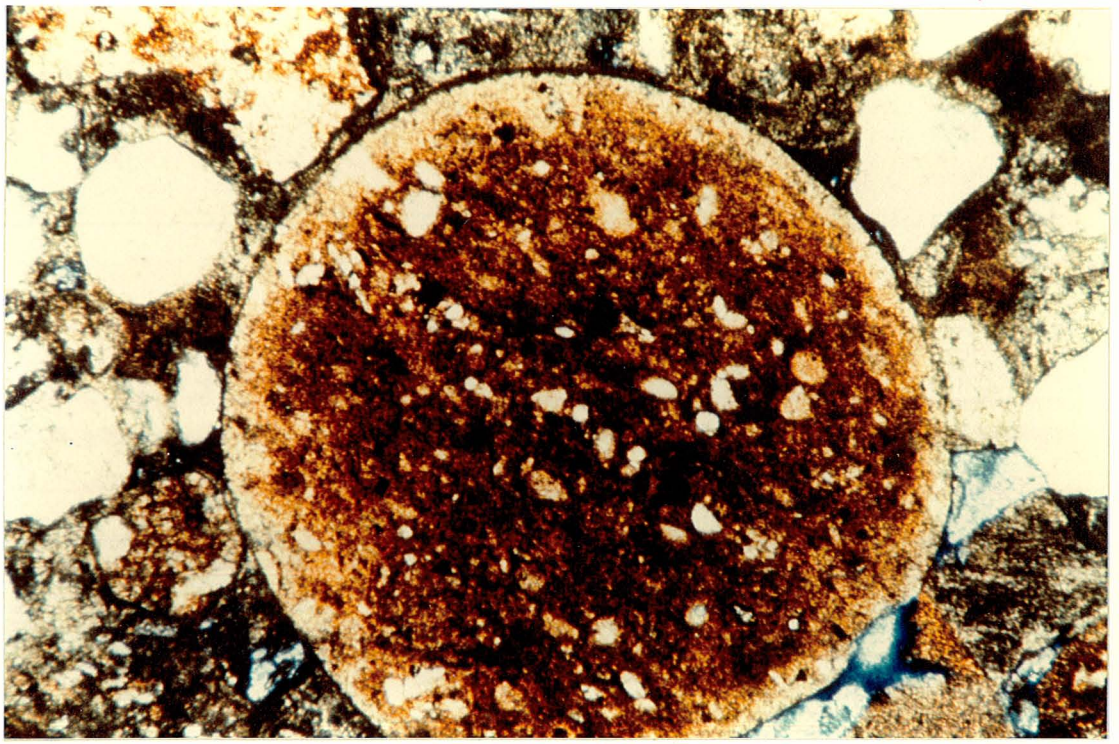

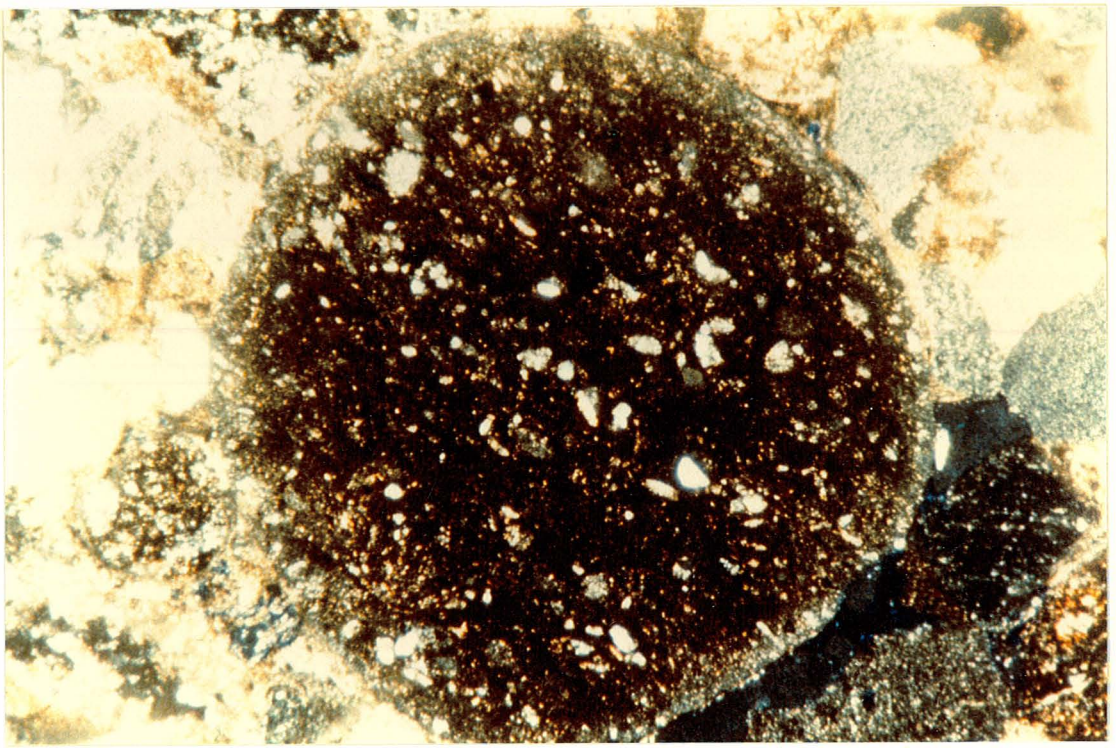

PLATE 39A : Thin Section 3-33-30-8W5 8535.5 ft Caroline Field, magnification 63x. Plain light photograph of a composite chert clast composed of nearly 100% siderite. Note the Opague nature of the clast.

PLATE 39B : Same as above, but under crossed nicols.

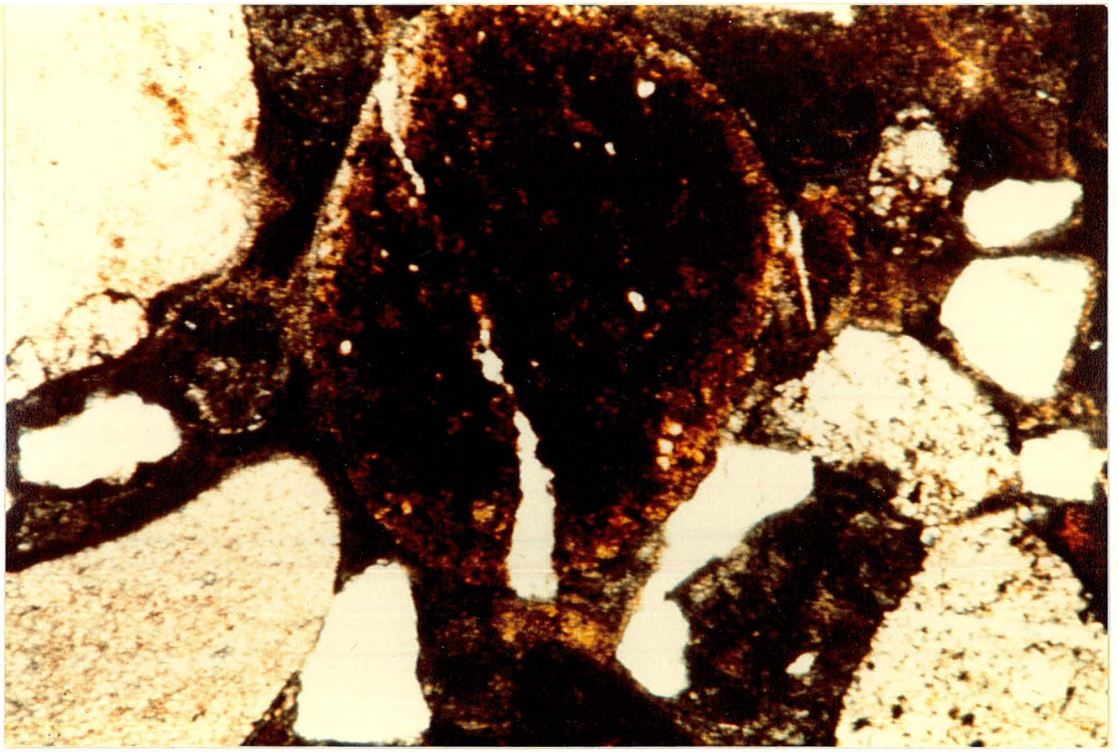

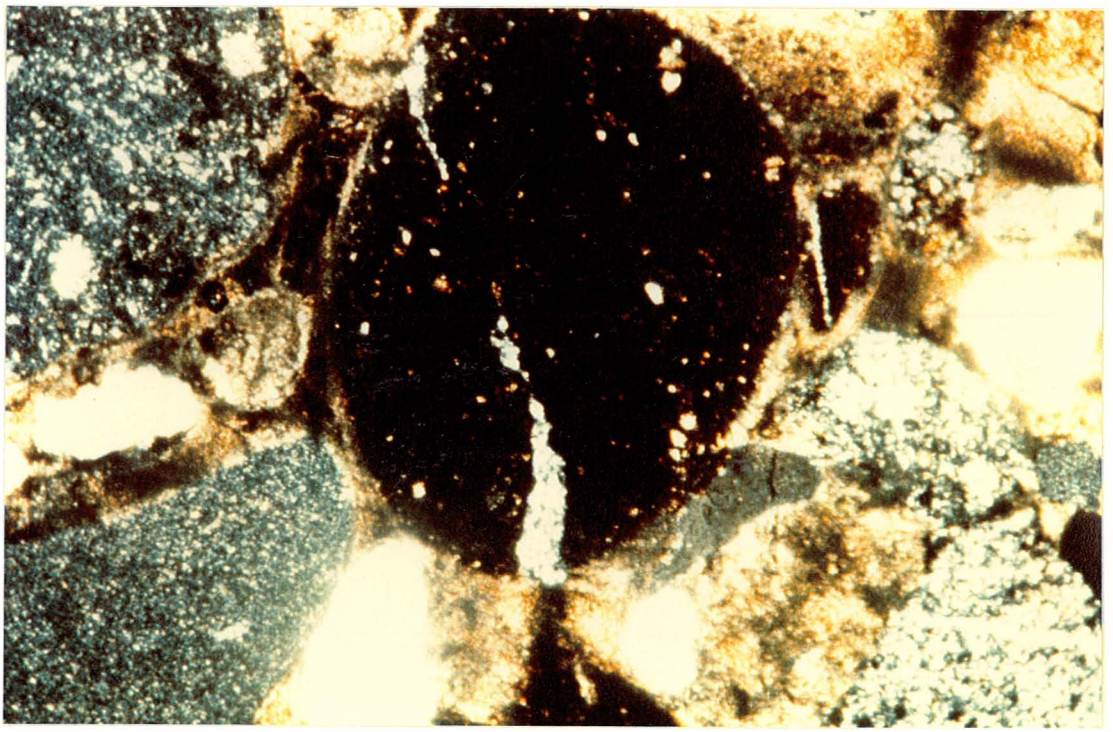

PLATE 40A : Conglomeratic sandstone,
magnification 5x.

PLATE 40B : Coarse grained sandstone,
magnification 5x.

PLATE 40C : Fine grained sandstone,
magnification 5x.

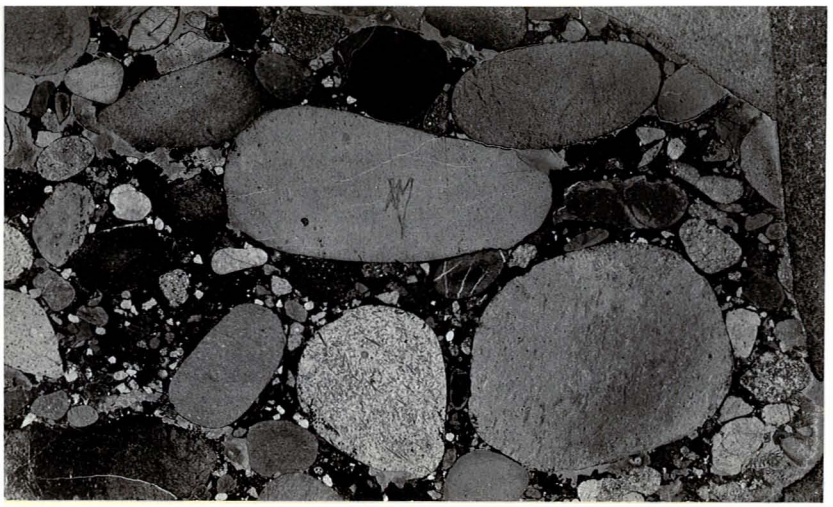

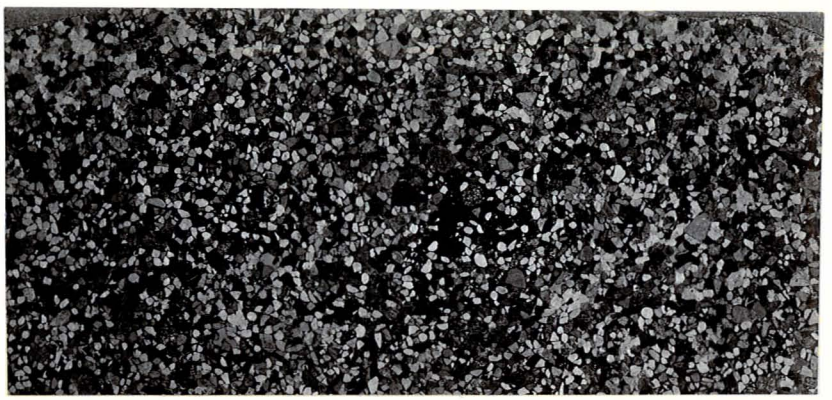

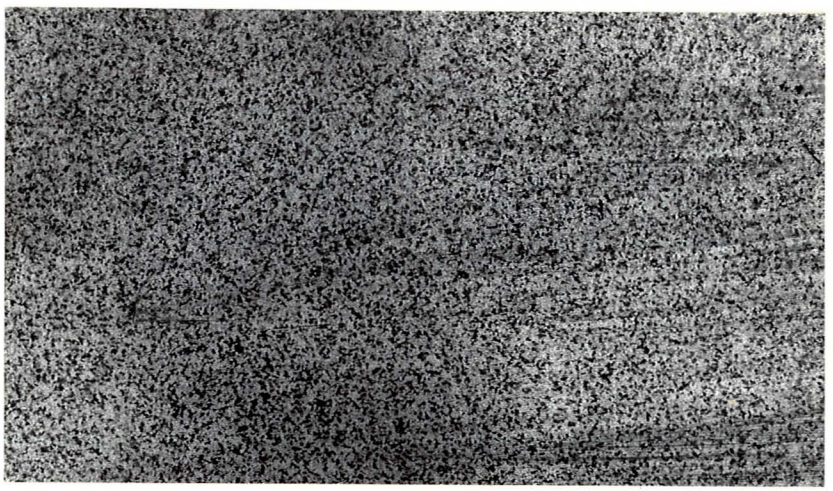

APPENDIX I

Well Number Designation and Location

RICINUS FIELD

Well#	Location And Depth	Well#	Location And Depth
1	7-9-33-7W5 6555.0′ R63	22	7-19-35-8W5 8853.0′ R28
2	7-9-33-7W5 6565.0′ R64	23	6-8-36-8W5 8887.0′ R27
3	7-9-33-7W5 6575.0′ R65	24	10-7-36-8W5 8910.0′ R30
4	7-9-33-7W5 6579.0′ R66	25	10-7-36-8W5 8931.0′ R29
5	2-1-34-8W5 6843.0′ R55	26	6-24-31-9W5 9112.0′ R77
6	2-1-34-8W5 6871.0′ R52	27	6-24-31-9W5 9109.0′ R78
7	8-10-34-8W5 8090.0′ R73	28	6-24-36-9W5 9060.0′ R79
8	8-10-34-8W5 8154.0′ R68	29	16-26-36-9W5 8889.0′ R26
9	11-21-34-8W5 7081′ R35	30	16-26-36-9W5 8925.0′ R25
10	11-21-34-8W5 7041′ R36	31	6-28-36-9W5 9215.0′ R11
11	7-28-34-8W5 5802.0′ R41	32	8-32-36-9W5 9467.5′ R8
12	7-28-34-8W5 5847.5′ R40	33	8-32-36-9W5 9215.0′ R7
13	7-28-34-8W5 5855.0′ R39	34	11-33-36-9W5 9442.0′ R2
14	3-29-34-8W5 9350.0′ R61	35	11-33-36-9W5 9460.0′ R1
15	3-29-34-8W5 9361.5′ R60	36	2-34-36-9W5 9225.0′ R16
16	3-29-34-8W5 9387.0′ R59	37	2-34-36-9W5 9226.0′ R17
17	3-5-35-8W5 8846.0′ R45	38	2-34-36-9W5 9244.0′ R14
18	10-11-35-8W5 8378′ R58	39	2-34-36-9W5 9250.0′ R13
19	10-11-35-8W5 8749′ R57	40	2-34-36-9W5 9254.0′ R12
20	7-19-35-8W5 8749.0′ R46	41	2-34-36-9W5 9336.0′ R15
21	7-19-35-8W5 9020.0′ R47		

APPENDIX I

Well Nunber Designation And Location

CAROLINE AND GARRINGTON FIELDS

Well#	Location And Depth		Well#	Location And Depth	
42	11-31-34-6W5	8175.0′ C6	64	11-27-34-6W5	7801.0′
43	11-31-34-6W5	8171.0′ C5	65	10-33-34-6W5	7880.0′ C4
44	3-7-35-6W5	8086.0′ C7	66	10-33-34-6W5	7889.0′ C2
45	3-7-35-6W5	8097.37′ C8	67	10-33-34-6W5	7899.5′ C1
46	5-22-35-7W5	8256.0′ T/3	68	10-33-34-6W5	7884.0′ C3
47	16-31-35-7W5	8355.0′ Top	69	16-9-35-6W5	7742.0′
48	16-31-35-7W5	8355.0′ Mid	70	2-25-35-7W5	7441.0′
49	16-31-35-7W5	8359.0′ Top	71	10-20-37-7W5	7441.0′
50	16-31-35-7W5	8359.0′ Bot	72	10-20-37-7W5	7445.75′
51	16-31-35-7W5	8359.0′ Mid	73	10-20-37-7W5	7437.3′
52	16-31-35-7W5	8355.0′ Bot			
53	11-17-35-8W5	9187.0′ R42	74	10-35-31-2W5	5976.0′
54	11-17-35-8W5	9267.5′ R43	75	16-6-34-3W5	6538.0′
55	11-17-35-8W5	9274.0′ R44	76	16-12-34-4W5	6611.0′
56	10-22-36-8W5	8665.5′ T/3			
57	10-22-36-8W5	8665.5′ T/4	77	16-6-34-3W5	6429.0′
58	10-22-36-8W5	8665.5′ T/2	78	4-21-37-6W5	7174.0′
59	10-22-36-8W5	8660.5′ B/2	79	4-21-37-6W5	7017.0′
60	10-22-36-8W5	8660.5′ B/1			
61	3-23-36-8W5	8535.5′ T/3			
62	3-23-36-8W5	8535.5′ T/4			
63	12-33-36-8W5	8514.0′ T/?			

APPENDIX II

Mineralogic Point Count Percentages

RICINUS FIELD

Well #	Qtz.	Chert	R.Frag	Fspar.	Por.	Cmt.	Mtx.	Other
1	40.0	35.0	3.0	0.0	9.0	10.0	10.25	2.75
2	56.0	20.0	4.0	.5	6.25	11.25	11.0	2.25
3	30.0	51.0	6.75	0.0	5.75	6.0	4.5	2.0
4	34.75	49.0	6.5	0.0	6.0	5.0	3.75	0.0
5	65.25	0.0	5.0	.75	24.5	6.5	4.5	0.0
6	70.75	0.0	15.75	1.5	6.0	14.0	4.5	1.5
7	63.25	2.0	7.75	0.0	23.5	0.0	3.5	0.0
8	66.25	1.25	3.5	1.0	24.0	0.0	4.0	0.0
9	61.0	21.0	3.25	0.0	12.75	12.0	2.0	0.0
10	62.75	19.25	1.5	.5	14.75	9.5	1.25	.5
11	64.25	15.5	8.75	0.0	9.25	10.0	2.25	0.0
12	56.75	27.5	8.0	0.0	7.25	5.0	0.0	0.0
13	38.0	34.0	18.0	1.0	4.0	6.0	5.0	0.0
14	50.0	12.75	10.25	3.5	13.75	15.0	9.75	0.0
15	54.0	17.5	7.0	2.75	.5	8.0	18.25	0.0
16	38.5	31.75	12.75	0.0	3.75	3.0	14.5	0.0
17	63.25	2.0	28.0	0.0	3.75	13.5	3.0	0.0
18	6.75	30.25	33.5	0.0	1.5	0.0	2.75	2.0
19	64.75	.25	30.0	.5	3.5	19.5	1.5	0.0
20	71.5	5.0	10.75	.5	11.25	7.0	1.0	0.0
21	65.5	23.75	7.0	0.0	3.75	10.0	0.0	0.0
22	63.0	3.0	23.25	.25	7.25	12.5	3.25	0.0

Mineralogic Point Count Percentages

RICINUS FIELD

Well #	Qtz.	Chert	R.Frag	Fspar.	Por.	Cmt.	Mtx.	Other
23	62.75	8.25	23.25	.75	1.0	12.5	4.0	0.0
24	62.0	10.0	4.5	0.0	20.0	9.5	3.5	0.0
25	64.0	1.5	4.0	0.0	15.0	13.0	2.0	0.0
26	46.0	33.0	3.0	0.0	12.75	7.0	5.25	0.0
27	62.0	11.25	3.5	0.0	22.75	9.0	.5	0.0
28	23.0	53.25	7.0	0.0	4.75	1.0	12.0	0.0
29	65.0	17.0	5.75	0.0	8.5	10.0	3.5	.25
30	63.25	5.25	13.5	0.0	15.75	13.0	2.75	0.0
31	65.0	16.0	5.0	1.75	8.5	10.0	3.5	.25
32	58.25	17.25	8.25	.75	14.75	9.0	.75	0.0
33	67.0	10.25	9.5	0.0	9.25	10.0	4.0	0.0
34	57.25	16.75	8.5	0.0	15.0	8.5	2.5	0.0
35	62.0	18.75	8.25	0.0	2.5	19.0	3.5	0.0
36	48.25	43.25	2.25	3.0	2.5	10.0	.75	0.0
37	47.0	44.0	6.5	0.0	1.25	15.0	1.25	0.0
38	71.0	8.5	6.75	0.0	10.25	18.0	2.5	1.0
39	57.75	9.25	14.5	0.0	14.25	9.5	3.75	0.0
40	55.0	32.0	4.0	0.0	4.0	14.5	4.0	1.0
41	63.25	15.75	8.25	.25	10.75	10.0	1.75	0.0

Mineralogic Point Count Percentages

CAROLINE FIELD (U)

Well #	Qtz.	Chert	R.Frag	Fspar.	Por.	Cmt.	Mtx.	Other
64	58.0	25.25	2.0	.5	1.0	0.0	13.25	0.0
65	36.5	4.0	4.5	0.0	1.0	0.0	51.0	3.0
66	58.0	10.0	8.75	0.0	5.25	6.0	8.25	9.75
67	53.25	10.0	4.25	2.0	.5	12.0	17.25	12.75
68	56.0	10.0	3.75	.5	2.25	11.0	13.75	13.75
69	53.75	17.5	4.0	0.0	0.0	22.5	22.5	2.25
70	49.0	19.0	4.75	1.0	0.0	18.0	22.75	4.0
71	52.0	18.0	4.0	1.0	13.0	10.0	12.0	0.0
72	47.75	23.0	4.5	.75	11.5	4.0	12.5	0.0
73	53.75	16.25	4.5	.75	11.0	12.0	13.75	0.0
		GARRINGTON FIELD (L)						
74	19.5	53.0	3.0	0.0	12.5	0.0	12.0	0.0
75	9.75	61.0	3.0	.75	19.5	0.0	6.0	0.0
76	10.25	64.5	4.0	0.0	2.25	1.0	19.0	0.0
		GARRINGTON FIELD (U)						
77	50.75	4.75	20.0	0.0	2.5	5.0	20.0	2.0
78	20.25	57.5	1.5	.75	13.75	5.0	6.25	0.0
79	42.5	31.0	1.75	.75	5.5	10.0	18.25	0.0

Mineralogic Point Count Percentages

CAROLINE FIELD (L)

Well #	Qtz.	Chert	R.Frag	Fspar	Por.	Cmt.	Mtx.	Other
42	41.25	30.0	8.5	0.0	14.75	4.0	4.5	0.0
43	21.25	45.0	9.0	0.0	7.75	1.0	17.0	0.0
44	25.75	49.5	7.0	0.0	11.0	4.0	6.5	0.0
45	39.75	43.0	4.75	1.0	7.75	8.0	4.0	0.0
46	20.0	40.0	.25	0.0	4.25	0.0	35.5	0.0
47	27.25	31.0	7.0	0.0	5.5	4.5	29.25	0.0
48	19.25	31.5	12.75	0.0	4.5	2.0	32.0	0.0
49	48.0	29.0	9.5	0.0	8.5	4.0	5.0	0.0
50	43.25	30.5	11.0	0.0	8.5	11.0	7.0	0.0
51	45.5	29.0	8.0	0.0	9.5	11.0	8.0	0.0
52	19.0	31.0	9.25	0.0	3.25	2.0	37.5	0.0
53	60.75	24.0	9.0	.25	3.5	15.0	2.5	0.0
54	12.0	35.0	16.5	2.0	5.5	16.5	16.75	0.0
55	53.75	34.5	6.5	0.0	5.25	5.0	0.0	0.0
56	23.75	43.0	4.25	.25	3.75	4.0	25.0	0.0
57	22.5	49.5	3.0	0.0	5.75	3.0	19.0	0.0
58	17.5	47.0	3.25	0.0	6.25	4.0	26.0	0.0
59	14.25	52.0	10.0	0.0	10.0	0.0	13.75	0.0
60	18.0	51.0	7.0	0.0	10.0	1.0	14.0	0.0
61	8.75	55.0	10.0	.25	.5	1.0	25.5	0.0
62	18.0	41.0	8.5	0.0	2.0	1.0	30.5	0.0
63	54.75	37.75	2.25	.25	3.0	0.0	2.0	0.0

APPENDIX III

Quartz Analysis And Grain Size Statistics

RICINUS FIELD

Well #	Poly. <3 gns	Ploy. >3 gns	Undu-lose	Non Und.	Average Gn. Size	Sphericity
1	0%	20%	80%	0%	.5mm	Subangular
2	0	0%	100%	0%	.65mm	Subrounded
3	0%	0%	80%	0%	3.5mm	Subrounded
4	0%	20%	80%	0%	4.0mm	Subrounded
5	20%	0%	60%	20%	.17mm	Subangular
6	0%	0%	80%	20%	.35mm	Subangular
7	0%	0%	80%	20%	.12mm	Subangular
8	0%	0%	40%	60%	.15mm	Angular
9	0%	0%	100%	0%	.15mm	Angular
10	0%	0	100%	0%	.175mm	Subangular
11	0%	0%	80%	20%	.075mm	Subangular
12	0%	0%	100%	0%	.2mm	Subangular
13	0%	0%	100%	0%	1.5mm	Rounded
14	0%	20%	80%	0%	.1mm	Angular
15	20%	0%	80%	0%	.1mm	Angular
16	0%	20%	80%	0%	.3mm	Subangular
17	0%	0%	40%	60%	.15mm	Subangular
18	0%	40%	20%	40%	2.0mm	Rounded
19	0%	0%	80%	20%	.16mm	Subangular
20	0%	0%	80%	20%	.15mm	Angular
21	0%	20%	60%	40%	.125mm	Subangular
22	0%	20%	80%	0%	.2mm	Subangular

APPENDIX III

Quartz Analysis And Grain Size Statistics

RICINUS FIELD

Well #	Poly. <3 Gns	Poly. >3 Gns	Undu-lose	Non Und.	Average Gn. Size	Sphericity
23	0%	0%	20%	40%	.12mm	Subangular
24	0%	20%	60%	20%	.10mm	Subangular
25	0%	0%	20%	80%	.15mm	Subangular
26	0%	0%	100%	0%	.25mm	Angular
27	0%	0%	100%	0%	.15mm	Angular
28	0%	20%	60%	20%	2.5mm	Rounded
29	0%	0%	80%	20%	.15mm	Subangular
30	0%	0%	100%	0%	.15mm	Subangular
31	0%	0%	80%	20%	.15mm	Angular
32	0%	0%	100%	0%	.15mm	Subangular
33	0%	0%	100%	0%	.15mm	Angular
34	0%	0%	100%	0%	.15mm	Angular
35	0%	0%	80%	20%	.20mm	Angular
36	20%	0%	60%	20%	.30mm	Subangular
37	0%	0%	100%	0%	1.0mm	Rounded
38	0%	0%	80%	20%	.15mm	Subangular
39	0%	0%	80%	20%	.15mm	Subangular
40	0%	20%	60%	20%	1.0mm	Subrounded
41	0%	0%	80%	20%	.15mm	Subangular

APPENDIX III

Quartz Analysis And Grain Size Statistics

LOWER CAROLINE

Well #	Poly. <3 Gns	Poly >3 Gns	Undu-lose	Non Und.	Average Gn. Size	Sphericity
42	20%	0%	60%	20%	.35mm	Subangular
43	0%	20%	60%	20%	.60mm	Round
44	20%	20%	40%	20%	.25mm	Subrounded
45	20%	20%	40%	20%	.35mm	Subrounded
46	20%	20%	40%	20%	.25mm	Subrounded
47	0%	20%	20%	60%	.30mm	Subrounded
48	0%	20%	60%	20%	.35mm	Subrounded
49	20%	20%	60%	0%	.45mm	Subangular
50	0%	20%	20%	60%	.35mm	Subangular
51	0%	20%	20%	60%	.40mm	Subangular
52	20%	0%	60%	20%	.25mm	Subrounded
53	0%	0%	60%	40%	.15mm	Subangular
54	20%	20%	40%	20%	.45mm	Subrounded
55	0%	20%	40%	40%	.40mm	Subrounded
56	0%	20%	60%	20%	.30mm	Subrounded
57	0%	20%	60%	20%	.25mm	Subangular
58	0%	20%	40%	40%	.40mm	Subangular
59	0%	20%	80%	0%	3.5mm	Subrounded
60	0%	20%	40%	40%	1.0mm	Subrounded
61	0%	20%	40%	40%	2.5mm	Rounded
62	0%	20%	40%	40%	1.5mm	Subrounded
63	0%	0%	20%	80%	.35mm	Subangular

APPENDIX III

Quartz Analysis And Grain Size Statistics

UPPER CAROLINE

Well #	Poly. <3 Gns	Poly. >3 Gns	Undu-lose	Non Und.	Average Gn. Size	Sphericity
64	0%	0%	100%	0%	.05mm	Subangular
65	0%	20%	40%	40%	.125mm	Subangular
66	0%	0%	40%	60%	.075mm	Angular
67	0%	0%	40%	60%	.05mm	Angular
68	0%	0%	40%	60%	.75mm	Angular
69	0%	20%	60%	20%	.10mm	Subangular
70	0%	0%	80%	20%	.075mm	Subangular
71	0%	0%	80%	20%	.05mm	Subangular
72	0%	0%	100%	0%	.05mm	Subangular
73	0%	20%	60%	20%	.10mm	Subangular
		LOWER GARRINGTON SAND				
74	0%	40%	60%	0%	5.0mm	Rounded
75	20%	20%	40%	20%	3.5mm	Rounded
76	0%	20%	40%	40%	4.0mm	Rounded
		UPPER GARRINGTON SAND				
77	0%	20%	40%	40%	.025mm	Subangular
78	0%	20%	60%	20%	.75mm	Subrounded
79	0%	0%	80%	20%	.075mm	Angular

Point Count Summary Statistics

APPENDIX IV

Sand Body	Qtz.	Chert	R. Frag	Fspar.	Por.	Cmt.	Mtx.	Other
RICINUS								
Average	56.0%	19.0%	9.5%	.5%	9.5%	9.5%	5.0%	.5%
Standard Deviation	14.8	15.5	7.8	1.1	6.8	4.8	5.5	.7
LOWER CAROLINE								
Average	30.0%	38.5%	7.5%	.25%	7.0%	4.5%	16.5%	0.0%
Standard Deviation	15.6	9.7	3.6	.5	3.5	4.5	11.8	
UPPER CAROLINE								
Average	52.0%	15.5%	4.5%	.5%	4.5%	9.5%	18.5%	4.5%
Standard Deviation	6.4	6.6	1.7	.6	5.3	7.3	12.2	5.5
LOWER GARRINGTON								
Average	13.5%	59.5%	3.5%	.25%	11.0%	.25%	12.0%	0.0%
Standard Deviation	5.3	5.9	.6	.4	8.7	.5	5.3	
UPPER GARRINGTON								
Average	38.0%	31.0%	7.75%	.5%	7.25%	6.5%	15.0%	.5%
Standard Deviation	15.8	26.4	10.6	.5	5.8	3.0	7.5	1.0

Point Count Results From The Error Analysis

APPENDIX V

Thin Section # 50	Qtz.	Chert	R. Frag	Fspar	Por.	Cmt.	Mtx.	Other
First Point Count First Operator	43.0%	30.5%	11.0%	0.0%	8.5%	11.0%	7.0%	0.0%
Second Point Count First Operator	48.0%	36.0%	6.0%	0.0%	8.0%	----	2.0%	0.0%
Third Point Count Second Operator	41.0%	36.0%	10. %	0.0%	9.0%	----	4.0%	0.0%

APPENDIX VI
(Scholle, 1981)

Comparison Chart For Visual Percentage Estimation (After Terry and Chilingar, 1955).

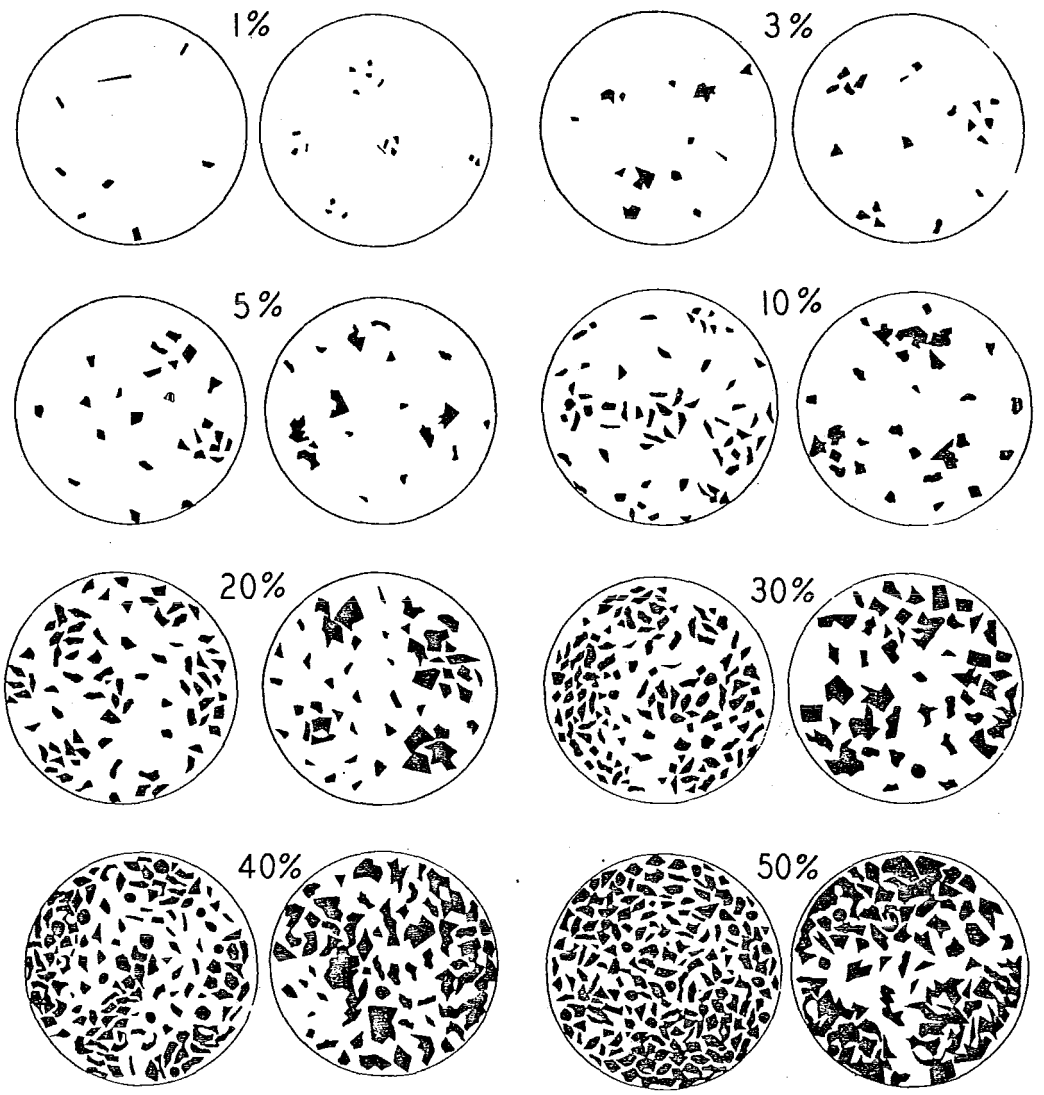

APPENDIX VII
(Scholle, 1981)

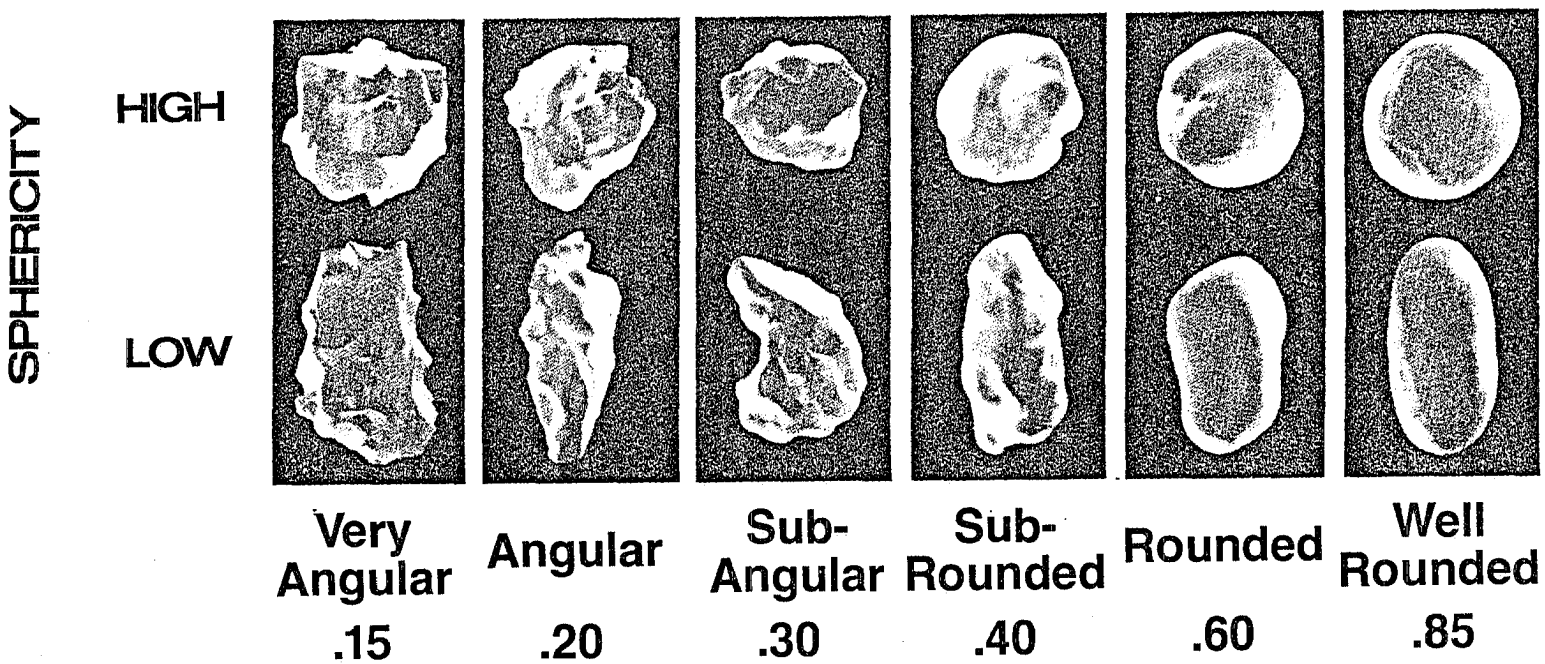

(from: Powers, 1953)

REFERENCES

Almon, W.R., 1979, Petrophysical Evidence of Cementation Differences in the Cardium Sandstone: in Transactions of the CWLS Seventh Formation Evaluation Symposium, Oct. 21-24, 1979, Section K.

Berven, R.J., 1966, Cardium Sandstone bodies, Crossfield-Garrington area, Alberta: Bull. Can. Petrol. Geol., V. 41, pg. 208-240.

Berner, R.A., 1971, Principles of Chemical Sedimentology: McGraw-Hill Inc., New York, 240 pp.

Blatt, B and Middleton, C., 1980, Origin of Sedimentary Rocks, Prentice Hall Inc., "Cementation and Deep Disgenesis of Sandstones".

Burk, C.F., 1963, "Structure, Isopach, and Facies Maps of Upper Cortaceous Marine Succession, West Central Alberta and Adjacent British Columbia", Geological Society of Canada, paper 61-31

Currie, J.B. and Nwachukwa, S.O., 1974, Evidence of incipient fracture porosity in reservoir rocks at depth: Bull, Can. Petrol. Geol., V. 22, pp. 42-58.

Curtis, C.D. and Spears, D.A., 1968, The formation of sedimentary iron minerals: Econ. Geol., V. 63, pp. 257-270.

Curtis, C.D., Pearson, M.J. and Somogyi, V.A., 1975, Mineralogy, chemistry and origin of a concretionary siderite sheet (clay-ironstone band) in the Westphalian of Yorkshire: Mineralog. Mag., V. 40 pp. 385-393.

Dickinson, W.R. and Suczek, C.A., 1978, Plate Tectonics and Sandstone Composition, American Association of Petroleum Geologists, Vol. 62, pp. 2164-2182.

Ehleis, E.C. and Blatt, H., 1982, Petrology Igneous Sedimentary and Metamorphic, Diagenesis of Sandstone, Wilt Freeman & Co., pp. 386-423

Franks, P.C., 1969, Synaeresis features and genesis of siderite concretions, Kiowa Formation (early Cretaceous): J. Sed. Petrology, V. 39, pp. 799 - 803.

Hallam, A., 1967, Siderite and Calcite-bearing concretionary nodules in the Lias of Yorkshire: Geol. Mag., V. 104, pp. 222-227.

Hodgson, W.R., 1968, The diagenesis of spherulitic carbonate concretions and other rocks from Mangakahia Group Sediements, Kaipara Harbour, New Zealand: J. Sed. Petrology, V. 38, pp. 1254-1263

Hoyowitz, A.S. and Petter, P.E., 1971, Introductory Petrography of Fossils, Springer-Verlag Berlin,

Krause, F.F., 1982, "Geology of the Pembina Cardium Pool" in John C. Hopkins Depositional environments and Reservoir Facies In Some Western Canadian Oil And Gas Fields, University of Calgary Core Conference, pp. 3-15

MacDonald, W.D., 1957, The upper Cretaceous Cardium Formation Between the Athabasca River and the Peace River: Alberta Soc. Petrol. Geol. Jor., V. 5, pp. 82-88

Mellon, G.B., 1962, Petrology of Upper Cretaceous colitic iron-rich rocks from Northern Alberta: Economic Geology, V. 57, pp. 921-940

Michaelis, E.R., 1957, Cardium sedimentation in the Pembina River area: Amer. Assoc. Petrol. Geol. Jour., V. 5, pp. 73-77

Michaelis, E.R. and Dixon, G., 1969, Interpretation of depositional process from sedimentary structures in Cardium sand: Can. Soc. Petrol. Geol. Bull., V. 17, pp. 410-433

Nickel, E., 1978, "The Present Status at Cathode Luminescence As a Tool in Sedimentology: Mineral Science Engineering Sedimentology, Vol. 10, pp. 73-99

Pendergast, R.D., 1969, Correlating Cardium Stratigraphy using static bottom hole pressures: Canadian Well Logging Soc. Jour., V. 2, pp. 19-27

Scholle, P.A., 1981, Constituents, Textures, Cements and Porosities of Sandstones, and Associated Rocks, AAPL memoir 28.

Sinha, R.N., 1970, Cardium Formation, Edson area, Alberta: Geol. Sur. Canada Paper 68-30.

Spencer, E., 1925, On some occurrences of spherulitic siderite and other carbonates in sediments:

Geol. Soc. London Quart. Journ., V. 81, pp. 667-705.

Stott, D.F., 1963, The Cretaceous Alberta Group and equivalent rocks, Rocky Mountain Foothills, Alberta: Geol. Sur. Canada Memoir 137.

Swagor, N.S., Oliver, T.A. and Johnson, B.A., 1976, Carrot Creek Field, Central Alberta: in M. Lerand, (ed), The Sedimentology of Selected Clastic Oil and Gas Reservoirs in Alberta: Can. Soc. Petrol. Geol., Calgary, p. 78-95.

Thomas, M.B. and Oliver T.A., 1979, Depth porosity relationships in the Viking and Cardium Formations of Central Alberta: Can. Soc. Petrol. Geol. Bull., V. 27, pp. 209-228.

Walker, R.G., 1983, "Cardium Formation 2" Sand Body Geometry and Stratigraphy in the Garrington-Caroline-Ricinus Area, Alberta -- The "Ragged Blanket" McDel Bulletin of Canadian Petroleum Geologists, V. 31, pp. 3-18.

Wright, M.E. and Walker, R.G., 1980, Cardium Formation (Upper Cretaceous) at Seebe, Alberta - storm-transported sandstones and conglomerates in shallow marine depositional enviornments below fair-weather wave base: Can. J. Earth Sci., V. 18, pp. 795-809.